Patient-specific B-cell lymphoma modeling identifies cooperating genetic alterations and the critical influence of patient context

Fabian Konrath

Mathematical Modelling of Cellular Processes, Max-Delbrück-Center for Molecular Medicine in the Helmholtz Association (MDC), Berlin, Germany https://orcid.org/0000-0002-6843-6252

Sophy Denker

Charité - Universitätsmedizin, corporate member of Freie Universität Berlin, Humboldt-Universität zu Berlin, Department of Hematology, Oncology and Tumor Immunology, and Molekulares Krebsforschungszentrum – MKFZ, Campus Virchow Klinikum, Berlin, Germany Berlin Institute of Health at Charité - Universitätsmedizin Berlin, Berlin, Germany

Clemens Schmitt

Charité - Universitätsmedizin, corporate member of Freie Universität Berlin, Humboldt-Universität zu Berlin, Department of Hematology, Oncology and Tumor Immunology, and Molekulares Krebsforschungszentrum – MKFZ, Campus Virchow Klinikum, Berlin, Germany Cancer Genetics and Cellular Stress Responses, Max-Delbrück-Center for Molecular Medicine in the Helmholtz Association (MDC), Berlin, Germany Kepler University Hospital, Department of Hematology and Oncology, Medical Faculty, Johannes Kepler University, Linz, Austria https://orcid.org/0000-0002-4731-2226

Björn Chapuy

Charité - Universitätsmedizin, corporate member of Freie Universität Berlin, Humboldt-Universität zu Berlin, Department of Hematology, Oncology, and Cancer Immunology, Campus Benjamin Franklin, Berlin, Germany German Consortium for Translational Cancer Research (DKTK), partner site Berlin, German Cancer Research Center (DKFZ), 69120 Heidelberg, Germany https://orcid.org/0000-0002-6485-8773

Jana Wolf

jana.wolf@mdc-berlin.de

Mathematical Modelling of Cellular Processes, Max-Delbrück-Center for Molecular Medicine in the Helmholtz Association (MDC), Berlin, Germany Department of Mathematics and Computer Science, Free University Berlin, Berlin, Germany https://orcid.org/0000-0003-3254-5868

Article

Keywords:

Posted Date: March 12th, 2026

DOI: https://doi.org/10.21203/rs.3.rs-9022766/v1

Additional Declarations: There is **NO** Competing Interest.

Patient-specific B-cell lymphoma modeling identifies cooperating genetic alterations and the critical influence of patient context

Fabian Konrath[1], Sophy Denker[2,3], Clemens A. Schmitt[2,4,5], Björn Chapuy[6,7], Jana Wolf[1,8]

1 Mathematical Modelling of Cellular Processes, Max-Delbrück-Center for Molecular Medicine in the Helmholtz Association (MDC), Berlin, Germany

2 Charité - Universitätsmedizin, corporate member of Freie Universität Berlin, Humboldt-Universität zu Berlin, Department of Hematology, Oncology and Tumor Immunology, and Molekulares Krebsforschungszentrum – MKFZ, Campus Virchow Klinikum, Berlin, Germany

3 Berlin Institute of Health at Charité - Universitätsmedizin Berlin, Berlin, Germany

4 Cancer Genetics and Cellular Stress Responses, Max-Delbrück-Center for Molecular Medicine in the Helmholtz Association (MDC), Berlin, Germany

5 Kepler University Hospital, Department of Hematology and Oncology, Medical Faculty, Johannes Kepler University, Linz, Austria

6 Charité - Universitätsmedizin, corporate member of Freie Universität Berlin, Humboldt-Universität zu Berlin, Department of Hematology, Oncology, and Cancer Immunology, Campus Benjamin Franklin, Berlin, Germany

7 German Consortium for Translational Cancer Research (DKTK), partner site Berlin, German Cancer Research Center (DKFZ), 69120 Heidelberg, Germany

8 Department of Mathematics and Computer Science, Free University Berlin, Berlin, Germany

corresponding: jana.wolf@mdc-berlin.de

Abstract

Diffuse large B-cell lymphoma (DLBCL) is a molecularly heterogeneous disease with high genetic complexity and interpatient variability. Sequencing studies of representative patient cohorts have identified a comprehensive set of genetic driver alterations, enabling patient stratification for personalized treatment strategies. To date, it remains insufficiently understood how these oncogenic driver alterations operate in concert and shape malignant cell states. Here, we use a computational approach that embeds patient data and experimentally characterized molecular perturbations in mechanism-based mathematical modeling to study the effect of genetic alterations in a network context. Based on a detailed pathway model capturing key cellular processes, including apoptosis, cell division, and B-cell differentiation, we created personalized models for a cohort of 284 patients, of which 90.5% reflect an aberrant cell state. Systematic assessment of the functional effects of individual and combinatorial alterations within these models identified previously not appreciated cooperating alterations that operate in synergy, such as mutated *NFKBIE* and *BCL6* structural variant. Notably, we identify a strong context dependency of functional effects, as identical alterations exert varying effects in different patient models. Incorporation of the network context is therefore essential for understanding DLBCL heterogeneity and selecting therapeutic targets for personalized and more efficient treatment strategies.

Introduction

Diffuse large B-cell lymphoma (DLBCL) is the most common Non-Hodgkin lymphoma, accounting globally for approximately 150 000 new cases each year[1]. The current first-line standard-of-care for DLBCL patients is an immunochemotherapy (R-CHOP-like), which leads to a cure in approximately two-thirds of the patients. A sizeable fraction of the remaining patients still succumb to their disease despite modern salvage strategies[2]. Molecularly, DLBCL is a heterogeneous disease, and these differences impact on biology and treatment (in)sensitivity, thereby affecting curability, disease progression, or relapse, and eventual death from the disease[3–5].

To characterize the molecular heterogeneity and understand the impact of molecular-defined substructure to treatment response, DLBCL patient samples have been subjected to transcriptomic and genetic profiling[6–15]. Transcriptional stratification based on the putative cell-of-origin of the disease led to the identification of the activated B-cell (ABC) or germinal center-type B-cell (GCB) DLBCL subtypes[6]. Accordingly, GCB DLBCL exhibit high expression of germinal center markers, *e.g. BCL6*, and frequently harbor genetic alterations such as *EZH2* mutations, or *BCL2* and *MYC* translocations. ABC DLBCL originate from post-germinal center B-cells, frequently exhibits *MYD88* and *CD79* mutations, and are characterized by chronic-active B-cell receptor and associated NF-κB pathway signaling[16].

Genetically, DLBCL is characterized by a considerable interindividual heterogeneity due to the variety, number, and composition of altered genes as well as the type of those alterations, comprising somatic mutations, copy number (CN) aberrations (CNAs) and structural variants (SVs). Sequencing of large DLBCL patient cohorts facilitated the

identification of driver alterations and cosegregated genetic signatures[6–15]. Among the identified genetically perturbed genes are regulators of NF-κB activity such as *NFKBIA* (IκBα) or *TNFAIP3* (A20), but also well-known oncogenes and tumor suppressors, including *MYC*, *TP53*, *BCL6* and *PTEN*.

The centrality of the NF-κB pathway in DLBCL biology is due to its involvement in the regulation of critical cellular functions, including life-death cell fate decisions, cell-cycle control and B-cell differentiation. Of note, NF-κB is a family of transcription factors consisting of RELA, CREL, RELB, p105/p50 (NFKB1) and p100/p52 (NFKB2) that induce the expression of a multitude of target genes, *e.g.* cyclin D1, D2, D3, anti-apoptotic factors BCL2 and BCL-XL, as well as the transcription factor BLIMP1. Moreover, NF-κB mediates the expression of its own direct and indirect inhibitors, namely IκBs and *TNFAIP3* (A20), and drives expression of many cytokines and chemokines.

To stratify patients based on their genetic signatures, classifiers have been developed (DLB*class* and Lymphgen)[13,17,18], enabling a better biological subgrouping and more detailed stratification of patients regarding treatment options and prediction of expected outcomes. In parallel, computational disease models have been developed to predict responses and to improve patient stratification of DLBCL patients[19–23] (recently reviewed in detail[24]). Among those approaches, mechanistic mathematical models have been used to study patient data by creating patient-specific models. In earlier work, we developed logical models to assess the effect of genetic alterations, single inhibitors, and inhibitor combinations in a patient-specific manner[20]. These models allowed to characterize patients based on the impact of the respective inhibitors on the individual NF-κB signaling

activity. In an alternative published patient-specific model, patients are stratified based on defined signaling patterns of the model[21].

These approaches enable predictive insights into stratification and treatment responses, but systematic modeling of individual and cosegregated genetic alterations and their functional relationships in patient contexts is missing. The crucial role of functional relationships between alterations has been demonstrated in molecular studies, *e.g.* for the anti-apoptotic factor BCL2. While a delay or abrogation of apoptosis induction is associated with cancer[25], an overexpression of BCL2 in mice, cell lines and human primary cells is not sufficient to cause malignant transformations or tumor development[26,27]. However, the combination with increased expression of the proliferation-promoting oncogene *MYC* results in a synergistic effect, causing strongly increased proliferation and the development of tumors[28]. This combination is known as double hit lymphoma and is associated with poor outcomes in patients[16]. Alterations of other drivers, including *MYC*, *CCND3*, *BCL6* and *TP53* were alone also insufficient to cause a strong cellular expansion of primary B-cells[27]. While combinations of BCL2 and MYC overexpression, or BCL2 and BCL6 overexpression, strongly prolonged primary B-cell survival, in immunodeficient mice, four of the five alterations are required for *in vivo* tumor formation[27]. These results strongly emphasize the importance to understand mutual effects of alterations and assessing the combined effect of patient-specific compositions of alterations.

We therefore employed here a computational approach that combines detailed mechanistic network modeling with patient cohort data and experimentally characterized functional effects of alterations to study the effect of genetic alterations in a network

context. The combined analysis of alteration insertions and drop out simulations in patient-specific models reveals previously unrecognized synergistic interactions and highlights the strong context dependency created by each individualized alteration signature.

Results

Constructing patient-specific models

To assess the impact of all genetic alterations in DLBCL patients on signaling network dynamics and their contribution to putative cancerous cell states, we first created a reference model and thereafter patient-specific models. We chose as a basis the model of Roy *et al.*[29], in which crucial cellular functions, including apoptosis, cell division and B-cell differentiation, are described and which allows us to analyze the derived state of a cell. To enable efficient simulations and capture additional regulatory processes that play an important role in DLBCL, we substantially refined and expanded the model (Fig. 1A and Methods, Construction of the reference model). We visualized the complex underlying network of our reference model, representing a wild-type (WT) activated B-cell, in an automated way (Fig. 1A, Methods, Model visualization), highlighting the model wiring of important network components, their interconnection, and distinct subnetworks (Fig. 1B).

To investigate the heterogeneity of patients based on their individual composition of alterations, we created patient-specific models based on our reference model. We therefore captured key alterations that were directly or indirectly implemented into the reference model. From a recently published cohort consisting of 304 DLBCL patients[13], we incorporated the molecular profiles at the timepoint of diagnosis of 284 patients based on mutations, CNAs and SVs of genes that could be mapped to components of the network model (for details, see Methods, Implementation of genetic alterations). The remaining patients did not show significant alterations that could be linked to our model components. Regarding the mutations, we distinguished between loss-of-function (LOF)

mutations, activating or inactivating mutations, and gain-of-function (GOF) mutations. In total, we were able to map 105 distinct alterations from the patient cohort onto our reference model. The implementation of the functional effects of 104 alterations (Table 1) was achieved by using the databases cBioPortal[30–32] and oncoKB[33,34]. Moreover, we performed a thorough literature search to collect information about functional effects of relevant mutations (Table S1). Among those is also the formation of the My-T-BCR super-complex in the presence of *MYD88* and *CD79B* mutations that accounts for chronic NF-κB and PI3K activity[35]. To incorporate the quantitative impact of the alterations, we defined perturbation strengths based on accessible quantitative data and sensitivity analyses (Fig. 1A). By combining patient-individual compositions of all implemented alterations, we successfully created 284 patient models capturing in total 638 mutations, 1778 CN gains, 539 CN losses and 142 SVs (Fig. S1, Table 1). The number and type of alterations differed substantially among patients, ranging from 1 to 33 alterations per case implemented into the model (Fig. 1C). Simulating all patient models revealed diverse dynamics of key components (Fig. 1D), reflecting the heterogeneity of the patients (Fig. S1).

Patient models reflect aberrant cellular states

We first investigated whether the implemented patient-specific genetic signatures cause an aberrant cellular state for each patient model. Aberrant cell states differ from the reference cell state in terms of proliferation and/or cellular survival and contribute to the malignant transformation and eventual tumor formation in the patient. As we incorporated the patient-specific genetic signature into the patient models, we therefore simulated the network dynamics and estimated the timepoint of apoptosis and the division rate of each model (see Methods, Creating and simulating patient models).

The combination of both readouts, the apoptosis timepoint and the division rate define the cell state. Based on the physiological state of the reference model (Fig. 2, empty square), the division rate of the WT state is extrapolated for all time points of apoptosis (Fig. 2, dotted line). Importantly, from the 284 patient models developed, 257 (90.5%) show an aberrant state (Fig. 2). This data demonstrates that the specific combination of alterations present in a given patient model promote for the vast majority an aberrant state. The patient models in this state can be divided into two groups. While the proliferation rate is increased in both groups compared to the reference model, apoptosis is either entirely suppressed or is still induced - earlier or later than in the reference model. There are 27 models (9.5%) showing a “physiological state”.

The extensive coverage of aberrant states in the patient models provides a valuable baseline for dissecting the impact of individual and combined alterations as well as their functional interdependencies within patient-specific network contexts.

Individual alteration effects explain only a limited number of aberrant states

To investigate the effect of individual alterations on the cell state, we used the reference model to simulate each alteration that is found in the patients and quantified the change in the timepoint of apoptosis and the division rate (Fig. 3A). From the 104 alterations, 42 (40.4%) have the potential to individually promote an aberrant state (Table S2). These 42 alterations correspond to 21 genes (45.7%). The strongest effects are observed for *TNFAIP3* mutations, SVs of *MYC* and the LOF mutation of *NFKBIA*. All these alterations strongly increase the division rate and, except for *MYC*, also prevent apoptosis induction

during the simulation time. The analysis reveals that specific alterations affecting the cell division directly or indirectly via the regulation of NF-κB are sufficient to promote an aberrant state. This is in line with the known tumor suppressor roles of *TNFAIP3* and *NFKBIA,* as their LOF mutations can cause constitutive NF-κB activity and thereby promote an aberrant cell state[36–41].

In patients with DLBCL, genetic alterations usually occur not in isolation but as co-segregated genetic signatures[12,13]. Moreover, certain genetic alterations cooperate functionally and prominent examples include the synergy of *BCL2* SV and *MYC* SV (also known as double hit lymphoma)[26,27,42].

Wet laboratory testing of all possible combinatorial effects of alterations is currently not feasible. To this end, we performed a systematic analysis of alteration effects by simulating the model, including all possible combinations of the 104 alterations. The simulation results show that 3,113 out of 5,356 pairs (58.1%) promote an aberrant state (Fig. 3B). From these 3,113 pairs, 27.7% are pairs in which both alterations already individually promote an aberrant state, while 71.6% contain one such alteration (Table 2). Interestingly, there are 22 pairs (0.7%) for which only their combined effect causes an aberrant state, but none of the individual perturbations. In contrast, from the 3,465 pairs containing at least one alteration causing an aberrant state, 11% show a WT-like state. Interestingly, this reveals the possibility of neutralizing and compensatory effects between alterations.

Identification of synergistic interaction effects

To compare the effect of individual and cosegregated alteration pairs, we defined a metric that captures the malignancy potential of alterations and computed it for all single

220 alterations and all pairs. This ‘malignancy score’ captures the shortest distance between
221 the alteration-promoted state and the reference state, which we define here as the WT
222 state (Fig. S2 and for details, see Methods, Defining a malignancy score to quantify effect
223 sizes of alterations). A positive score indicates changes towards aberrant states, while
224 negative scores cover physiological states. To assess whether the scores of alteration
225 pairs reflect purely additive effects of the corresponding individual alterations, we
226 computed an expected score for each alteration pair capturing the additive contribution
227 alone. This is compared to the calculated true malignancy score (Fig. 4A).

228 The comparison of the true and expected scores reveals that 64% of all alteration pairs
229 show a simple additive effect, *i.e.* the true value corresponds to the expected value.
230 However, there are pairs with strong deviations between both values. We were most
231 interested to identify those cases in which the combined effect causes an aberrant state
232 while a physiological state was expected from the individual effects alone (true score > 0,
233 expected score ≤ 0) or the aberrant state is more severe than expected (true score >
234 expected score), (light orange and light red regions, respectively, Fig. 4A). The
235 physiological-vs-aberrant region (light orange) contains the 22 pairs which only in
236 combination, but not individually, promote an aberrant state (Table 2). Most of these pairs
237 contain alterations affecting BCR signaling and mutations of *NFKBIE*. Interestingly, the
238 detected combination *CARD11* mutation & *NFKBIE* mutation is also found in two patients
239 (CARD11 & NFKBIE, Fig. 4A).

240 We detected 372 pairs that promote an aberrant state stronger than expected (Fig. 4A,
241 light red region). Notably, among the identified alteration pairs are the *BCL2* SV and *MYC*
242 SV, which are known for their synergistic effect[28]. Interestingly, we find similar

discrepancies between scores for combinations of *MYC* SV and mutations of either *FAS, KMT2D, TP53,* or *MYD88*. The mutations cause, such as the *BCL2* SV, a cooperative effect by delaying or abrogating apoptosis and thereby potentiating the pro-proliferative *MYC* SV effect (Table 3). These additional *MYC* SV pairs are also found in the patient cohort (Table 3), supporting their contribution to the aberrant state in the patient context.

Pairs with even stronger cooperative effects are combinations in which the level of active BLIMP1 is affected, for example, by a LOF *PRDM1* mutation (the locus encoding BLIMP1) or *BCL6* translocation, together with a LOF mutation of *NFKBIE*. Intriguingly, their combined effect causes a synergy with a strongly enhanced proliferation and prolonged cellular survival (Fig. 4B). A list of alterations affecting the level of active BLIMP1 and therefore forming a synergy with *NFKBIE* mutations is given in table S3.

We checked if such a combination of mutated *NFKBIE* and alterations affecting BLIMP1 is present in patient models and found ten patients in which *NFKBIE* is mutated. Six of them harbor an additional alteration such as *BCL6* SV, *CARD11* mutation or *EZH2* amplification that alone can cause a reduction in the level of BLIMP1 (Fig. S4B). In four patients, BCL6 SV is present, including one patient in which only three alterations are present in the corresponding individual model: *BCL6* SV, *NFKBIE* mutation, and *CCND3* CN gain. Five out of the six patient models show indeed strongly increased levels of nuclear cREL:P50 and RELA:P50 (Fig. S4B), a dynamic pattern that was also observed in the corresponding alteration pair simulations (Fig. 4B and S4A).

In the broader signaling pathway context, this synergy indicates that alterations promoting both, the inactivation of BLIMP1 and activation of NF-κB synergize. This finding is further corroborated experimentally by two studies in mice, already reporting a strong

cooperative effect between constitutive active NF-κB and dysfunctional BLIMP1 with respect to increased cell numbers and shortened lifetime of mice[43,44]. We therefore analyzed if other alterations than *NFKBIE* mutations show a cooperative effect with *BCL6* SV alterations or *PRDM1* mutations. Interestingly, we find, although with a less pronounced effect compared to *BCL6* SV & *NFKBIE* mutation, alterations of *TNFAIP3* and *MYD88* causing a synergistic effect with *BCL6* and *PRDM1* alterations (Table 4). Strikingly, among those alteration pairs, *TNFAIP3* CN loss in combination with *PRDM1* CN loss are found in 91 patients (Table 4).

This demonstrates, that our identified synergistic effects might also be relevant for the cellular aberrant state in patient models. The results give a mechanistic insight how mutant *NFKBIE*, which was reported as driver in DLBCL[11,13], cooperates with other alterations and allows to resolve how alterations in the NF-κB regulation cooperate with alterations affecting BLIMP1. Still, since we focused here on alteration pairs, the presence of additional alterations in the patient models opens the possibility of their interference with the synergistic effect, inducing variability in the models and affecting the aberrant state. This is exemplified by one patient model, that does not show strongly increased levels of cREL:P50 and RELA:P50 despite the *NFKBIE* mutation and the *BCL6* SV. This highlights the requirement for context-specific analyses of alteration effects.

Alterations causing the aberrant state are patient-specific

To comprehensively assess the impact of alterations in a patient-specific context, we used the personalized models, including all perturbations per patient and performed a drop out analysis in which we initially removed each alteration individually and then all possible

289 combinations of alteration pairs, triplets and quadruplets. This allowed the identification
290 of alteration drop outs restoring the physiological state (Methods, Defining a malignancy
291 score to quantify effect sizes of alterations). The identified alterations represent in each
292 patient model a specific minimal genetic signature that causes the aberrant state. This
293 way, we identified 54 patient models with single causative alterations (Fig. 5A). For other
294 patient models, two (57 patients), three (55 patients) or four alterations (36 patients) have
295 to be taken out simultaneously to reverse the aberrant state (Fig. 5A). Strikingly, for 55
296 patient models removing all possible combinations of four alterations was not sufficient to
297 reverse the aberrant state, revealing a very robust composition of alterations.

298 In the 202 patient models, where causative alterations were identified that way, we found
299 overall 32 out of the 47 implemented genes including the MYD88-CD79B supercomplex
300 to promote, upon alteration, an aberrant state (Fig. 5B). In our previous analysis,
301 alterations in 21 genes were sufficient to individually promote an aberrant state in the
302 reference model (Fig. 3A). Nineteen of those genes overlap with the 32 genes identified
303 here by the drop out analysis as causative. Intriguingly, alterations in the remaining 13
304 genes are causative in the patient models but do not induce an aberrant cell state when
305 introduced into the WT model. These results show that the patient-specific signature
306 strongly modulates the functional impact of genetic alterations.

307 Among the most frequent alterations that individually cause the aberrant state are
308 *TNFAIP3*, *EZH2*, *BCL6* as well as *MYC* (Fig. 5B), which are well-known cancer drivers in
309 DLBCL (Fig. S5). In some patient models, different individual drop outs have the potential
310 to restore the physiological state, for example patient index 20 (Fig. 5B). In other patient
311 models, those cancer drivers alone are not sufficient to restore a physiological state, but

require the drop out of additional alterations. This is evident from the fact that alterations of these genes are very frequently found in combinations with two or more alterations. Interestingly, there are alterations which only cause an aberrant state in combination with other alterations. For example, *MYD88* alterations are frequently found in combinations consisting of at least two alterations (Fig. 5B, *e.g.* patient index 64, 80 and 140), demonstrating that causative alteration combinations are variable in different patient models.

For the most frequent causative alterations comprising *TNFAIP3*, *EZH2* and *BCL6*, the analysis shows that they are also found in combination with each other in some of the patients (Fig. 5B, *e.g.* patient index 56 and 116). Of note, the pairs we identified in our previous analysis showing a synergistic effect between dysfunctional BLIMP1 and NF-κB regulation are found here responsible for the aberrant state of the patient models. Beside the drop outs of the pairs *BCL6* SV - *NFKBIE* mutation and *MYD88* - *PRDM1* mutation, that of *PRDM1* deletion - *TNFAIP3* deletion also restore the physiological state. The latter pair is also involved in causative drop outs of three and four alterations and occurs in 24 patient models. Additionally, in 6 patient models, the pair is present and due to the synergy, the drop out of either *TNFAIP3* deletion or *PRDM1* deletion is sufficient to restore the physiological state.

Finally, we summarized how often identified genetic alterations occur as causative alterations in the drop out analysis of 1 to 4 alterations (Fig. 5C, red bars). The most prominent genes, *TNFAIP3*, *EZH2* and *BCL6* show frequent alterations in the patient cohort (between 100 and 150 patients) and are frequently part of the causative alterations. Interestingly, alterations of *MYC* and *NFKBIA* are less frequent in the cohort,

but are often identified as causative alterations for the altered cell state. In contrast, while *BCL2* is the most frequently altered gene in this patient model cohort, we only find it in very few cases to be the causative alteration. Such a low frequency is also true for *TP53*, *FAS* and *NFKBIE*. These results show that alterations that occur with high frequency not necessarily drive the aberrant state in patient models, and low frequent gene alterations can be causative. Intriguingly, the overall alteration signature of a patient model creates the context, enabling alteration interaction effects and therefore dictates the role of individual alterations.

Discussion

In this mathematical modeling approach, we integrated the genetic alterations of DLBCL patients into mechanism-based network modeling to infer the impact and mutual effects of highly heterogeneous alterations in patient-specific contexts. The use of recent cohort data to establish 284 patient models enabled us to dissect the effects of these alterations in a personalized manner, identifying established genetic drivers and predicting so far unknown combinatorial effects with a strong cancer-promoting potential.

While the effects of genetic alterations have been modeled before[20,21], a detailed mechanistic analysis and understanding of combinatorial effects on the cell fate within individual patients is not covered. We addressed this here by a thorough analysis of individual and combinatorial alteration effects. Our study expands both the considered alteration types and the range of effect sizes exceeding previous approaches. We here

356 implemented CNAs, SVs, and mutations separated in LOF, modified activity and GOF
357 mutations. For *CCND3* and *TP53* mutations, we were able to integrate quantitative data
358 capturing the effect of the mutations on the degradation rate of *CCND3* and the
359 transcription rate of the p53 target gene *BAX* (Table S1 and Schmitz *et al.*[45], Kato et al.[46]).
360 With this approach, we substantially expanded the coverage of distinct alterations
361 captured in mathematical models. From the 127 high-confidence driver genes, defined by
362 Coyle *et al.*[47], 23 are included in our model. Drivers that are found by Coyle et al. in all
363 twelve considered studies are *CREBBP*, *MYD88*, *EZH2*, *CD79B,* and *TP53,* all of which
364 are not only included in our model but were also identified here as cancer-causing genes
365 (Fig. 5). By implementing more alterations, we were able to cover 284 patients of the 304
366 patients of a recent study[13], which corresponds to 93.4%. The 284 models cover all
367 DLB*class*-identified DLBCL subtypes[17].

368 Our analysis of alteration effects is based on a malignancy score derived from model
369 readouts for apoptosis and proliferation, which allows to distinguish between aberrant and
370 physiological cell states. This score reflects important experimental observations. Caeser
371 *et al.*[27] experimentally tested the effects of *MYC*, *CCND3*, *BCL6* and a non-functional
372 variant of *TP53* in addition to the effect of *BCL2* overexpression, demonstrating that none
373 of those alterations caused a strong increase in cell viability[27]. For *BCL2*, *CCND3* and
374 *TP53,* these results are fully in line with our model, which predicts a score of zero for
375 these cases. However, MYC overexpression in primary GC B-cells cause a reduced cell
376 viability, whereas our model predicts a positive score and increased proliferation but does
377 not capture the pro-apoptotic effect[27]. This is likely due to the multiple effects exerted by
378 MYC including the promotion of apoptosis, global protein synthesis causing proteotoxic

379 stress[48], and activation of p53 by triggering the DNA damage response[49] which are
380 currently not captured by our model. Future model extensions incorporating DNA damage
381 response[50] and more comprehensive p53 signaling[51,52] will not only allow for a refinement
382 of the impact of dysfunctional p53 on the DNA damage response and the aberrant cell
383 state, but also facilitate simulation of chemotherapeutic-based treatment responses.
384 Additionally, integrating the DNA damage-induced activation of the NF-κB pathway would
385 be important to capture the balance between pro- and anti-apoptotic signals upon DNA
386 damage[53,54].

387 To untangle the complexity of alteration combinations, we here performed simulations of
388 more than 500.000 alteration combinations. This analysis prioritizes and short lists now
389 putative oncogenic and synergistic combinations that should be explored functionally in
390 the wet laboratory. For instance, one prediction of a striking synergy is the *NFKBIE*
391 mutation in combination with a second alteration affecting BLIMP1 levels. Interestingly,
392 LOF mutations of *NFKBIE* are markers for Aggressive Chronic Lymphocytic Leukemia
393 and for poor prognosis in Primary Mediastinal B-cell Lymphoma[55,56]. Moreover, in six out
394 of the twelve studies analyzed by Coyle *et al.*, *NFKBIE* was identified as a cancer driver
395 and is defined as a tier 1 driver[47]. As detailed above, constitutive activation of NF-κB
396 synergizes in mouse models with the deletion of BLIMP1[43,44], and we find this alteration
397 pair also in our model simulations, suggesting that these alterations promote NF-κB
398 signaling and enhance the effect of dysfunctional BLIMP1 in a non-additive way. Such a
399 cooperative effect is also supported by *ex vivo* culture of human primary GC B-cells
400 overexpressing *BCL2* and *BCL6*, followed by a CRISPR knockout screen of almost 700
401 genes. Strikingly, *NFKBIE* has the twelfth highest CRISPR gene score[27]. As *BCL6*

overexpression downregulates BLIMP1 due to transcriptional repression[57], those results show the critical role of dysfunctional *NFKBIE* in this alteration context.

Our approach and findings distilled thereby have important clinical implications. While DLBCL-treating lymphoma specialists are well aware of the highly variable outcomes their patients achieve, and see this diversity linked to the underlying molecular heterogeneity of the disease, systematic interrogations of the functional cooperativity between key genetic aberrations and their impact on individual patients' long-term responses are largely missing., Mathematical network modeling allows to link basal cellular growth properties and major recurrent driver mutations and thereby enabled us to derive here various cell states that reflect specific functional properties and dependencies. We identified those dependencies in a personalized manner and mechanistically resolved their functional effects. While our framework recapitulates the well-established synergistic effect of the BCL2-MYC double hit lymphomas, the approach also predicts multiple additional candidates of synergistic hit combinations observed in patients of the cohort. These insights will facilitate the prioritization of genetic alterations that might synergize functionally for wet laboratory validation and eventually enhance the molecular understanding of genetically defined patient subtypes.

Overall our results highlight the critical impact of integrating patient-specific alteration data and mechanism-derived network models capturing nonlinear effects for the prediction of functional alteration effects, demonstrating the necessity of personalized computational modeling for the reliable prediction of targeted therapeutic strategies in DLBCL.

Methods

1. Construction of the reference model

Based on the goal to implement many genetic alterations and comprehensively test their individual and combinatorial effects, efficient model simulations are required. In order to reduce the computational costs, we transformed the population model of Roy *et al.*[29] into a single reference model that allows to simulate the processes of a representative WT B-cell. We first simulated a population of 500 cells without additional sampling of parameters for daughter cells and then selected a representative cell based on the following criteria: the cell i) differentiates into a plasma cell, ii) differentiates at a later timepoint than 24 hours and iii) undergoes apoptosis in a time frame of 2 to 6 days.

To further increase the efficiency of model simulations, we replaced the delay differential equations (DDEs) describing the delayed transcription of *REL*, *NFKBIE* and *NFKB1* (P50) by ordinary differential equations (ODEs). To preserve the dynamics, we applied the linear chain trick[58] by adding a chain of intermediate components and reactions representing the process of transcription. To estimate the parameter values of these reactions, we trained the ODE model on simulated time course data (0 to 240 minutes) of *REL*, *NFKBIE* and *NFKB1* from the DDE model. For simulations and optimization, the tools AMICI[59] and PESTO[60] for MATLAB (R2023b, The Mathworks Inc., Natick, MA) and pyPESTO[61] for Python (version 3.12, Python Software Foundation, https://www.python.org/) were used. As the chain length can be variable, we trained the model on different chain lengths (1, 2, 3, 5). Using the corrected Akaike Information Criterion[62,63], we identified an optimal length of one and replaced the DDEs by one intermediate step (Text S1, eq. 1.16 and eq. 1.141, eq. 1.7 and eq. 1.139, eq. 1.13 and eq. 1.40). Additionally, we adapted the originally

447 discontinuous piecewise differential equation describing the transcription of *BCL2* by
448 removing the conditional rule for a threshold for the RELA:P50 and cREL:p50-promoted
449 *BCL2* transcription (eq. 1.114 and 2.4). This was necessary to enable a continuous effect
450 of our implemented genetic alterations on *BCL2* expression and it allows for more stable
451 simulations.

452 In the original model (Roy *et al.*[29]) two inputs initiate signal transduction. Both inputs are
453 not implemented as ODEs but as hard-coded time course data. To include genetic
454 alterations that affect upstream processes of the inputs as well as alterations directly
455 affecting the regulation of the input components, we replaced the two inputs by ODEs.
456 For the pIKK regulation, we included the negative regulator of NF-κB activity TNFAIP3
457 (A20) based on the model of Mothes *et al.*[64] (Text S1, eq. 1.142, eq. 143, eq. 144).
458 Importantly, by including *TNFAIP3*, we capture a frequently altered gene in DLBCL
459 patients (Fig. S1, 43% of patient samples contain a *TNFAIP3* alteration). For the second
460 input, we implement ODEs for the transcription factor AKT which is regulated by PTEN
461 (Text S1, eq. 1.145, eq. 1.146, eq. 1.147). The transcription of *PTEN* is regulated by
462 multiple transcription factors among which NF-κB RELA:P50 is a suppressor[65]. Thus, we
463 included an inhibitory term into the regulation of PTEN expression (Text S1, eq. 1.146).
464 To reproduce the input dynamics, we trained the model based on the hard-coded time
465 course data of the two inputs and additionally included simulated time course data of
466 RELA:P50, BLIMP1 and cleaved PARP1 for model training. Note, that we only fitted the
467 newly implemented parameters and fixed almost all remaining parameters to their
468 nominal value. One exception is the parameter k2_13, which was changed from
469 $0.0102s^{-1}$ to $0.0162s^{-1}$ to enhance the E2F-mediated expression of *CCNE*. Simulations

showed that this modification allows to reproduce the stronger impact of the *MYC* and *BCL2* double hit scenario. With the abovementioned steps, we constructed a reference model that allows for efficient and comprehensive simulations of the WT state. For the manuscript publication, the model will be made accessible at Biomodels (biomodels.org).

2. Model visualization

To visualize the model in an automated manner, we created the reference model as described in the previous section. We then created a YAML file that was converted into an SBML file using the python package yaml2sbml[66]. To create a model scheme, we used Cytoscape (version 3.10.1, https://cytoscape.org/) in combination with the plugin cy3sbml (version 0.3.0, König *et al.*[67]). Since the ODE-based input did not result in a clear model overview, we converted the ODE system into rate equations using the atomize function of the python package PyBioNetGen (version 0.7.4, https://pypi.org/project/bionetgen/). With the final conversion of the rate equation based Bionetgen model format into SBML using the pysb python package (version v1.13.2, Lopez *et al.*[68]), the model can be visualized using the Prefuse Force Directed Layout algorithm. The algorithm produces a force-directed graph with clearly distinguishable modules of the model structure (Fig. 1B). The modules represent regulatory networks of apoptosis, B-cell differentiation, cell cycle and NF-κB signaling.

3. Implementation of genetic alterations

We implemented three different alteration types into the model: copy number alterations, structural variants and mutations (Table 1). We first identified all genes and proteins in the model that are affected by genetic alterations in the cohort of 304 DLBCL patients (Chapuy *et al.*[13]). To map genetic alterations to genes and proteins, we converted the corresponding labels of model variables into HUGO Gene Nomenclature Committee (HGNC) symbols (https://www.genenames.org/) using HGNChelper (Oh *et al.*[69], version 0.8.1). We extended the resulting list of genetic alterations by additional frequent genetic alterations that affect implemented processes without the direct inclusion of the altered gene or protein in the model. Those “indirect” alterations include for example upstream processes of IKK and AKT activation. To include those alterations, we map them to the affected processes in the model. Moreover, some components of the model represent complexes where not all individual proteins are modelled. Additionally, model components not necessarily represent only a specific isoform or homologue. Thus, we also mapped isoforms and homologues to the corresponding model component. The list of all implemented alterations including the specification about direct and indirect implementations is given in table S4.

To implement the effect of the collected genetic alterations into the model, we assessed the functional consequence of a given alteration and defined a perturbation value. Details are shown below.

Functional effects of alterations

Copy Number Alterations

We implemented the copy number alterations (loss or gain) by modulating the parameter representing the synthesis of a given gene or gene product.

Structural Variants

Structural variants are implemented by assuming that the chromosomal translocation of a given gene changes the regulation of its transcription. Particularly, we introduce a new parameter that represents an ectopic expression rate and that has an increased value compared to the nominal transcription rate constant. Additionally, the regulatory processes including co-activators and co-repressors are no longer affecting transcription of the given gene and are therefore set to zero. Due to their relevance and available biological characterization, we focus on structural variants of the genes *MYC*, *BCL2* and *BCL6*[16]. In the lymphoma context, these genes can be translocated into the immunoglobulin loci[26]. Consequently, their expression becomes dysregulated as the endogenous regulation is lost but strongly promoted by enhancers of immunoglobulin expression. The concomitant overexpression of BCL2 counteracts apoptosis or in case of MYC promotes proliferation[26]. Dysregulation of BCL6 expression by mimicking a translocation was shown to cause DLBCL in mice[70].

Mutations

Based on the variant classifications of mutations specified in the MAF-file of the analyzed DLBCL cohort[13], we defined four mutation categories: loss-of-function (LOF), modified activity (MA), mutations missing additional information (info n/a) and gain-of-function

(GOF). To the first category we assign non-sense, splice site, frame shift indels, non-stop, de novo start in frame mutations which lead to a non-functional protein. For the second category, we assume that missense or in frame indel mutations lead to i) a reduced activity of the protein, such as reduced binding affinity towards its binding partners or ii) an increased activity. To determine if a mutation causes a reduced or increased activity or results in a GOF, we searched in literature for effects of mutations of the given genes and checked the frequency of the given alterations in DLBCL using cBioportal[30–32] (using the datasets of Chapuy *et al.*[13], Lohr *et al.*[8], Reddy *et al.*[11] and Morin *et al.*[9]) as well as the annotation of oncoKB[33,34] for the functional effect and if its oncogenic in DLBCL or not (Table S1). If there was no information for its oncogenic effect in DLBCL, neither for LOF nor MA mutations, and there was no information in literature for given mutations causing oncogenic effects, we neglected the alteration. Based on these criteria, we did not implement an effect for the following alterations:

CCNA1 (MA & LOF), CCNA2 (MA), CCNB3 (MA & LOF), CCNE1 (MA), CD79A (MA), CDC20 (MA), CDK1 (MA), E2F1 (MA), FADD (MA), FZR1 (MA), MCL1 (MA), NFKB1 (LOF), PIK3CA (CN gain), PPP4C (MA), REL (MA), XIAP (MA)

Silent mutations are not considered to have an effect and were therefore not included. For the mutations with missing information about the variant classification, the mutation effect is defined similar to the effect in the category modified activity (MA) if not stated otherwise (Table S4).

Defining perturbation strengths

Copy Number Alterations

The parameter value is multiplied with a perturbation strength of 1.5 for amplifications and 0.67 for deletions to resemble the addition or loss of one copy. To test the impact of stronger or weaker effects of copy number alterations, we perturbed the corresponding parameters (Fig. S6, S7).

Structural Variants

The perturbation strength for structural variants is chosen in a way that this strength is small while an effect is still present. We tested different parameter values and quantified the corresponding impact on the malignancy score (Fig. S8A, S8D, S8G), timepoint of apoptosis (Fig. S8B, S8E, S8H) and number of divisions (Fig. S8C, S8F, S8I). We selected the lowest tested value that still shows the expected effect.

Mutations

To implement the effect of LOF, MA and GOF mutations, we select the processes that are affected by a given alteration and change the corresponding model parameters by a factor that is specific for the different mutation types. The link between alterations, parameters and perturbation values are given in table S4. As a gene in a patient sample can have multiple point mutations, we take the amount of point mutations into account by assigning to each point mutation the specified factor and multiplying the factors.

For LOF mutations, we assume the corresponding protein to be non-functional and therefore set the affected rate constants to a value close to zero (1e-10). Exceptions are truncating mutations of *BCL10* which have been observed to result in increased activity (for details and experimental references see Table S1) and are therefore assigned to the increased activity factor of 3.2 (log10 value of 0.5). MA mutations causing an increased protein activity are also associated with this factor. In contrast, MA mutations causing a decreased protein activity are multiplied with a factor of 1e-2. Note that for MA mutations the specified factor is multiplied to the corresponding model parameter in contrast to the LOF mutations for which the corresponding parameter value is set to an absolute value of 1e-10. For GOF mutations, we introduce processes into the model that have a rate of zero if the mutation is absent and change it to a value of 100 a.u./min (MYD88 gain-of-function) or 1 a.u./min (My-T-BCR supercomplex), if the mutation is present (Table S1).

We chose the abovementioned perturbation strengths for mutations in a way that they are in a physiological range, biologically meaningful and show, if applicable, an impact on the malignancy score. We therefore tested the impact of different perturbation strengths on the malignancy score, apoptosis timepoint and proliferation (Fig. S9, S10, S11, S12).

For missense mutations of *TP53*, we use experiment-derived information from the study of Kato *et al.*, in which a yeast-based assay of 2314 *TP53* point mutations was performed to assess p53 functionality (Kato *et al.*[46], The *TP53* Database (R21, Jan 2025): https://tp53.cancer.gov, deAndrade *et al.*[71]). The quantified readout of expression level changes of p53 target genes can be used to simulate the effects of *TP53* mutations[72]. If multiple point mutations of *TP53* are present within one patient sample, we average the value of the given point mutations. Moreover, if the information about the point mutation

599 in the patient sample causes a LOF, we set the expression rate constant for BAX
600 expression to 1e-10.

601

602 Handling the effect sizes of multiple alterations of the same gene

603 Within a patient sample, the same gene can be affected by multiple alterations. We model
604 different alteration types in an accumulative manner. For LOF mutations, we set the
605 affected processes to a value close to zero instead of multiplying a factor to the rate
606 constants to prevent compensating effects between copy number gains and LOF
607 mutations.

608 4. Creating and simulating patient models

609 After associating genetic alterations to model parameters and defining perturbation
610 strengths, patient models can be created by defining patient-specific parameter sets.
611 Each patient model is thereby based on the reference model (Methods, section 1) and
612 only those parameters are perturbed that are affected by the patient-specific set of genetic
613 alterations. From the 292 patients with significant alterations (Chapuy *et al.*[13]), we were
614 able to create 284 patient models. For 8 individuals there were no alterations that could
615 be mapped to our model. We ran the simulations using MATLAB (R2023b, The
616 Mathworks Inc., Natick, MA) and Python (version 3.12, Python Software Foundation,
617 https://www.python.org/) in combination with AMICI[59]. For all our analyses, we define the
618 simulation end point at 10 days. The timepoint of apoptosis is defined as cPARP reaching
619 a level of 2500 a.u.[29] While the reference model shows apoptosis induction upon 6.4 days,
620 perturbations can lead to shorter or longer survival times. Note that in the latter case, the

simulation end point can be reached and the apoptosis timepoint is then given as endpoint of simulations. To assess the impact of the simulation end point on our score, we simulated the 284 patient models for 30 days (Fig. S3). Most of the models that showed no apoptosis induction before 10 days also did not show apoptosis until the end point of 30 days. Only a small number of patient models undergo apoptosis between 10 and 30 days. This shows that 10 day-simulation robustly capture apoptosis decisions. To quantify the number of divisions, we track CDH1 crossing a threshold value of 0.02 a.u. as it was defined in the original model of Roy *et. al* [29].

5. Defining a malignancy score to quantify effect sizes of alterations

We here use the timepoint of apoptosis and the division rate as readout. We separate the space of apoptosis timepoint and division rate into a physiological and aberrant state based on the state of the reference model. We assume that increased cell numbers compared to the reference model correspond to an aberrant state and less or equal numbers are physiological. The separator of these two cell states is therefore the calculated reference division rates for each timepoint of apoptosis with the separator function

$$f(x) = \frac{5}{x}\frac{divisions}{days}$$

Using the separator function, one can relate an alteration-mediated change to the reference-like state by computing the shortest Euclidean distance, the perpendicular, between the changed cell state and the separator function (Fig. S2). This way, the score represents the distance between the changed cell state and the reference-like state. We define a negative sign for the score, if the division rate at the given timepoint of apoptosis

643 is smaller than the reference value. Consequently, a positive score represents a change
644 causing an aberrant cell state and a negative or zero score is associated with a
645 physiological state.
646
647 For the analyses of causative alterations (Fig. 5), we check if a drop out causes a state
648 that is equal or below the separator function of the reference WT model. If this is the case
649 and the patient model is in the aberrant cell state, the tested alteration is defined as
650 causative.
651

652 ## 6. Computing expected effects for alteration pairs

653 To determine the expected state, we performed a vector addition of the two individual
654 alteration-induced changes in the state. From this expected state we then calculated the
655 score as described in Methods. This expected score is then compared to the simulated
656 true score which is the result of simulating the two alterations simultaneously. The
657 deviations between expected and simulated true effect of alteration pairs are shown in
658 Fig. 4A.

659 Note that the vector addition can result in some cases to infeasible states. In these cases,
660 the states are corrected by setting the value to zero for negative values, or to the
661 simulation end point for values exceeding the end point.

662 **Definition of additive, synergistic and dominating effects**

663 For the definition of additive effects, we compare for each alteration pair its true and
664 expected score. We consider effects as purely additive if the absolute difference between

665 true and expected effect is smaller than or equal to 0.01. Changes higher than 0.01 show
666 unexpected effects that can be synergistic, compensating or dominating. We define
667 synergistic effects as the combined effect of an alteration pair that show a greater effect
668 in combination than the expected sum of the individual effects. Unexpected effects are
669 also observed for alterations affecting similar regulations or parts of the model network.
670 In these cases, one alteration can show a dominant effect compared to the second
671 alteration resulting in a deviation between the expected and true score.

References

1. Sehn, L. H. & Salles, G. Diffuse Large B-Cell Lymphoma. *N. Engl. J. Med.* **384**, 842–858 (2021).
2. Coiffier, B. *et al.* Long-term outcome of patients in the LNH-98.5 trial, the first randomized study comparing rituximab-CHOP to standard CHOP chemotherapy in DLBCL patients: a study by the Groupe d'Etudes des Lymphomes de l'Adulte. *Blood* **116**, 2040–2045 (2010).
3. Staudt, L. M. & Dave, S. The Biology of Human Lymphoid Malignancies Revealed by Gene Expression Profiling. in *Advances in Immunology* vol. 87 163–208 (Academic Press, 2005).
4. Ren, W. *et al.* Genetic and transcriptomic analyses of diffuse large B-cell lymphoma patients with poor outcomes within two years of diagnosis. *Leukemia* **38**, 610–620 (2024).
5. Walker, J. S. *et al.* Integrated genomics with refined cell-of-origin subtyping distinguishes subtype-specific mechanisms of treatment resistance and relapse in diffuse large B-cell lymphoma. *Blood Cancer J.* **15**, 120 (2025).
6. Alizadeh, A. A. *et al.* Distinct types of diffuse large B-cell lymphoma identified by gene expression profiling. *Nature* **403**, 503–511 (2000).
7. Monti, S. *et al.* Integrative Analysis Reveals an Outcome-Associated and Targetable Pattern of p53 and Cell Cycle Deregulation in Diffuse Large B Cell Lymphoma. *Cancer Cell* **22**, 359–372 (2012).
8. Lohr, J. G. *et al.* Discovery and prioritization of somatic mutations in diffuse large B-cell lymphoma (DLBCL) by whole-exome sequencing. *Proc. Natl. Acad. Sci.* **109**, 3879–3884 (2012).
9. Morin, R. D. *et al.* Mutational and structural analysis of diffuse large B-cell lymphoma using whole-genome sequencing. *Blood* **122**, 1256–1265 (2013).

10. Pasqualucci, L. *et al.* Inactivating mutations of acetyltransferase genes in B-cell lymphoma. *Nature* **471**, 189–196 (2011).
11. Reddy, A. *et al.* Genetic and Functional Drivers of Diffuse Large B Cell Lymphoma. *Cell* **171**, 481-494.e15 (2017).
12. Schmitz, R. *et al.* Genetics and Pathogenesis of Diffuse Large B-Cell Lymphoma. *N. Engl. J. Med.* **378**, 1396–1407 (2018).
13. Chapuy, B. *et al.* Molecular subtypes of diffuse large B cell lymphoma are associated with distinct pathogenic mechanisms and outcomes. *Nat. Med.* **24**, 679–690 (2018).
14. Karube, K. *et al.* Integrating genomic alterations in diffuse large B-cell lymphoma identifies new relevant pathways and potential therapeutic targets. *Leukemia* **32**, 675–684 (2018).
15. Liu, F. *et al.* Unraveling the enigma of B cells in diffuse large B-cell lymphoma: unveiling cancer stem cell-like B cell subpopulation at single-cell resolution. *Front. Immunol.* **14**, 1310292 (2023).
16. Basso, K. & Dalla-Favera, R. Germinal centres and B cell lymphomagenesis. *Nat. Rev. Immunol.* **15**, 172–184 (2015).
17. Chapuy, B. *et al.* DLBclass: a probabilistic molecular classifier to guide clinical investigation and practice in diffuse large B-cell lymphoma. *Blood* **145**, 2041–2055 (2025).
18. Wright, G. W. *et al.* A Probabilistic Classification Tool for Genetic Subtypes of Diffuse Large B Cell Lymphoma with Therapeutic Implications. *Cancer Cell* **37**, 551-568.e14 (2020).
19. Du, W. *et al.* Effective combination therapies for B-cell lymphoma predicted by a virtual disease model. *Cancer Res.* **77**, 1818–1830 (2017).

20. Thobe, K., Konrath, F., Chapuy, B. & Wolf, J. Patient-Specific Modeling of Diffuse Large B-Cell Lymphoma. *Biomedicines* **9**, 1–22 (2021).

21. Norris, R. *et al.* Patient-specific computational models predict prognosis in B cell lymphoma by quantifying pro-proliferative and anti-apoptotic signatures from genetic sequencing data. *Blood Cancer J.* **14**, 1–11 (2024).

22. Pomeroy, A. E. & Palmer, A. C. A Model of Intratumor and Interpatient Heterogeneity Explains Clinical Trials of Curative Combination Therapy for Lymphoma. *Blood Cancer Discov.* **6**, 254–269 (2025).

23. Goldstein, J. S., Phillips, N. A. & Alizadeh, A. A. Beyond Trial and Error: A Mathematical Model Wrangles DLBCL Heterogeneity Toward Optimizing Combination Therapy. *Blood Cancer Discov.* **6**, 153–156 (2025).

24. Jayawant, E. S. *et al.* Computational modelling of aggressive B-cell lymphoma. *Biochem. Soc. Trans.* BST20253039 (2025) doi:10.1042/BST20253039.

25. Hanahan, D. & Weinberg, R. A. Hallmarks of cancer: the next generation. *Cell* **144**, 646–74 (2011).

26. Willis, T. G. & Dyer, M. J. S. The role of immunoglobulin translocations in the pathogenesis of B-cell malignancies. *Blood* **96**, 808–822 (2000).

27. Caeser, R. *et al.* Genetic modification of primary human B cells to model high-grade lymphoma. *Nat. Commun.* **10**, 4543 (2019).

28. Strasser, A., Harris, A. W., Bath, M. L. & Cory, S. Novel primitive lymphoid tumours induced in transgenic mice by cooperation between myc and bcl-2. *Nature* **348**, 331–333 (1990).

29. Roy, K. *et al.* A Regulatory Circuit Controlling the Dynamics of NFκB cRel Transitions B Cells from Proliferation to Plasma Cell Differentiation. *Immunity* **50**, 616-628.e6 (2019).
30. Cerami, E. *et al.* The cBio Cancer Genomics Portal: An Open Platform for Exploring Multidimensional Cancer Genomics Data. *Cancer Discov.* **2**, 401–404 (2012).
31. Gao, J. *et al.* Integrative Analysis of Complex Cancer Genomics and Clinical Profiles Using the cBioPortal. *Sci. Signal.* **6**, pl1–pl1 (2013).
32. de Bruijn, I. *et al.* Analysis and Visualization of Longitudinal Genomic and Clinical Data from the AACR Project GENIE Biopharma Collaborative in cBioPortal. *Cancer Res.* **83**, 3861–3867 (2023).
33. Chakravarty, D. *et al.* OncoKB: A Precision Oncology Knowledge Base. *JCO Precis. Oncol.* 1–16 (2017) doi:10.1200/po.17.00011.
34. Suehnholz, S. P. *et al.* Quantifying the Expanding Landscape of Clinical Actionability for Patients with Cancer. *Cancer Discov.* **14**, 49–65 (2024).
35. Phelan, J. D. *et al.* A multiprotein supercomplex controlling oncogenic signalling in lymphoma. *Nature* **560**, 387–391 (2018).
36. Schmitz, R. *et al.* TNFAIP3 (A20) is a tumor suppressor gene in Hodgkin lymphoma and primary mediastinal B cell lymphoma. *J. Exp. Med.* **206**, 981–989 (2009).
37. Compagno, M. *et al.* Mutations of multiple genes cause deregulation of NF-κB in diffuse large B-cell lymphoma. *Nature* **459**, 717–721 (2009).
38. Escudero-Ibarz, L., Wang, M. & Du, M.-Q. Significant functional difference between TNFAIP3 truncation and missense mutants. *Haematologica* **101**, e382–e384 (2016).

39. Zheng, H. *et al.* Whole-exome sequencing identifies multiple loss-of-function mutations of NF-κB pathway regulators in nasopharyngeal carcinoma. *Proc. Natl. Acad. Sci.* **113**, 11283–11288 (2016).
40. Cabannes, E., Khan, G., Aillet, F., Jarrett, R. F. & Hay, R. T. Mutations in the IkBa gene in Hodgkin's disease suggest a tumour suppressor role for IkappaBalpha. *Oncogene* **18**, 3063–3070 (1999).
41. Roy, P., Sarkar, U. A. & Basak, S. The NF-κB Activating Pathways in Multiple Myeloma. *Biomedicines* **6**, 59 (2018).
42. Sesques, P. & Johnson, N. A. Approach to the diagnosis and treatment of high-grade B-cell lymphomas with MYC and BCL2 and/or BCL6 rearrangements. *Blood* **129**, 280–288 (2017).
43. Mandelbaum, J. *et al.* BLIMP1 Is a Tumor Suppressor Gene Frequently Disrupted in Activated B Cell-like Diffuse Large B Cell Lymphoma. *Cancer Cell* **18**, 568–579 (2010).
44. Calado, D. P. *et al.* Constitutive Canonical NF-κB Activation Cooperates with Disruption of BLIMP1 in the Pathogenesis of Activated B Cell-like Diffuse Large Cell Lymphoma. *Cancer Cell* **18**, 580–589 (2010).
45. Schmitz, R. *et al.* Burkitt lymphoma pathogenesis and therapeutic targets from structural and functional genomics. *Nature* **490**, 116–120 (2012).
46. Kato, S. *et al.* Understanding the function-structure and function-mutation relationships of p53 tumor suppressor protein by high-resolution missense mutation analysis. *Proc. Natl. Acad. Sci. U. S. A.* **100**, 8424–8429 (2003).
47. Coyle, K. M., Dreval, K., Hodson, D. J. & Morin, R. D. Audit of B-cell cancer genes. *Blood Adv.* **9**, 2019–2031 (2025).

48. Gong, C. *et al.* Sequential inverse dysregulation of the RNA helicases DDX3X and DDX3Y facilitates MYC-driven lymphomagenesis. *Mol. Cell* **81**, 4059-4075.e11 (2021).
49. Das, S. K. *et al.* Excessive MYC-topoisome activity triggers acute DNA damage, MYC degradation, and replacement by a p53-topoisome. *Mol. Cell* **84**, 4059-4078.e10 (2024).
50. Jackson, S. P. & Bartek, J. The DNA-damage response in human biology and disease. *Nature* **461**, 1071–8 (2009).
51. Batchelor, E., Loewer, A., Mock, C. & Lahav, G. Stimulus-dependent dynamics of p53 in single cells. *Mol. Syst. Biol.* **7**, 488 (2011).
52. Konrath, F., Mittermeier, A., Cristiano, E., Wolf, J. & Loewer, A. A systematic approach to decipher crosstalk in the p53 signaling pathway using single cell dynamics. *PLoS Comput. Biol.* **16**, e1007901 (2020).
53. McCool, K. W. & Miyamoto, S. DNA damage-dependent NF-κB activation: NEMO turns nuclear signaling inside out. *Immunol. Rev.* **246**, 311–26 (2012).
54. Konrath, F., Willenbrock, M., Busse, D., Scheidereit, C. & Wolf, J. A computational model of the DNA damage-induced IKK/ NF-κB pathway reveals a critical dependence on irradiation dose and PARP-1. *iScience* **26**, 107917 (2023).
55. Mansouri, L. *et al.* Functional loss of IκBε leads to NF-κB deregulation in aggressive chronic lymphocytic leukemia. *J. Exp. Med.* **212**, 833–843 (2015).
56. Mansouri, L. *et al.* Frequent NFKBIE deletions are associated with poor outcome in primary mediastinal B-cell lymphoma. *Blood* **128**, 2666–2670 (2016).
57. Tunyaplin, C. *et al.* Direct Repression of *prdm1* by Bcl-6 Inhibits Plasmacytic Differentiation. *J. Immunol.* **173**, 1158–1165 (2004).

58. MacDonald, N. *Time Lags in Biological Models*. vol. 27 (Springer, Berlin, Heidelberg, 1978).
59. Fröhlich, F. *et al.* AMICI: high-performance sensitivity analysis for large ordinary differential equation models. *Bioinformatics* **37**, 3676–3677 (2021).
60. Stapor, P. *et al.* PESTO: Parameter EStimation TOolbox. *Bioinformatics* **34**, 705–707 (2018).
61. Schälte, Y. *et al.* pyPESTO: a modular and scalable tool for parameter estimation for dynamic models. *Bioinformatics* **39**, btad711 (2023).
62. Akaike, H. A new look at the statistical model identification. *IEEE Trans. Autom. Control* **19**, 716–723 (1974).
63. Hurvich, C. M. & Tsai, C. L. Regression and time series model selection in small samples. *Biometrika* https://doi.org/10.1093/biomet/76.2.297 (1989) doi:10.1093/biomet/76.2.297.
64. Mothes, J. *et al.* A Quantitative Modular Modeling Approach Reveals the Effects of Different A20 Feedback Implementations for the NF-kB Signaling Dynamics. *Front. Physiol.* **11**, 896 (2020).
65. Brito, M. B., Goulielmaki, E. & Papakonstanti, E. A. Focus on PTEN regulation. *Front. Oncol.* **5**, 1–15 (2015).
66. Vanhoefer, J., Matos, M. R. a, Pathirana, D., Schälte, Y. & Hasenauer, J. yaml2sbml: Human-readable and -writable specification of ODE models and their conversion to SBML. *J. Open Source Softw.* **6**, 3215 (2021).
67. König, M., Dräger, A. & Holzhütter, H.-G. CySBML: a Cytoscape plugin for SBML. *Bioinformatics* **28**, 2402–2403 (2012).
68. Lopez, C. F., Muhlich, J. L., Bachman, J. A. & Sorger, P. K. Programming biological models in Python using PySB. *Mol. Syst. Biol.* **9**, 646 (2013).

69. Oh, S. *et al.* HGNChelper: identification and correction of invalid gene symbols for human and mouse. Preprint at https://doi.org/10.12688/f1000research.28033.2 (2022).
70. Cattoretti, G. *et al.* Deregulated BCL6 expression recapitulates the pathogenesis of human diffuse large B cell lymphomas in mice. *Cancer Cell* **7**, 445–455 (2005).
71. de Andrade, K. C. *et al.* The TP53 Database: transition from the International Agency for Research on Cancer to the US National Cancer Institute. *Cell Death Differ.* **29**, 1071–1073 (2022).
72. Migueles, O. Analyzing disturbed signaling pathways in cancer employing bioinformatic and mathematical modeling approaches. (Humboldt University Berlin, 2022).
73. Gu, Z., Eils, R. & Schlesner, M. Complex heatmaps reveal patterns and correlations in multidimensional genomic data. *Bioinformatics* **32**, 2847–2849 (2016).
74. Gu, Z. Complex heatmap visualization. *iMeta* **1**, e43 (2022).

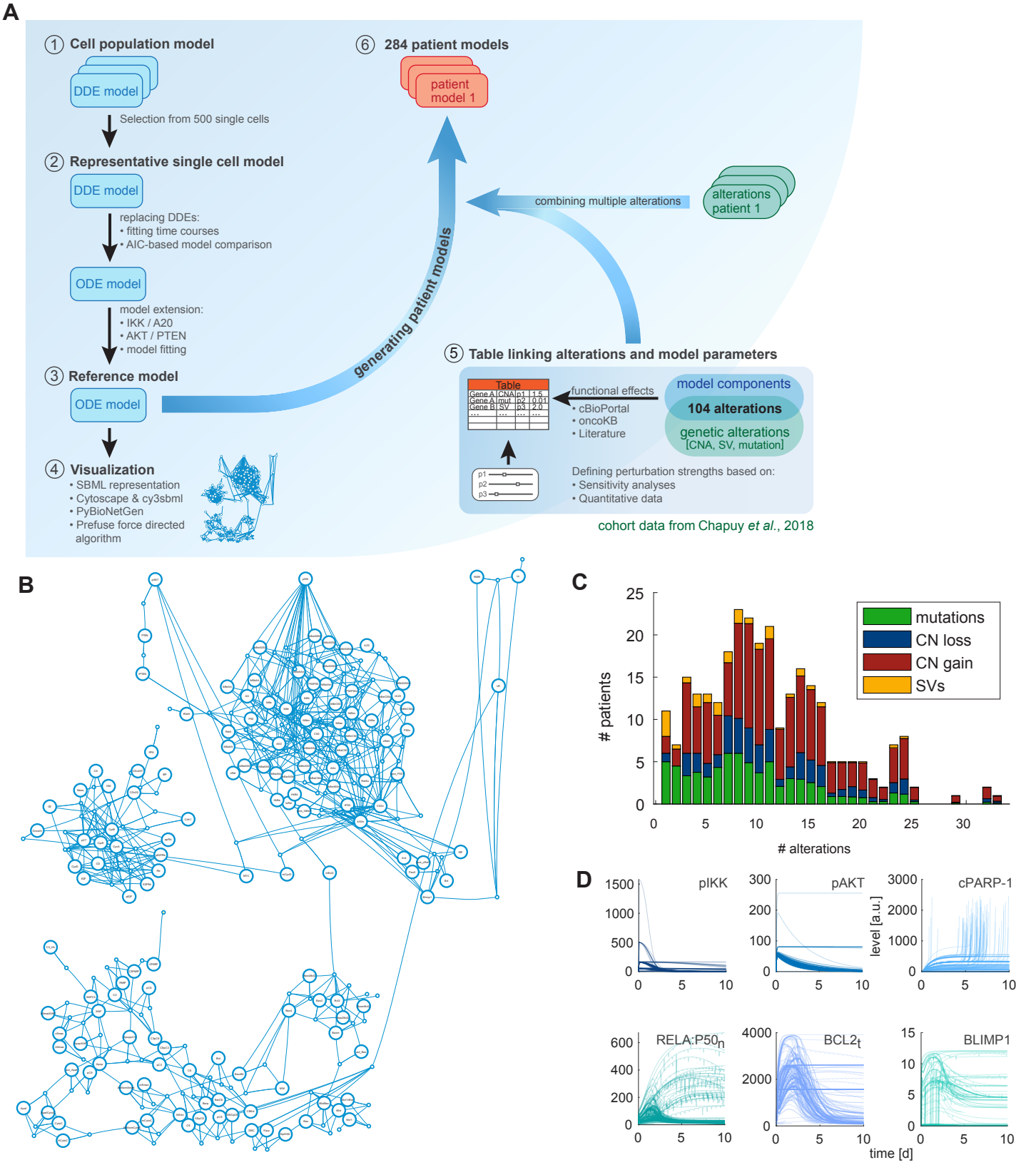

Figure 1. Generation of patient-specific DLBCL models.
(A) Workflow describing the development of patient-specific models based on the population model of Roy et al.[29]. We reduced the cell population model into a representative single cell model (1), transformed the delay differential equations into ordinary differential equations (2) and extended the initial model to capture TNFAIP3 (A20) and the PTEN-PI3K-AKT-mediated signaling (3). For the latter, we included the negative feedback regulation of NF-κB via A20, and PI3K signaling via AKT and its regulation by PTEN. After visualizing the reference model (4), we created a table linking all mapped alterations with model parameters and specific perturbation strengths (5). Incorporation of the patient-specific alterations led to 284 patient models (6). For details of all workflow steps, see Methods. **(B)** Scheme of the derived computational model. The network model consists of 158 variables, 544 parameters and describes regulatory interactions of NF-κB signaling, differentiation of naïve B-cells to antibody-producing cells, proliferation as well as apoptosis. **(C)** The number of alterations is given per DLBCL patient. Moreover, the distribution of implemented alteration types (mutations, copy number (CN) loss, CN gain and structural variants (SV)) is given for each amount of alterations. **(D)** Dynamics of six selected model components for all patient models. Cleaved Parp-1 (cPARP-1) is used as marker for the timepoint of apoptosis. pIKK: phosphorylated IKK, pAKT: phosphorylated AKT, RELA:P50n: nuclear complex of RELA and P50, BCL2t: BCL2 mRNA and BLIMP1: BLIMP1 protein, a marker for B-cell differentiation.

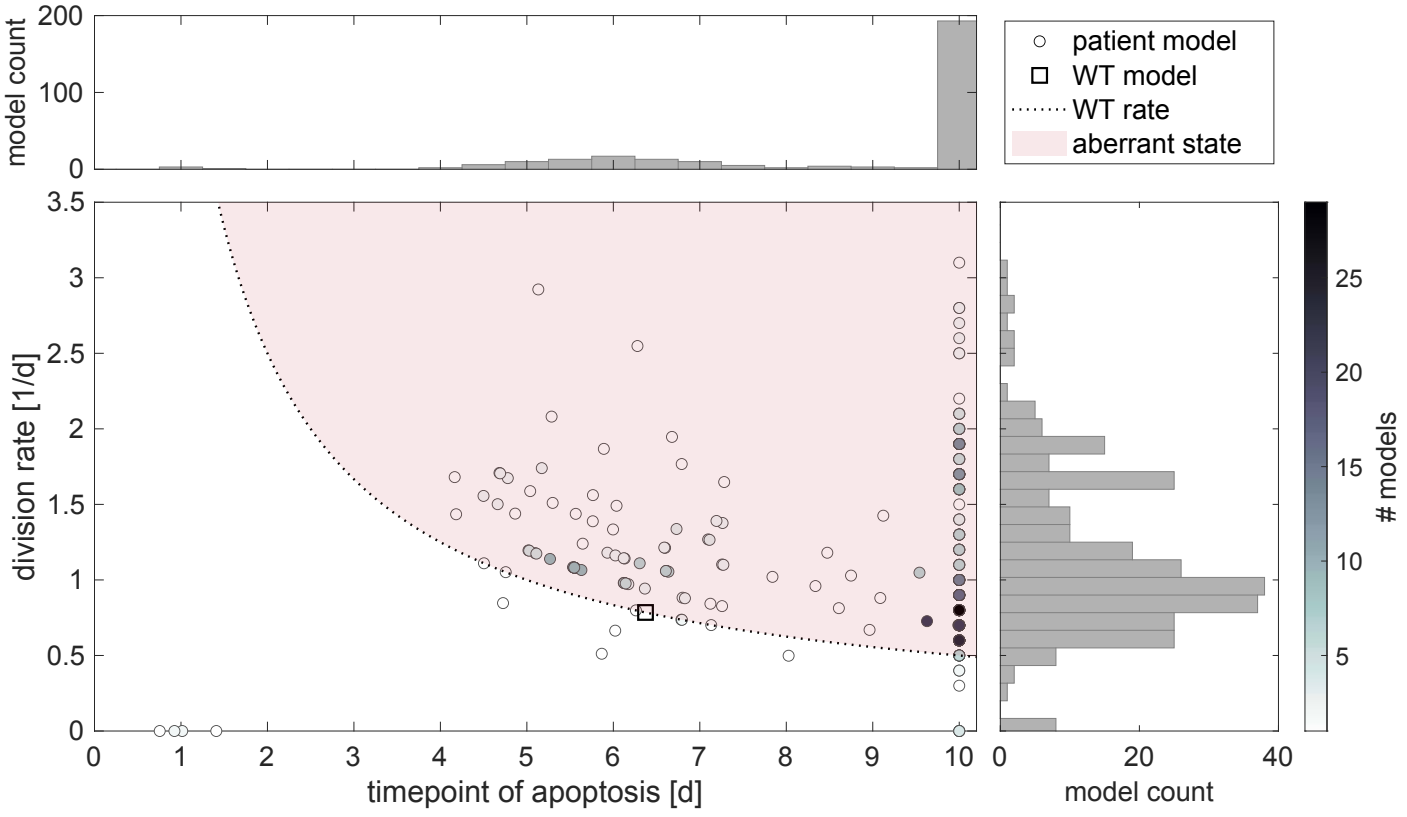

Figure 2. Cellular state of 284 patient models.
In the WT model (indicated by an empty square), the cell undergoes apoptosis upon around 6.4d and divides 5 times resulting in a division rate of around $0.8d^{-1}$. The dotted line marks the reference division rate at which cells are in a WT-like state according to the given timepoint of apoptosis. Empty circles show patient models; the color intensity represents the amount of models found in a given state. 90.5% of patient models are above the dotted line and thereby show, compared to the reference division rate, increased proliferation. These models therefore represent an aberrant state. The simulation end point is 10 days. Patient models in which apoptosis is induced later than 10 days or never, are therefore plotted at a timepoint of apoptosis of 10 days, longer simulation time does not change the results (Fig. S3). Histograms depict the model count for specific timepoints of apoptosis (top) or the number of divisions (right).

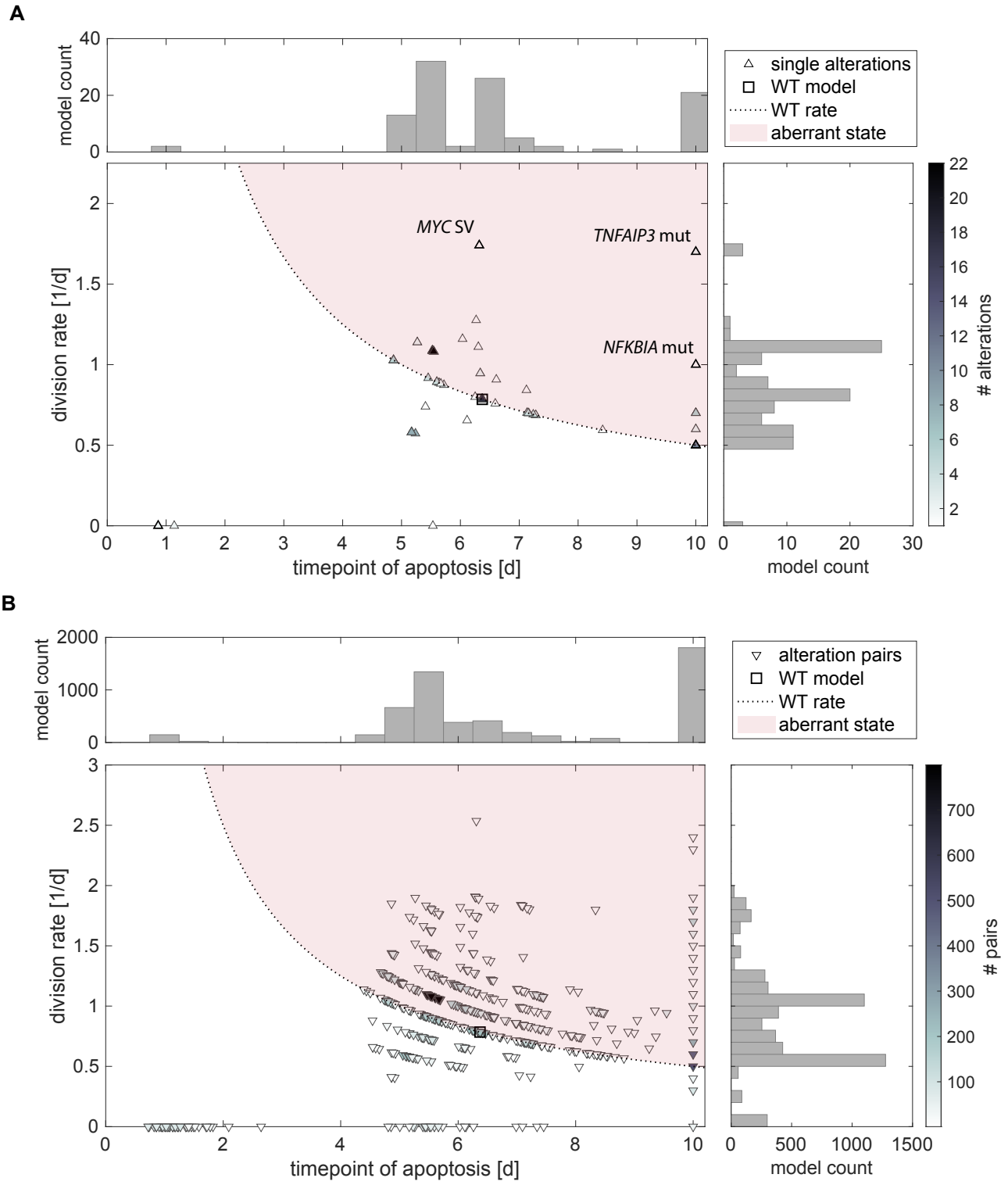

Figure 3. Effects of single and paired alterations in the WT model.
(A) Effect of single alterations on the cell state. 40.4% of single alterations promote an aberrant state. Example alterations labeled: *MYC* SV: structural variant of *MYC*, *TNFAIP3* mut: LOF mutation of *TNFAIP3*, *NFKBIA* mut: LOF mutation of *NFKBIA*. **(B)** Simulated effect of all possible combinations of two alterations. For 58.1% of all pairs, the combined effect results in an aberrant state.

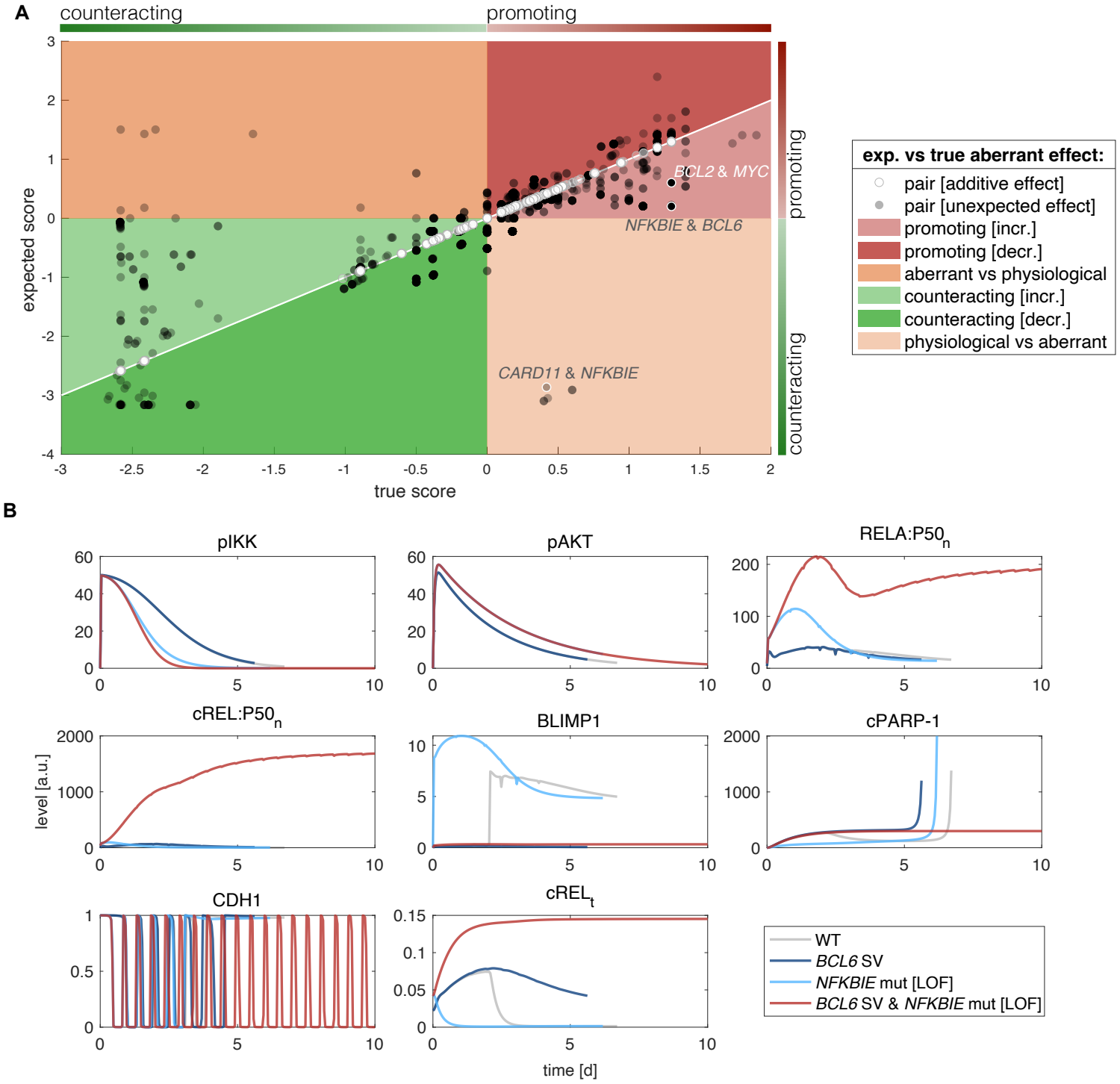

Figure 4. Identification of synergistic effects of alteration pairs.
(A) The expected score of all alteration pairs is plotted against the corresponding true calculated score. The bars on the top and on the right mark aberrant state promoting effects for positive scores (red) and counteracting effects for negative scores (green). The different colored regions allow to classify the combinatorial effects. The white line marks the effects where the true score corresponds to the expected score, that is, the alteration pairs have a purely additive effect. All alteration pairs with an absolute difference between true and expected score smaller or equal than 0.01 are defined as additive and are given by white dots. The grey and black dots represent all pairs with an unexpected effect. **(B)** Simulated time courses of selected model components mechanistically explain the identified synergistic effect between a *BCL6* SV and an *NFKBIE* LOF mutation. While both alterations individually reduce the survival time and number of divisions (dark and light blue lines), their combination (red line) causes a strong increase in the proliferation rate (CDH1) with abrogated apoptosis induction (cPARP-1). The *NFKBIE* mutation alone causes a dysfunctional inhibition of NF-κB family members and in turn a transient hyperactivation of the NF-κB system, i.e. a strongly increased activity of RELA:P50 and cREL:P50. In addition, PRDM1 transcription is induced by NF-κB signaling and its hyperactivation triggers a fast increase in the BLIMP1 (PRDM1) protein level, which, in turn, leads to a reduced transcription of cREL (Fig. 4B, cRELt). Together, this regulation prevents the transition to an aberrant state which is why IκBε alone is not sufficient to promote an aberrant state. However, the case of additional genetic alterations that diminish BLIMP1 activity, such as *BCL6* SV, allow elevated levels of cREL. This effect can be reproduced by simulating the *NFKBIE* mutation in combination with a reduced transcription rate of PRDM1 (Fig. S4A).

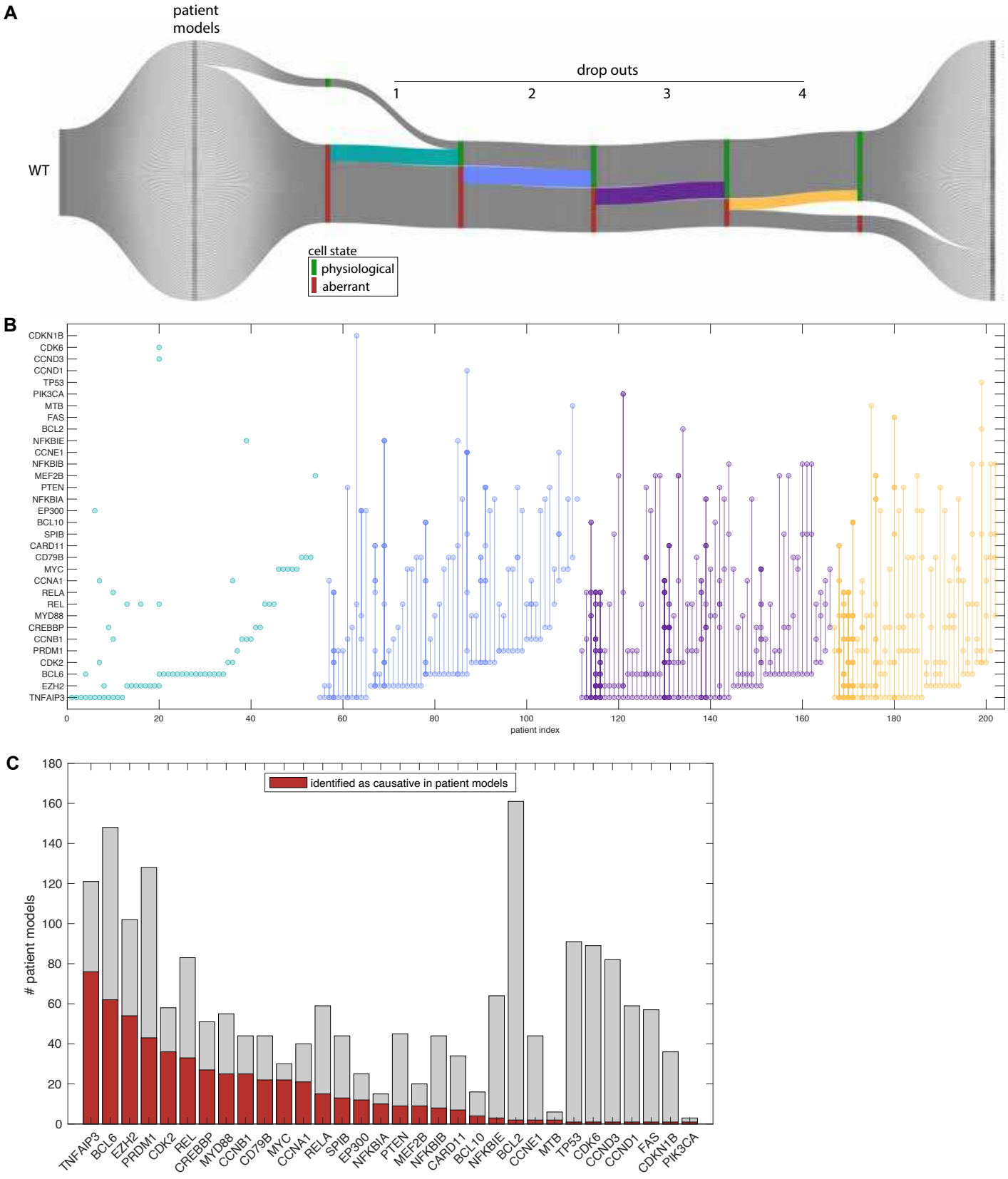

Figure 5. Identification of personalized aberration-causing alterations.
(A) Representation of all 284 patient models by individual lines. The cellular state of the models is physiological (green bars) for 27 (9.5%) models or aberrant (red bars) for 257 (90.5%). From left to right: successive removal of 1, 2, 3 or 4 alterations from models in aberrant states. For each removal all possible combinations are tested. Out of the 257 patient models with an aberrant state, 54 show a switch from the aberrant state to a physiological state after dropping out a single alteration (turquoise). Therefore, these alterations are identified as a single aberration-causing alteration. For the remaining patient models, the removal of more than one alteration is required for a switch to a benign state: For 57 patient models two alterations (light blue), for 55 models three alterations (purple), for 36 models four alterations (yellow). For 55 patient models, more than four alterations need to be removed in order to reach a benign state. The plot was created using plotly (version 5.3.1, https://plotly.com/graphing-libraries/). **(B)** Causative genes and their combinations for 202 patient models (given by patient index). Colors present the number of required causative genes, see Fig. 5A. Each circle represents a causative gene in a given patient model. Multiple causative genes within a patient model are connected through a line. Since there can be multiple combinations promoting a cancer state in the same patient model, circles and lines can overlap. **(C)** Number of patient models in which a causative genetic alteration is present (height of bars), and number of patients in which it is the aberration-causing gene (red part of the bars).

Table 1. Implemented genetic alterations. For each alteration, the number of patients harboring the specified genetic alteration are shown. CN: Copy number, SV: Structural variant, GOF: Gain-of-function mutation, MA: Modified activity (mutation causing increased or decreased activity), LOF: Loss-of-function mutation, mutation [info n/a]: mutation with missing information about the mutation type (assigned to LOF or MA).

Gene	CN gain	CN loss	SV	mutation [info n/a]	mutation [LOF]	mutation [MA]	mutation [GOF]
APAF1	58	0	0	0	0	0	0
BAX	44	0	0	0	0	0	0
BCL10	0	0	0	10	4	3	0
BCL2	116	0	61	23	0	56	0
BCL6	88	25	56	5	1	12	0
CARD11	0	0	0	16	1	22	0
CASP3	0	45	0	0	0	0	0
CCNA1	40	0	0	0	0	0	0
CCNB1	44	0	0	0	0	0	0
CCND1	59	0	0	0	0	0	0
CCND3	70	0	0	8	3	3	0
CCNE1	44	0	0	0	0	0	0
CD79B	0	0	0	24	5	15	0
CDK2	58	0	0	0	0	0	0
CDK4	58	0	0	0	0	0	0
CDK6	89	0	0	0	0	0	0
CDKN1B	0	35	0	0	1	0	0
CREBBP	0	0	0	23	17	28	0
CYCS	96	0	0	0	0	0	0
DIABLO	58	0	0	0	0	0	0
EP300	0	0	0	16	2	7	0
EZH2	89	0	0	13	0	10	0
FADD	59	0	0	0	0	0	0
FAS	0	36	0	15	9	3	0
FBXO11	0	0	0	0	2	2	0
IRF4	55	0	0	0	0	1	0
KMT2D	58	0	0	40	48	10	0
MALT1	116	0	0	0	0	0	0
MCL1	91	0	0	0	0	0	0
MEF2B	0	0	0	8	2	10	0
MTB	0	0	0	0	0	0	6
MYC	0	0	25	0	0	21	0
MYD88	0	0	0	33	0	22	0
NFKBIA	0	0	0	9	6	10	0
NFKBIB	44	0	0	0	0	0	0
NFKBIE	55	0	0	6	2	3	0
PARP1	63	25	0	0	0	1	0
PAX5	0	0	0	0	4	2	0
PIK3CA	0	0	0	0	1	2	0
PRDM1	0	120	0	11	8	4	0
PTEN	0	36	0	5	3	2	0
RB1	40	42	0	0	0	1	0
REL	83	0	0	0	0	0	0
RELA	59	0	0	0	0	0	0
SPIB	44	0	0	0	0	0	0
TNFAIP3	0	109	0	21	5	0	0
TP53	0	66	0	34	6	26	0

Table 2: Composition of aberrant states of pair alterations

number of individual alterations leading to an aberrant state	number of pairs in aberrant state [%]
both	861 [27.7%]
one	2230 [71.6%]
none of them	22 [0.7%]

Table 3. Pairs including *MYC* SV with a synergistic effect. For each alteration pair the malignancy score, expected score, FC (fold change: score divided by expected score) and number of patients harboring the alteration pair is given.

alteration 1	alteration 2	score	expected score	FC score	# patients
MYC SV	*BCL2* SV	1.3	0.6	2.16	9
	FAS mutation [info n/a]	1.3	0.6	2.16	2
	FAS mutation [MA]	1.3	0.6	2.16	0
	FAS mutation [LOF]	1.3	0.6	2.16	0
	KMT2D mutation [info n/a]	1.3	0.6	2.16	3
	KMT2D mutation [MA]	1.3	0.6	2.16	0
	KMT2D mutation [LOF]	1.3	0.6	2.16	3
	PARP1 mutation [MA]	1.3	0.6	2.16	0
	TP53 mutation [info n/a]	1.3	0.6	2.16	2
	TP53 mutation [MA]	1.3	0.6	2.16	2
	TP53 mutation [LOF]	1.3	0.6	2.16	0
	MYD88 mutation [info n/a]	1.4	0.7	1.99	4
	MYD88 mutation [MA]	1.4	0.7	1.99	0
	NFKBIA mutation [info n/a]	1.4	0.8	1.74	2
	NFKBIA mutation [MA]	1.4	0.8	1.74	1
	PTEN mutation [info n/a]	1.4	0.8	1.74	0
	PTEN mutation [MA]	1.4	0.8	1.74	0
	PTEN mutation [LOF]	1.4	0.8	1.74	0
	CASP3 CN loss	1.2	0.72	1.67	3
	CCNB1 CN gain	1.73	1.27	1.36	4
	BCL2 mutation [info n/a]	1.1	0.83	1.34	3
	BCL2 mutation [MA]	1.1	0.83	1.34	5
	BCL2 CN gain	1.13	0.84	1.34	7
	FAS CN loss	1.11	0.83	1.34	1
	MCL1 CN gain	1.12	0.84	1.34	6
	TP53 CN loss	1.12	0.84	1.34	4
Sum					24

Table 4. Pairs including *BCL6* SV or mutated *PRDM1* in combination with alterations affecting NF-κB activity. For each alteration pair the malignancy score, expected score, FC (fold change: score divided by expected score) and number of patients harboring the alteration pair is given.

alteration 1	alteration 2	score	expected score	FC score	# patients
BCL6 SV	*NFKBIE* mutation [info n/a]	1.1	0.2	5.37	4
MYD88 mutation [MA]	*PRDM1* mutation [LOF]	0.36	0.22	1.65	2
MYD88 mutation [info n/a]	*PRDM1* mutation [info n/a]	0.36	0.22	1.64	2
MYD88 mutation [info n/a]	*PRDM1* CN loss	0.35	0.22	1.62	19
MYD88 mutation [MA]	*PRDM1* CN loss	0.35	0.22	1.62	12
BCL6 SV	*MYD88* mutation [info n/a]	0.35	0.22	1.62	8
BCL6 SV	*MYD88* mutation [MA]	0.35	0.22	1.62	6
BCL6 SV	*TNFAIP3* CN loss	0.45	0.32	1.43	29
PRDM1 CN loss	*TNFAIP3* CN loss	0.45	0.32	1.43	91
PRDM1 mutation [LOF]	*TNFAIP3* CN loss	0.45	0.32	1.43	2
PRDM1 mutation [info n/a]	*TNFAIP3* CN loss	0.45	0.32	1.43	4
PRDM1 mutation [MA]	*TNFAIP3* CN loss	0.45	0.32	1.43	2
Sum					104

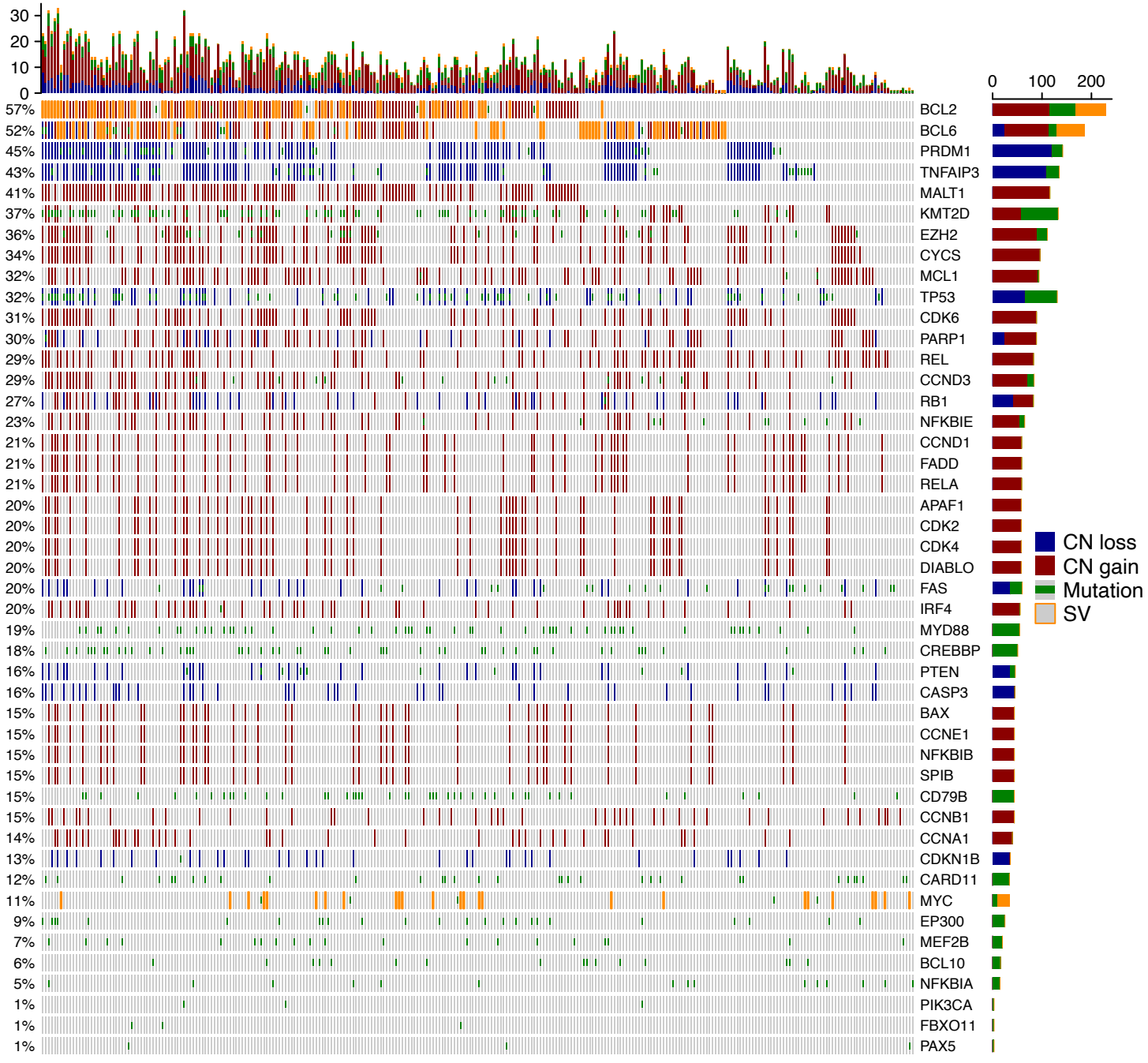

Figure S1. Oncoprint of the cohort data from Chapuy et al., 2018[13] for all genes that could be mapped to the model.

The shown alterations are the basis for creating the patient-specific DLBCL models. To create the oncoprint plot, the R (version 4.5.1, https://www.r-project.org) package ComplexHeatmap from the Bioconductor repository was used (version 2.24.0, Gu et al.[73,74]).

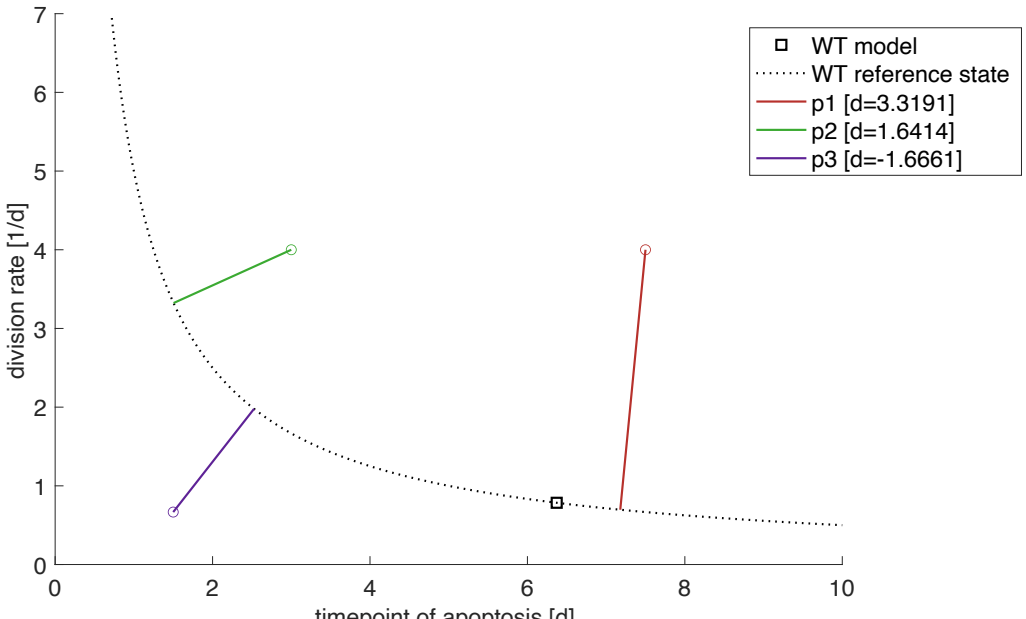

Figure S2. Illustration of malignancy score calculation.
Based on the WT model (empty square), we calculated a reference state (dotted line) representing for each timepoint of apoptosis the corresponding WT division rate. Examples p1 and p2 show alterations that cause increased proliferation rates and therefore result in an aberrant cell state. Example p3 shows a transition below the reference state and is therefore in a physiological cell state. The calculated score for each of the examples is given in brackets.

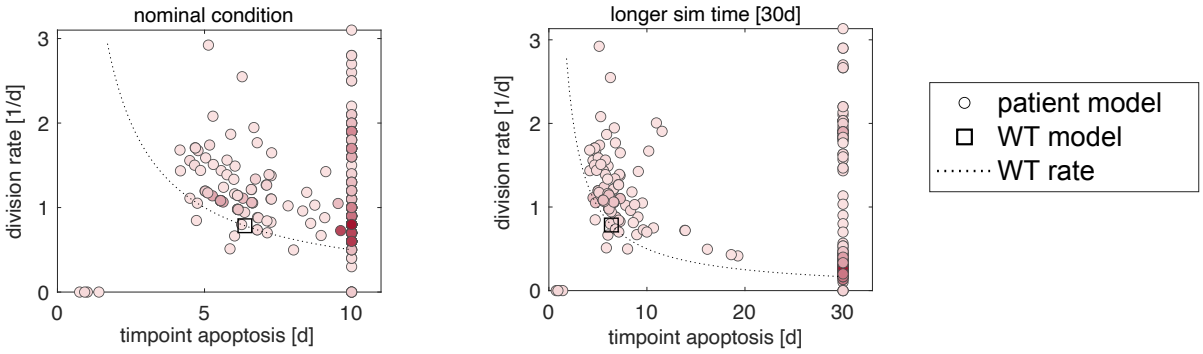

Figure S3. Predicted cell states for longer simulation time.
Shown are the cell states of the patient models with a simulation time of 10d (left, compare Fig 2) and a prolonged simulation time of 30d (right) The percentage of patient models with an aberrant state (90.5%) is not changed by the longer simulation time.

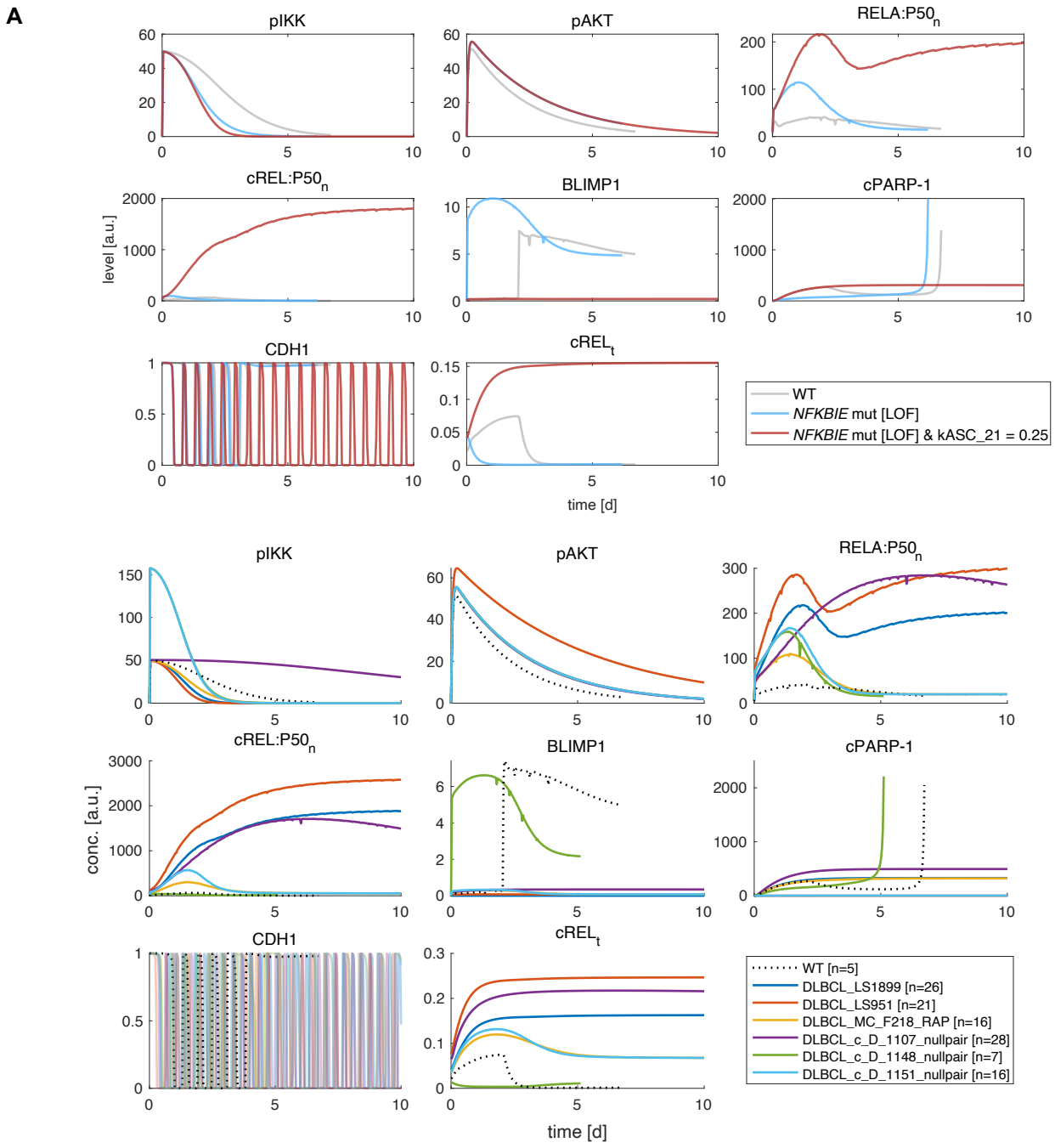

Figure S4. Simulation results capturing synergistic effects of NFKBIE mutations.
(A) Reducing the transcription rate of BLIMP1/PRDM1 to 0.25 demonstrates the effect of the NFKBIE synergy. **(B)** Simulation of patient models in which, NFKBIE is mutated and in addition one of the PRDM1 (BLIMP1)-enhancing alterations (Table S3) is present. The number in brackets gives the number of divisions that are observed for the given patient model.

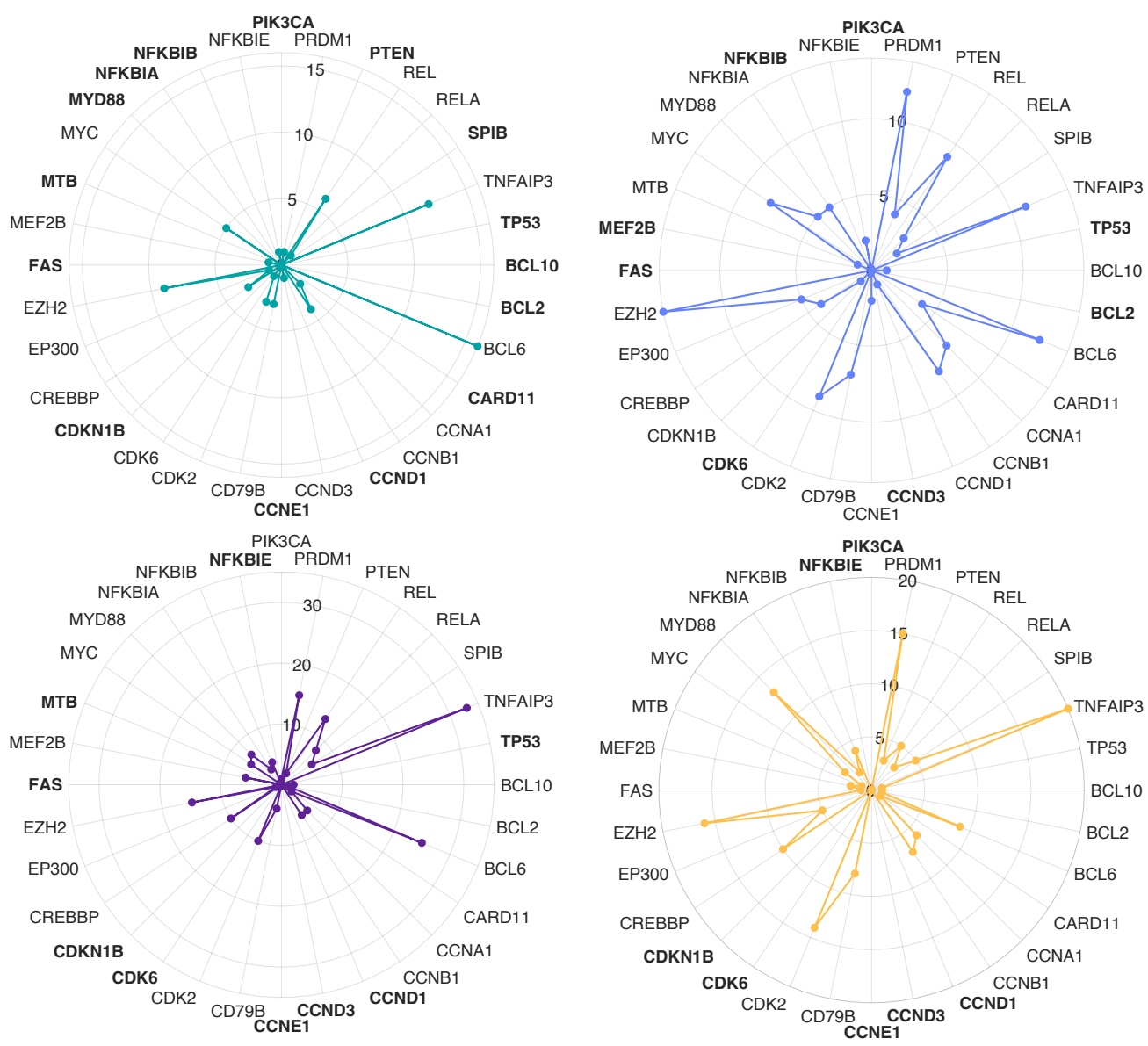

Figure S5. Frequency of causative genes in patient models based on drop out analyses.
For the 32 identified causative genes and the supercomplex MTB (labels given on outer circles), the number of patient models (radius) in which they are causative is shown. The four circles represent the different number of required causative genes in accordance to Fig. 5A (upper left: turquoise, one altered gene; upper right: light blue, two altered genes; lower left: purple, three altered genes; lower right: yellow, four altered genes).

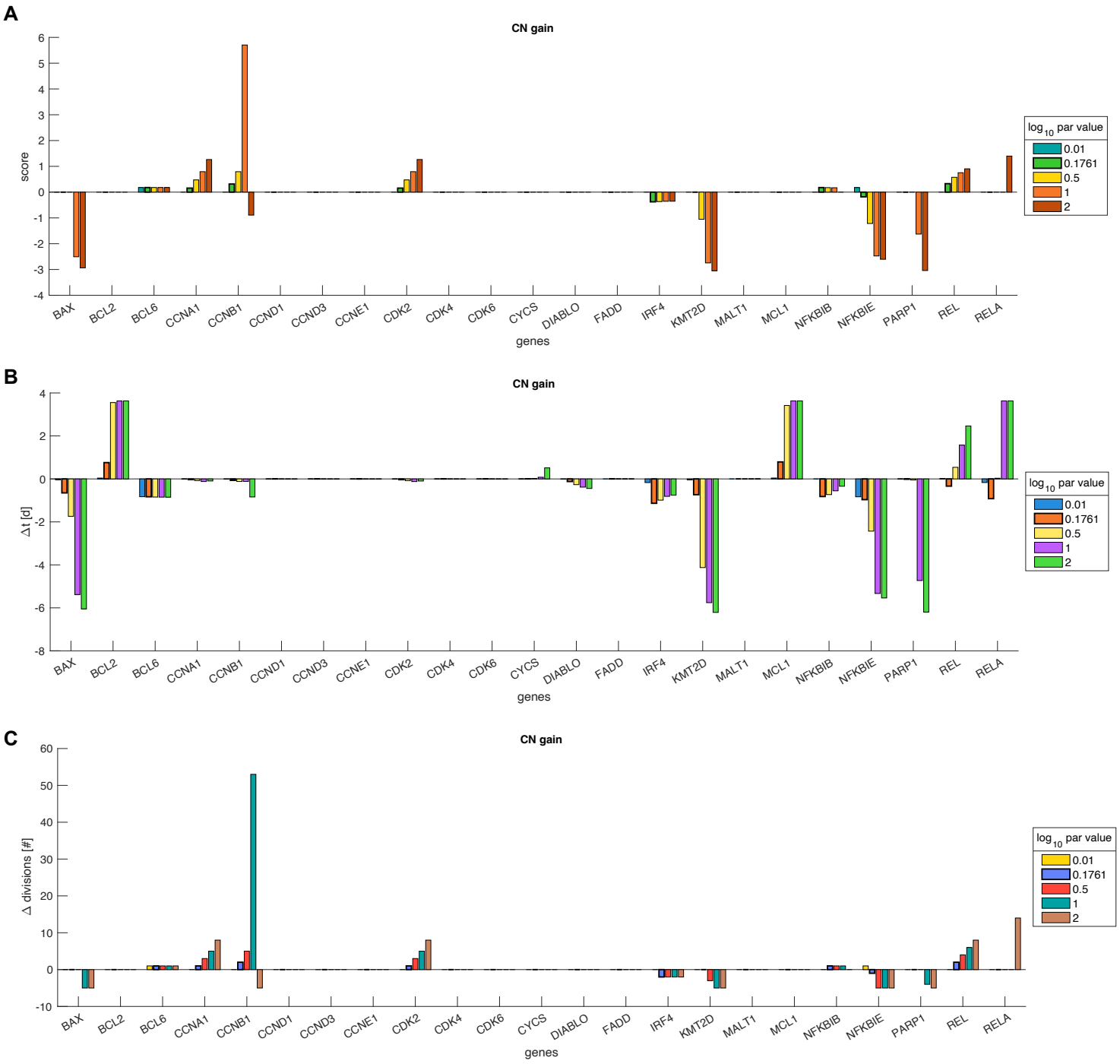

Figure S6. Perturbation strength analyses for CN gain alterations.
The effect of multiple perturbation strengths on the score **(A)**, difference in timepoint of apoptosis **(B)** and difference in division rate **(C)** was calculated. $\Delta t = t_{WT} - t$, where t is the timepoint of apoptosis for the given perturbation strength. $\Delta divisions = divisions_{WT} - divisions$, where divisions correspond to the number of divisions for the given alteration strength. For the copy number alterations affecting the score, the increasing perturbation strengths cause stronger effects on the score. The amplifications of the genes BAX and PARP-1 only show an effect on the score if the expression would be strongly increased (log_{10} factor >= 1).

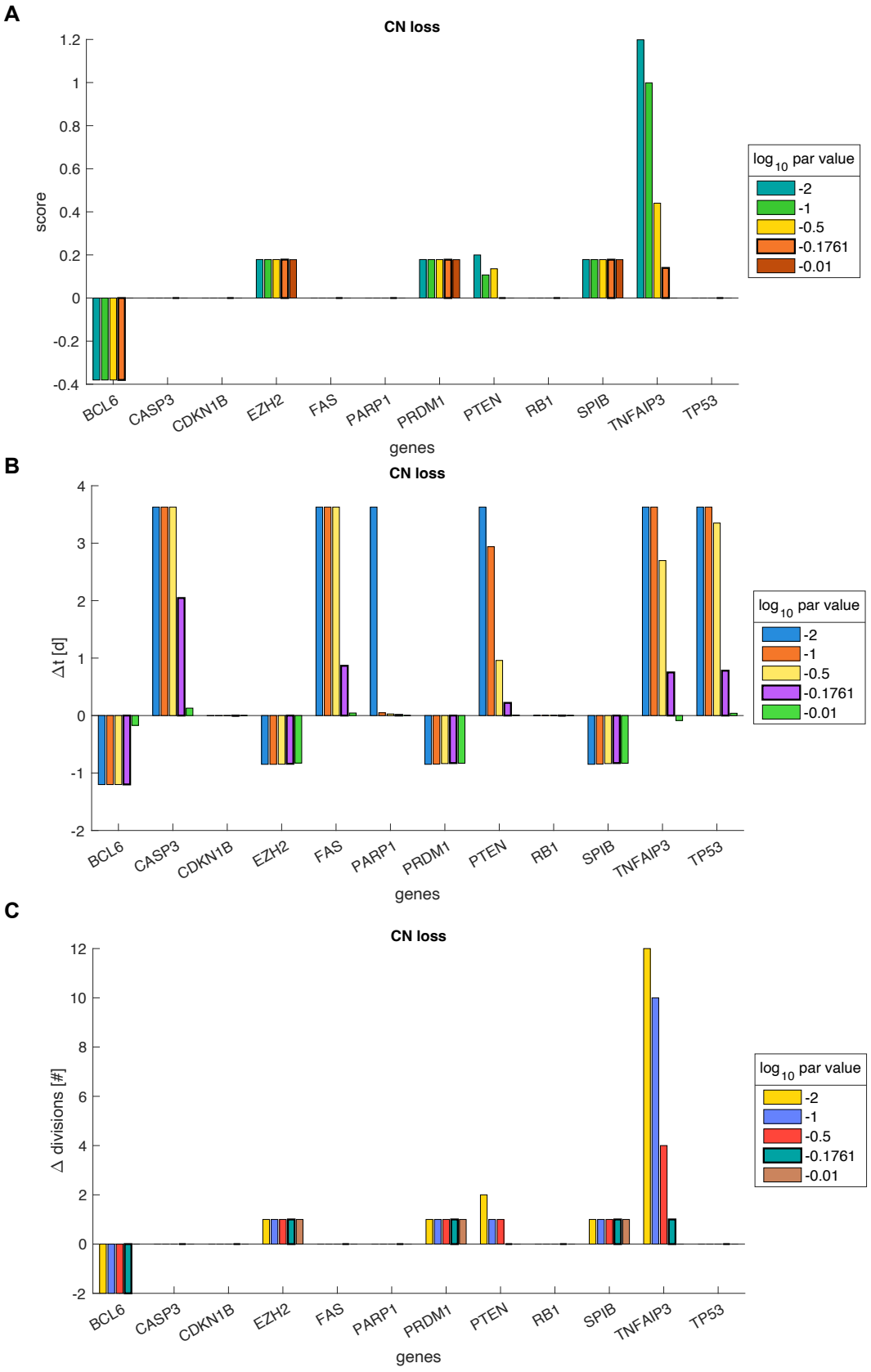

Figure S7. Perturbation strength analyses for CN loss alterations.
The effect of multiple perturbation strengths on the score **(A)**, difference in timepoint of apoptosis **(B)** and difference in division rate **(C)** was calculated. $\Delta t = t_{WT} - t$, where t is the timepoint of apoptosis for the given perturbation strength. $\Delta divisions = divisions_{WT} - divisions$, where divisions correspond to the number of divisions for the given alteration strength.

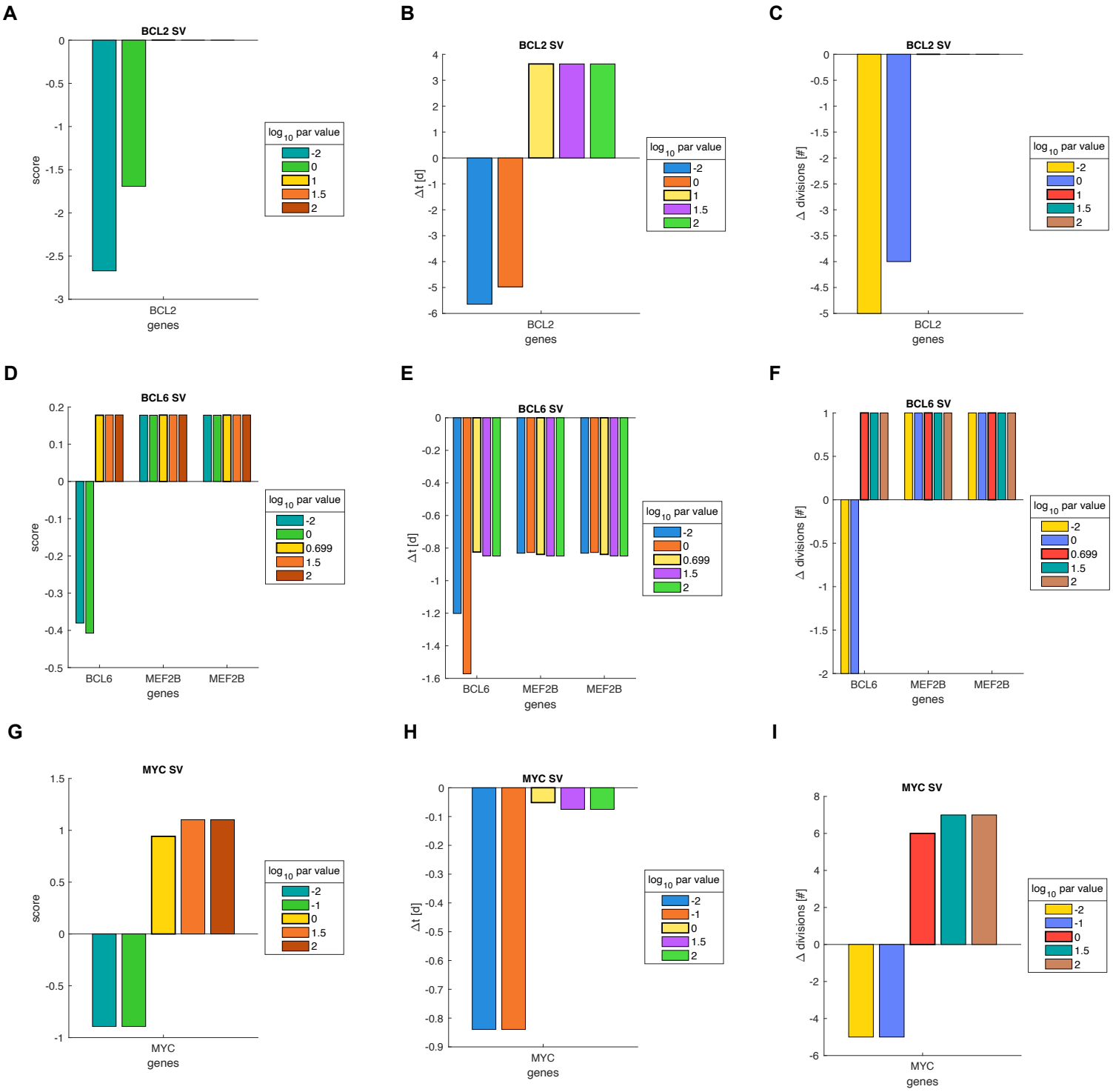

Figure S8. Perturbation strength analyses for SV alterations.
The effect of multiple perturbation strengths on the score **(A, D, G)**, difference in timepoint of apoptosis **(B, E, H)** and difference in division rate **(C, F, I)** was calculated. $\Delta t = t_{WT} - t$, where t is the timepoint of apoptosis for the given perturbation strength. $\Delta divisions = divisions_{WT} - divisions$, where divisions correspond to the number of divisions for the given alteration strength. For *BCL2* SV, we expect an increase in the timepoint of apoptosis. For $\log_{10}$ values of 0 and -2, the score, the timepoint of apoptosis and the number of divisions is reduced compared to the WT **(A-C)** and therefore unexpected. The reason for the unexpected effect is the implemented abrogation of its endogenous positive and negative regulation. In the scenario of a translocation, the gene expression is only dependent on the ectopic expression rate. By reducing the ectopic expression rate below a certain value (here $\log_{10}$ value of 0 or -2), the resulting expression rate of BCL2 is below the expression rate of the WT. Consequently, the anti-apoptotic effect of BCL2 is reduced and apoptosis is induced earlier **(B)** which coincides with less divisions **(C)**. We therefore chose for the ectopic basal expression rate constant a value of 10 a.u./min ($\log_{10}$ value of 1). For *BCL6* SV and *MYC* SV, an increase in the number of divisions is expected. We therefore chose a value of 5 a.u./min ($\log_{10}$ value of 0.7) and 1 a.u./min ($\log_{10}$ value of 0), respectively. The impact of the perturbation strengths on the number of divisions for *BCL6* SV and *MYC* SV is shown in **F** and **I**.

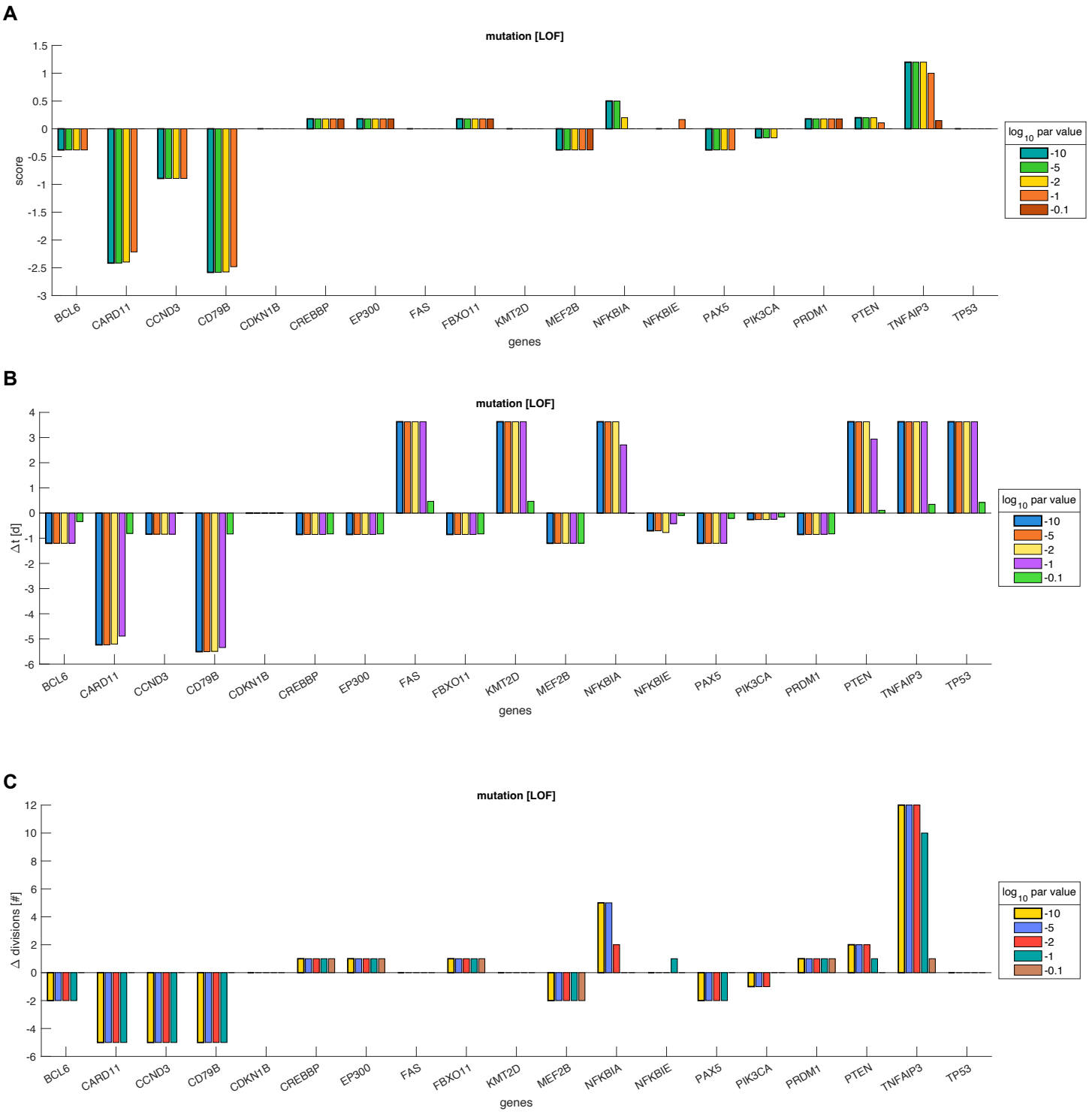

Figure S9. Perturbation strength analyses for LOF mutations.
The effect of multiple perturbation strengths on the score **(A)**, difference in timepoint of apoptosis **(B)** and difference in division rate **(C)** was calculated. $\Delta t = t_{WT} - t$, where t is the timepoint of apoptosis for the given perturbation strength. $\Delta divisions = divisions_{WT} - divisions$, where divisions correspond to the number of divisions for the given alteration strength. For LOF mutations, a value of 1e-10 is chosen.

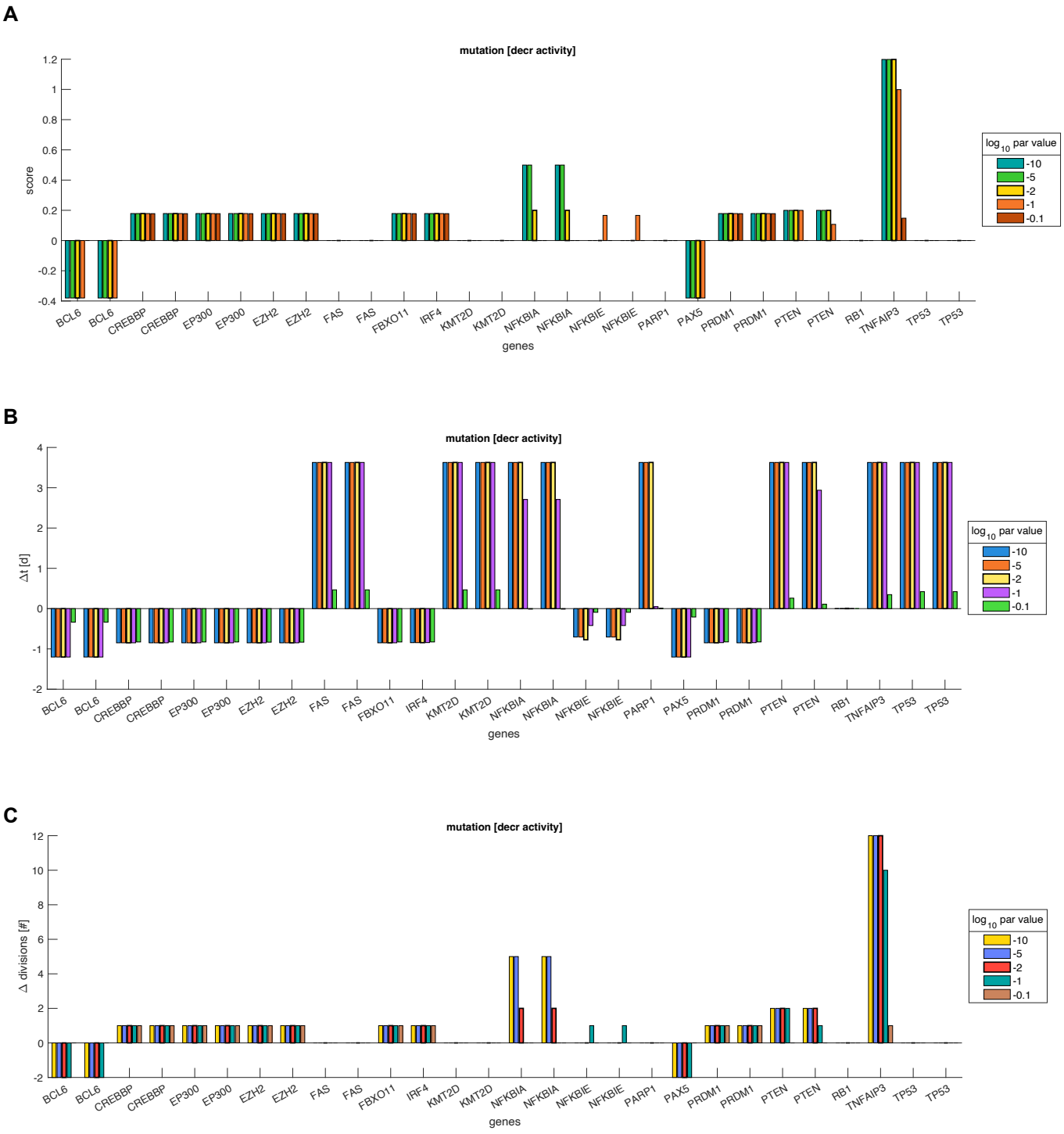

Figure S10. Perturbation strength analyses for decreased activity mutations.
The effect of multiple perturbation strengths on the score **(A)**, difference in timepoint of apoptosis **(B)** and difference in division rate **(C)** was calculated. $\Delta t = t_{WT} - t$, where t is the timepoint of apoptosis for the given perturbation strength. Δ divisions = divisions_{WT} – divisions, where divisions correspond to the number of divisions for the given alteration strength. For the MA mutations causing a reduced protein activity, we chose a value of 1e-2 as all MA mutations, except *NFKBIE* mutations, show an effect on the score **(A)**. *NFKBIE* mutations show a negative effect on the apoptosis time **(B)** but only an effect on the score and number of divisions for a $\log_{10}$ value of -1 **(A, C)**. For lower and higher values, *NFKBIE* mutations show no impact. This is due to the fact that if the activity of NF-κB is too strongly increased by a strong reduction (e.g. factor of 1e-5) of the functionality of the IκBε protein (*NFKBIE* gene product), the negative feedback mechanism via IκBα reduces NF-κB activity after an activation overshoot resulting in a shorter lifetime **(B)** but unchanged number of divisions and therefore an unchanged score **(A, C)**. If the reduction is too small (e.g. $\log_{10}$ value of -0.1) the effect on NF-κB activity is too small to result in any changes on the number of divisions and the score. As the *NFKBIE* mutation effect is specific for a single factor and leads to value-specific results while the effect of *NFKBIA* mutations is dose dependent and valid for a broader range of values, we decided for a factor of 1e-2. Nevertheless, the effect of the MA mutations causing a reduced activity and affecting the score is robust over a wide range of values except for *NFKBIA* and *NFKBIE*.

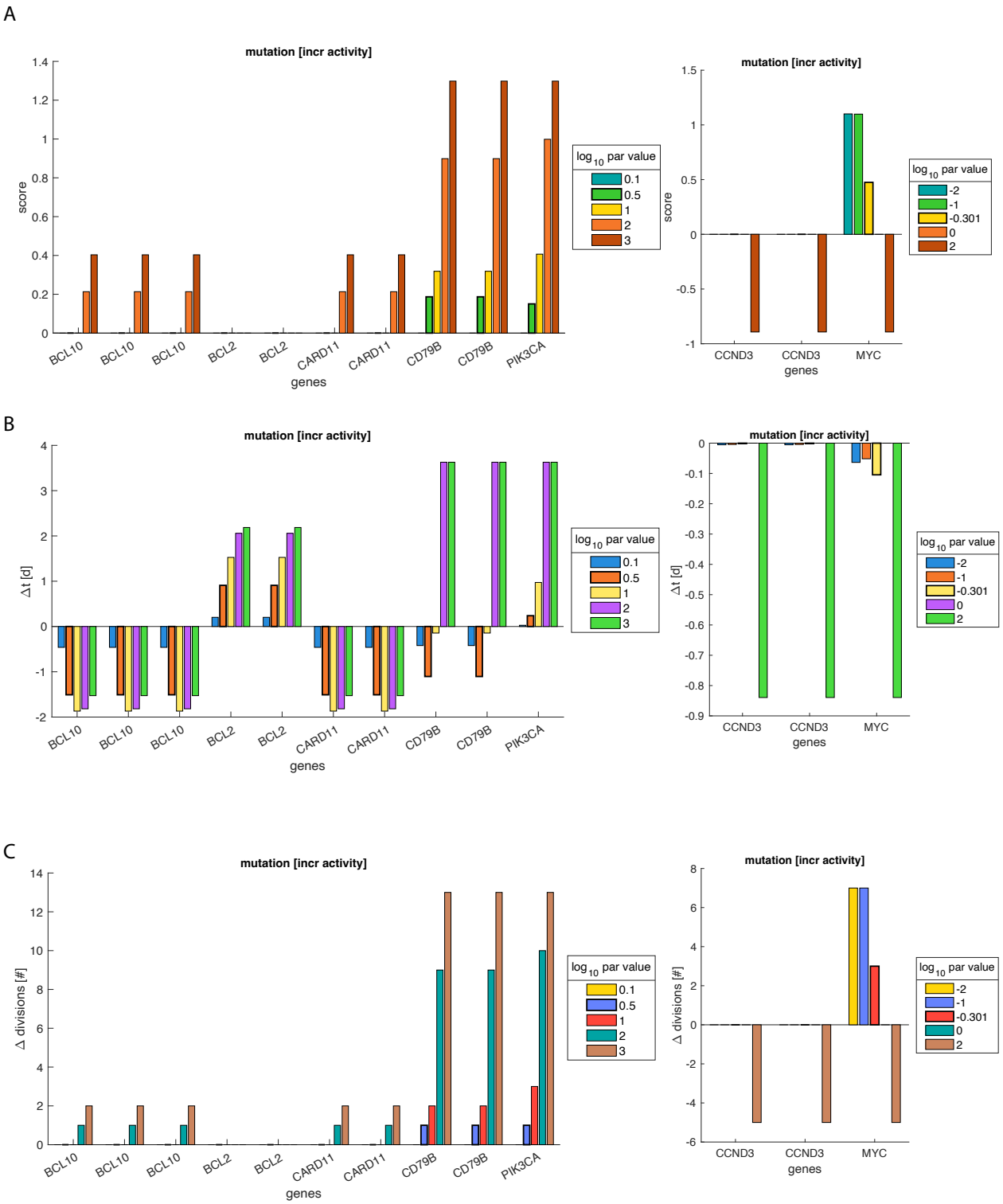

Figure S11. Perturbation strength analyses for increased activity mutations.
The effect of multiple perturbation strengths on the score **(A)**, difference in timepoint of apoptosis **(B)** and difference in division rate **(C)** was calculated. $\Delta t = t_{WT} - t$, where t is the timepoint of apoptosis for the given perturbation strength. $\Delta divisions = divisions_{WT} - divisions$, where divisions correspond to the number of divisions for the given alteration strength. For the MA mutations causing an increased activity, we chose a $\log_{10}$ value of 0.5 as this results in effects of the *CD79B*, *MYC* and *PIK3CA* mutations on the score **(A)**. However, the chosen value is not sufficient to enable an effect of *BCL10* and *CARD11* missense mutations (for an effect the value would need to be increased very strongly (>100)).

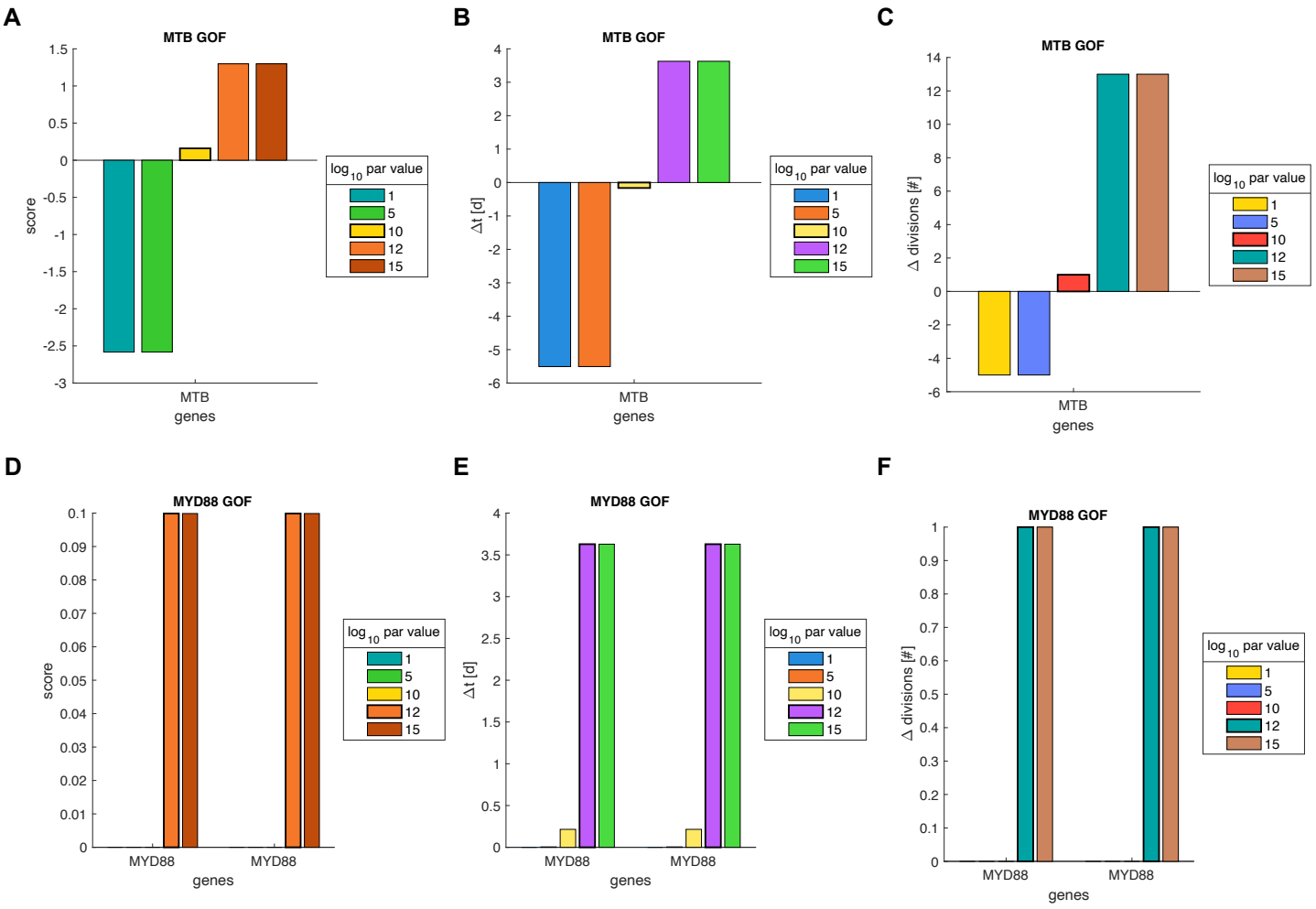

Figure S12. Perturbation strength analyses for GOF mutations.
The effect of multiple perturbation strengths on the score **(A, D, G)**, difference in timepoint of apoptosis **(B, E, H)** and difference in division rate **(C, F, I)** was calculated. $\Delta t = t_{WT} - t$, where t is the timepoint of apoptosis for the given perturbation strength. $\Delta divisions = divisions_{WT} - divisions$, where divisions correspond to the number of divisions for the given alteration strength.

Table S1. List of implemented modified activity (MA) mutations and gain-of-function (GOF) mutations with the corresponding assigned alteration effect and reference.

MA Mutations:

Gene	**Activity** increased: + decreased: -	**Description**	**Annotation based on cBioportal & oncoKB** [1] likely oncogenic: **O** oncogenic: **O+** likely GOF: **G** / likely LOF: **L** GOF: **G+** / LOF: **L+**
BCL10	+	Missense mutation R58Q and non-sense truncation E140X and K146Nfs lead to strongly increased NF-κB activity compared to WT BCL10 [1]. Increased levels of active NF-κB were also observed in DLBCL patients with *BCL10* mutations [1].	Most frequent missense mutation is R58Q [O/G]. Effect of other missense mutations is unknown. E140* nonsense mutation: [O/G] Other nonsense and frameshift mutations: [O/L]
BCL2	+	Missense mutations in the *BCL2* gene (G33R and A43T) can increase the affinity of BCL2 towards BIM and PUMA and thereby enhance its anti-apoptotic property [2]. In the model, only the binding of BCL2 to BAX is implemented. Based on the finding that a missense mutation can modify the binding affinity of BCL2 towards pro-apoptotic proteins, we assume that this can also be the case for the binding to BAX.	Several missense mutations: [O/G+] and [O/G]
BCL6	+/-	Missense mutations found in DLBCL can change binding sites of BCL6 and IRF4 to the BCL6 promotor and thereby cause a dysfunctional repression of BCL6 transcription ([3], [4], reviewed in [5]). We also assume that the BLIMP1-mediated repression of BCL6 is impaired as well as the BCL6-mediated repression of BLIMP1 transcription.	Effect of missense/nonsense mutations unknown. Only Fusions: [O/G]
CARD11	+	Multiple point mutations of *CARD11* cause elevated levels of activated basal NF-κB as well as elevated levels of activated NF-κB upon stimulation [6]. The gain-of-function phenotype was also demonstrated on the level of expression of NF-κB target genes.	Multiple missense mutations: [O+/G+] or [O/G]
CCND3	+	Multiple point mutations of *CCND3* cause increased levels of Cyclin D3 and consequently enhanced proliferation [7]. The increased protein levels were due to lower degradation rates [7]. Based on the conducted pulse chase experiment [7], we determined a change	Multiple missense mutations: [O+/G+] or [O/G]

		between WT CCND3 and mutated CCND3 in the degradation rate by a factor of around 0.5.	
CD79B	+	The most frequent missense mutations of *CD79B* in DLBCL (Y197H, Y197S, Y197D, cBioportal) can lead to chronic B-Cell-Receptor activity in DLBCL which promotes NF-κB signaling and AKT signaling [8]. The survival of ABC-DLBCL cell lines with missense mutations in *CD79B* and chronic B-Cell-Receptor signaling were thereby dependent on CD79B and NF-κB signaling [8].	for missense mutations Y197(C,N,F,H,D,S) and E198G: [O+/G+] or [O/G] other missense mutations: unknown effect
CREBBP	-	Most of tested missense mutations that were found in DLBCL patients are incapable to mediate BCL6 acetylation and therefore strongly reduce repression of BCL6 [9]. As CREBBP is not included in the model, we modulate the level of active BCL6 in presence of *CREBBP* missense mutations.	Majority of missense mutations: [O/L]
EP300	-	*EP300* mutations are also found in DLBCL although less frequent than *CREBBP* mutations [9]. Based on the structural and functional similarity of EP300 and CREBBP [9], we assume for *EP300* missense mutations a reduced functionality in inhibiting BCL6.	multiple missense mutations: [O/L]; for others unknown effect
EZH2	+	The most frequent missense mutations of *EZH2* are found for Y641 (Y646) in DLBCL ([10] and cBioportal taking [11], [12], [13], [14] data sets into account). This missense mutation was shown to enhance EZH2-mediated repression of BLIMP1 and IRF4 ([15], [16], reviewed in [5]).	vast majority variant: Y646N/F/H [O/G]
FAS	-	We assume a LOF effect due to the crucial role of FAS in the negative B-Cell selection in the germinal center ([17], [18], [19]). However, there is no information in literature about the experimentally assessed effects of *FAS* mutations. There is also no information in the oncoKB database about predictions of the oncogenic potential.	For non-sense mutations and fusions: [O/L] For missense mutations the effect is unknown
FBXO11	-	*FBXO11* missense mutations can reduce the degradation rate of BCL6 and therefore lead to increased BCL6 levels [20].	Non-sense mutations: [O/L] For missense mutations the effect is unknown
IRF4	-	*IRF4* missense mutations are present in DLBCL mostly in the IRF domain (cBioPortal). Based on the missense mutation (C99R) which is predicted to be likely-oncogenic, we assume a reduced activity of IRF4 which in turn causes reduced i) inhibition of BCL6, ii) expression of BLIMP1 and iii) expression of AID. As BCL6 is an oncogene due to its constitutive activation causing the development of lymphomas [21], the effect of IRF4 on BCL6 activity could link its reduced functionality to the likely-oncogenic effect.	For one missense mutation (C99R): [O/unknown]
KMT2D	-	A reduction in the level of KMT2D affects expression of multiple genes. One of them is the FAS receptor [22]. As most of the point mutations in DLBCL patients are predicted by OncoKB to be likely-LOF and likely-oncogenic, we assume a LOF mutation for *KMT2D*.	[O/L]

MCL1		The oncogenic effect of MCL1 in DLBCL is based on increased protein levels due to copy number gains or upstream signaling events [23]. The frequency of mutations of *MCL1* in DLBCL are low and the effect is unknown ([24], cBioportal). As we did not find reports about effects of non-sense or LOF mutations, we did not implement an effect for *MCL1* missense mutations.	effect unknown
MEF2B	+	The transcription factor MEF2B promotes BCL6 expression [25]. Missense mutations of *MEF2B* frequently found in DLBCLs increase the transcriptional activity of MEF2B and enhance BCL6 transcription [25]. We therefore implement a GOF effect for *MEF2B* missense mutations.	multipe mutations: [O+/L+] and [O/L]
MYC	+	Missense mutations can lead to a GOF protein due to less efficient degradation [26] (and can be oncogenic due to impaired/prolonged apoptosis induction [27]) (reviewed in [28]). Based on these reports, we assumed that the level of MYC is increased.	multiple mutations: [O/G]
NFKBIA	-	Based on the effects of deletions and LOF mutations of *NFKBIA*, the negative regulator of NF-κB is a known tumor suppressor ([29], [30]). Moreover, dysfunctional IκBα can cause constitutive NF-κB activity [31] which is one of the main characteristics of ABCs [32]. Consequently, we assume for the missense mutations of *NFKBIA* reduced affinity of the IκBα protein for NF-κBs (RELA:RELA, P50:P50, CREL:P50, RELA:P50).	non-sense mutations: [O/L] missense mutations: unknown
NFKBIE	-	*NFKBIE* is like *NFKBIA* a negative regulator of NF-κB activity. Deletions of *NFKBIE* can cause increased proliferation and survival of B-Cells [33]. Moreover, LOF mutations can be a marker for an aggressive form of chronic lymphocytic leukemia [34] and poor outcome in primary mediastinal B-Cell lymphoma [35]. For the missense mutations of *NFKBIE* we assume a reduced activity, i.e. reduced binding rates of the corresponding protein IκBε and NF-κBs (RELA:RELA, P50:P50, CREL:P50, RELA:P50).	effect unknown
PARP1	-	Based on the predicted likely-LOF and likely-oncogenic function of PARP-1 non-sense mutations by oncoKB (https://www.oncokb.org/gene/PARP1/Truncating%20Mutations, [36], we assume for missense mutations a reduced binding affinity towards caspases and thus a reduced amount of cleaved PARP-1.	non-sense mutations: [O/L] missense mutations: effect unknown
PAX5	-	The oncoKB prediction for non-sense mutations of *PAX5* are likely-LOF with a likely-oncogenic effect. Moreover, one missense mutation (V26G) is likely-LOF and likely-oncogenic as well. Consequently, we assume a reduced activity of PAX5 resulting in a reduced synthesis of BCL6 and AID.	1 missense mutation (V26G): [O/L] Others: effect unknown
PIK3CA	+	There are three missense mutations of *PIK3CA* mutations in DLBCL (E545K, R108H, H1047L) with a known GOF resulting in an oncogenic effect (oncoKB, cBioPortal). The gene is found to be frequently mutated in different cancers [37] and mutations can increase the enzymatic activity of PI3K and thereby lead to a constitutive activation of	multiple mutations: [O+/G+]

		AKT [38]. We therefore assume that missense mutations of *PIK3CA* are activating mutations enhancing the activation of AKT.	
PRDM1	-	Missense mutations of *PRDM1* can lead to altered splicing and reduced DNA binding affinity [39]. Thus, we assume a reduced level of the protein BLIMP1 (*PRDM1*) that can bind to DNA and repress PAX5 as well as BCL6.	non-sense mutations: [O/L] missense mutations: effect unknown
PTEN	-	Missense mutations are oncogenic or likely-oncogenic due to LOF (oncoKB, cBioportal, [40]).	[O+/L+] and [O/L]
RB1	-	Based on the observation that loss of *RB1* can cause enhanced proliferation (oncoKB, cBioPortal, [41]) and missense mutations are likely-oncogenic (oncoKB, [42]), we assume for *RB1* missense mutations a reduced binding affinity for E2F which in turn can lead to increased proliferation.	1 missense mutation: [O/L] Others: unknown effect Multiple nonsense mutations: [O/L]
TNFAIP3	-	Non-sense mutations and indel frameshifts lead to non-functional A20 (*TNFAIP3*) and consequently, as A20 is an inhibitor of NF-κB, constitutive NF-κB activity in Hodgkin lymphoma and primary mediastinal B-Cell lymphoma [43]. *TNFAIP3* is also frequently mutated in DLBCL and dysfunctional due to mutations or deletions [44]. Re-introducing functional A20 into cell lines, abrogates constitutive activity of NF-κB and restores apoptotic capability and cellular growth arrest ([43], [44]). *TNFAIP3* (A20) is therefore defined as a tumor suppressor. Seven tested missense mutations of *TNFAIP3* showed either no effect on NF-κB activity or a much less prominent effect compared to non-sense or indel frameshifts causing a truncated A20 variant [45].	missense mutations: unknown effect multiple nonsense mutations: [O/L]
TP53	-	The *TP53* gene is the most mutated gene across different cancers [46] and is among the most frequently mutated genes in DLBCL patients with poor outcomes [47]. The majority of mutations are missense mutations located in the DNA binding domain of P53 ([48] and for DLBCL: cBioportal taking [11], [12], [13], [14] data sets into account). Missense mutations in the DNA binding domain can lead to abrogated DNA binding and therefore dysfunctional P53 transcriptional activity [48]. Missense mutations can also cause a GOF of P53 but these variants are mostly associated with promoted metastasis which is not covered by our model and is also not relevant in non-solid tumors [49]. As P53 is not implemented in our model, we capture *TP53* mutations by altering the synthesis of one of its target genes BAX which is involved in inducing apoptosis. Here, we use additional information to capture the effects of point mutations on transcription of BAX (see Methods, “Defining perturbation strengths” for details).	[O+/L+]

GOF mutations:

Gene(s)	Label	Description	prediction oncogenicity
MYD88	MYD88	Most frequent and well-known point mutation in *MYD88* in DLBCL, specifically ABCs, is L265P [50]. This mutation causes K63-linked polyubiquitination of MYD88 and subsequent activation of NF-κB [51]. Depletion of A20 (*TNFAIP3*) further promotes the MYD88-mediated activation of NF-κB [51]. This GOF mutation alone induces DLBCL in mice [52]. But also other MYD88 variants (M232T, S243N, T294P, S222R) strongly enhance NF-κB activity [50]. To implement MYD88 alterations, we introduce a new term in the model representing a constant activation of IKK in presence of MYD88 GOF mutations (Text S1, eq. 1.142). As A20 can counteract the MYD88-mediated NF-κB activation [51], we included A20 as negative regulator of this process.	especially L265P mutation: [O+/G+] other point mutations: [O/G]
MYD88 + *CD79A/B*	MTB	In (ABC-)DLBCL cell lines and patient samples a My-T-BCR supercomplex was found that causes constitutive B-Cell receptor (BCR) signaling and concomitant NF-κB as well as PI3K activity [53]. The supercomplex consists of the toll-like receptor 9, MYD88, the BCR as well as the CARMA (CARD11-MALT1-BCL10) complex which interact with the IKK complex and thereby induce its activation. It could be shown that ABC-DLBCL cell lines with mutations of *CD79A/B* and *MYD88* (L265P) forming the supercomplex are dependent on the toll-like receptor 9, MYD88 as well as CD79A [53]. Based on these observations, we assume that in presence of both, *MYD88* missense mutations as well as *CD79A/B* missense mutations, a supercomplex exists that constitutively activates IKK and PI3K. Similar to the *MYD88* GOF mutation, we introduce in the model a term constantly activating IKK (Text S1, eq. 142) and increased AKT/PI3K-mediated expression of target genes (Text S1, eq. 1.113, 1.114, 1.133).	

[1] Prevalence information based on cBioportal ([54], [55], [56]) and [oncogenic annotation (likely oncogenic: O, oncogenic: O+) and predicted functional effect (likely GOF: G, GOF: G+, likely LOF: L, LOF: L+)] based on oncoKB ([57], [58]). We took the following data sets on DLBCL cohort studies in cBioportal into account: [11], [12], [13], [14].

[1] M. Xia *et al.*, “BCL10 Mutations Define Distinct Dependencies Guiding Precision Therapy for DLBCL,” *Cancer Discov.*, vol. 12, no. 8, pp. 1922–1941, Aug. 2022, doi: 10.1158/2159-8290.CD-21-1566.
[2] C. Correia *et al.*, “BCL2 mutations are associated with increased risk of transformation and shortened survival in follicular lymphoma,” *Blood*, vol. 125, no. 4, pp. 658–667, 2015, doi: 10.1182/blood-2014-04-571786.
[3] L. Pasqualucci, A. Migliazza, K. Basso, J. Houldsworth, R. S. K. Chaganti, and R. Dalla-Favera, “Mutations of the BCL6 proto-oncogene disrupt its negative autoregulation in diffuse large B-cell lymphoma,” *Blood*, vol. 101, no. 8, pp. 2914–2923, Apr. 2003, doi: 10.1182/blood-2002-11-3387.
[4] M. Saito *et al.*, “A Signaling Pathway Mediating Downregulation of *BCL6* in Germinal Center B Cells Is Blocked by *BCL6* Gene Alterations in B Cell Lymphoma,” *Cancer Cell*, vol. 12, no. 3, pp. 280–292, Sept. 2007, doi: 10.1016/j.ccr.2007.08.011.
[5] K. Basso and R. Dalla-Favera, “Germinal centres and B cell lymphomagenesis,” *Nat. Rev. Immunol.*, vol. 15, no. 3, pp. 172–184, 2015, doi: 10.1038/nri3814.
[6] G. Lenz *et al.*, “Oncogenic CARD11 mutations in human diffuse large B cell lymphoma,” *Science*, vol. 319, no. 5870, pp. 1676–1679, 2008, doi: 10.1126/science.1153629.
[7] R. Schmitz *et al.*, “Burkitt lymphoma pathogenesis and therapeutic targets from structural and functional genomics,” *Nature*, vol. 490, no. 7418, pp. 116–120, 2012, doi: 10.1038/nature11378.
[8] R. E. Davis *et al.*, “Chronic active B-cell-receptor signalling in diffuse large B-cell lymphoma,” *Nature*, vol. 463, no. 7277, pp. 88–92, Jan. 2010, doi: 10.1038/nature08638.
[9] L. Pasqualucci *et al.*, “Inactivating mutations of acetyltransferase genes in B-cell lymphoma,” *Nature*, vol. 471, no. 7337, pp. 189–196, 2011, doi: 10.1038/nature09730.
[10] R. D. Morin *et al.*, “Somatic mutations altering EZH2 (Tyr641) in follicular and diffuse large B-cell lymphomas of germinal-center origin,” *Nat. Genet.*, vol. 42, no. 2, pp. 181–185, Feb. 2010, doi: 10.1038/ng.518.
[11] B. Chapuy *et al.*, “Molecular subtypes of diffuse large B cell lymphoma are associated with distinct pathogenic mechanisms and outcomes,” *Nat. Med.*, vol. 24, no. 5, pp. 679–690, 2018, doi: 10.1038/s41591-018-0016-8.
[12] J. G. Lohr *et al.*, “Discovery and prioritization of somatic mutations in diffuse large B-cell lymphoma (DLBCL) by whole-exome sequencing,” *Proc. Natl. Acad. Sci.*, vol. 109, no. 10, pp. 3879–3884, Mar. 2012, doi: 10.1073/pnas.1121343109.
[13] A. Reddy *et al.*, “Genetic and Functional Drivers of Diffuse Large B Cell Lymphoma,” *Cell*, vol. 171, no. 2, pp. 481-494.e15, 2017, doi: 10.1016/j.cell.2017.09.027.
[14] R. D. Morin *et al.*, “Mutational and structural analysis of diffuse large B-cell lymphoma using whole-genome sequencing,” *Blood*, vol. 122, no. 7, pp. 1256–1265, Aug. 2013, doi: 10.1182/blood-2013-02-483727.
[15] M. Caganova *et al.*, “Germinal center dysregulation by histone methyltransferase EZH2 promotes lymphomagenesis,” *J. Clin. Invest.*, vol. 124, no. 4, pp. 1869–1869, Apr. 2014, doi: 10.1172/JCI75675.
[16] W. Béguelin *et al.*, “EZH2 Is Required for Germinal Center Formation and Somatic EZH2 Mutations Promote Lymphoid Transformation,” *Cancer Cell*, vol. 23, no. 5, pp. 677–692, May 2013, doi: 10.1016/j.ccr.2013.04.011.
[17] E. Kondo and T. Yoshino, “Expression of apoptosis regulators in germinal centers and germinal center-derived B-cell lymphomas: Insight into B-cell lymphomagenesis,” *Pathol. Int.*, vol. 57, no. 7, pp. 391–397, 2007, doi: 10.1111/j.1440-1827.2007.02115.x.

[18] M. Müschen, K. Rajewsky, M. Krönke, and R. Küppers, “The origin of CD95-gene mutations in B-cell lymphoma,” *Trends Immunol.*, vol. 23, no. 2, pp. 75–80, 2002, doi: 10.1016/S1471-4906(01)02115-9.
[19] S. Nagata, “Fas ligand-induced apoptosis.,” *Annu. Rev. Genet.*, vol. 33, pp. 29–55, Jan. 1999, doi: 10.1146/annurev.genet.33.1.29.
[20] S. Duan *et al.*, “FBXO11 targets BCL6 for degradation and is inactivated in diffuse large B-cell lymphomas,” *Nature*, vol. 481, no. 7379, pp. 90–94, 2012, doi: 10.1038/nature10688.
[21] G. Cattoretti *et al.*, “Deregulated BCL6 expression recapitulates the pathogenesis of human diffuse large B cell lymphomas in mice,” *Cancer Cell*, vol. 7, no. 5, pp. 445–455, May 2005, doi: 10.1016/j.ccr.2005.03.037.
[22] A. Ortega-Molina *et al.*, “The histone lysine methyltransferase KMT2D sustains a gene expression program that represses B cell lymphoma development,” *Nat. Med.*, vol. 21, no. 10, pp. 1199–1208, 2015, doi: 10.1038/nm.3943.
[23] S.-S. Wenzel *et al.*, “MCL1 is deregulated in subgroups of diffuse large B-cell lymphoma,” *Leukemia*, vol. 27, no. 6, pp. 1381–1390, June 2013, doi: 10.1038/leu.2012.367.
[24] V. M. Smith *et al.*, “Specific interactions of BCL-2 family proteins mediate sensitivity to BH3-mimetics in diffuse large B-cell lymphoma,” *Haematologica*, vol. 105, no. 8, pp. 2150–2163, 2020, doi: 10.3324/haematol.2019.220525.
[25] C. Y. Ying *et al.*, “MEF2B mutations lead to deregulated expression of the oncogene BCL6 in diffuse large B cell lymphoma,” *Nat. Immunol.*, vol. 14, no. 10, pp. 1084–1092, Oct. 2013, doi: 10.1038/ni.2688.
[26] F. Bahram, N. von der Lehr, C. Cetinkaya, and L.-G. Larsson, “c-Myc hot spot mutations in lymphomas result in inefficient ubiquitination and decreased proteasome-mediated turnover,” *Blood*, vol. 95, no. 6, pp. 2104–2110, Mar. 2000, doi: 10.1182/blood.V95.6.2104.
[27] F. Kuttler *et al.*, “c-myc box II mutations in Burkitt’s lymphoma-derived alleles reduce cell-transformation activity and lower response to broad apoptotic stimuli,” *Oncogene*, vol. 20, no. 42, pp. 6084–6094, Sept. 2001, doi: 10.1038/sj.onc.1204827.
[28] Z. Y. Xu-Monette *et al.*, “Clinical and Biologic Significance of MYC Genetic Mutations in De Novo Diffuse Large B-cell Lymphoma,” *Clin. Cancer Res.*, vol. 22, no. 14, pp. 3593–3605, July 2016, doi: 10.1158/1078-0432.CCR-15-2296.
[29] G. S. Kinker, A. M. Thomas, V. J. Carvalho, F. P. Lima, and A. Fujita, “Deletion and low expression of NFKBIA are associated with poor prognosis in lower-grade glioma patients,” *Sci. Rep.*, vol. 6, no. 1, p. 24160, Apr. 2016, doi: 10.1038/srep24160.
[30] H. Zheng *et al.*, “Whole-exome sequencing identifies multiple loss-of-function mutations of NF-κB pathway regulators in nasopharyngeal carcinoma,” *Proc. Natl. Acad. Sci.*, vol. 113, no. 40, pp. 11283–11288, Oct. 2016, doi: 10.1073/pnas.1607606113.
[31] E. Cabannes, G. Khan, F. Aillet, R. F. Jarrett, and R. T. Hay, “Mutations in the IkBa gene in Hodgkin’s disease suggest a tumour suppressor role for IkappaBalpha,” *Oncogene*, vol. 18, no. 20, pp. 3063–3070, May 1999, doi: 10.1038/sj.onc.1202893.
[32] R. E. Davis, K. D. Brown, U. Siebenlist, and L. M. Staudt, “Constitutive Nuclear Factor κB Activity Is Required for Survival of Activated B Cell–like Diffuse Large B Cell Lymphoma Cells,” *J. Exp. Med.*, vol. 194, no. 12, pp. 1861–1874, Dec. 2001, doi: 10.1084/jem.194.12.1861.
[33] B. N. Alves *et al.*, “IκBε Is a Key Regulator of B Cell Expansion by Providing Negative Feedback on cRel and RelA in a Stimulus-Specific Manner,” *J. Immunol.*, vol. 192, no. 7, pp. 3121–3132, 2014, doi: 10.4049/jimmunol.1302351.
[34] L. Mansouri *et al.*, “Functional loss of IκBε leads to NF-κB deregulation in aggressive chronic lymphocytic leukemia,” *J. Exp. Med.*, vol. 212, no. 6, pp. 833–843, May 2015, doi: 10.1084/jem.20142009.

[35] L. Mansouri *et al.*, “Frequent NFKBIE deletions are associated with poor outcome in primary mediastinal B-cell lymphoma,” *Blood*, vol. 128, no. 23, pp. 2666–2670, Dec. 2016, doi: 10.1182/blood-2016-03-704528.
[36] M. L. Agarwal, A. Agarwal, W. R. Taylor, Z. Q. Wang, E. F. Wagner, and G. R. Stark, “Defective induction but normal activation and function of p53 in mouse cells lacking poly-ADP-ribose polymerase,” *Oncogene*, vol. 15, no. 9, pp. 1035–1041, Aug. 1997, doi: 10.1038/sj.onc.1201274.
[37] Y. Samuels *et al.*, “High Frequency of Mutations of the PIK3CA Gene in Human Cancers,” *Science*, vol. 304, no. 5670, pp. 554–554, Apr. 2004, doi: 10.1126/science.1096502.
[38] M. Gymnopoulos, M.-A. Elsliger, and P. K. Vogt, “Rare cancer-specific mutations in PIK3CA show gain of function,” *Proc. Natl. Acad. Sci.*, vol. 104, no. 13, pp. 5569–5574, Mar. 2007, doi: 10.1073/pnas.0701005104.
[39] W. Tam, M. Gomez, A. Chadburn, J. W. Lee, W. C. Chan, and D. M. Knowles, “Mutational analysis of PRDM1 indicates a tumor-suppressor role in diffuse large B-cell lymphomas,” *Blood*, vol. 107, no. 10, pp. 4090–4100, May 2006, doi: 10.1182/blood-2005-09-3778.
[40] I. Rodríguez-Escudero, M. D. Oliver, A. Andrés-Pons, M. Molina, V. J. Cid, and R. Pulido, “A comprehensive functional analysis of PTEN mutations: implications in tumor- and autism-related syndromes,” *Hum. Mol. Genet.*, vol. 20, no. 21, pp. 4132–4142, Nov. 2011, doi: 10.1093/hmg/ddr337.
[41] Z. He *et al.*, “Deletion of Rb1 induces both hyperproliferation and cell death in murine germinal center B cells,” *Exp. Hematol.*, vol. 44, no. 3, pp. 161-165.e4, Mar. 2016, doi: 10.1016/j.exphem.2015.11.006.
[42] E. O. Berge *et al.*, “Identification and characterization of retinoblastoma gene mutations disturbing apoptosis in human breast cancers,” *Mol. Cancer*, vol. 9, p. 173, July 2010, doi: 10.1186/1476-4598-9-173.
[43] R. Schmitz *et al.*, “TNFAIP3 (A20) is a tumor suppressor gene in Hodgkin lymphoma and primary mediastinal B cell lymphoma,” *J. Exp. Med.*, vol. 206, no. 5, pp. 981–989, Apr. 2009, doi: 10.1084/jem.20090528.
[44] M. Compagno *et al.*, “Mutations of multiple genes cause deregulation of NF-κB in diffuse large B-cell lymphoma,” *Nature*, vol. 459, no. 7247, pp. 717–721, June 2009, doi: 10.1038/nature07968.
[45] L. Escudero-Ibarz, M. Wang, and M.-Q. Du, “Significant functional difference between TNFAIP3 truncation and missense mutants,” *Haematologica*, vol. 101, no. 9, Art. no. 9, Sept. 2016, doi: 10.3324/haematol.2016.148346.
[46] M. Sinkala, “Mutational landscape of cancer-driver genes across human cancers,” *Sci. Rep.*, vol. 13, no. 1, p. 12742, Aug. 2023, doi: 10.1038/s41598-023-39608-2.
[47] W. Ren *et al.*, “Genetic and transcriptomic analyses of diffuse large B-cell lymphoma patients with poor outcomes within two years of diagnosis,” *Leukemia*, vol. 38, no. 3, pp. 610–620, Mar. 2024, doi: 10.1038/s41375-023-02120-7.
[48] L. Bouaoun *et al.*, “TP53 Variations in Human Cancers: New Lessons from the IARC TP53 Database and Genomics Data,” *Hum. Mutat.*, vol. 37, no. 9, pp. 865–876, Sept. 2016, doi: 10.1002/humu.23035.
[49] Y. Stein, R. Aloni-Grinstein, and V. Rotter, “Mutant p53 oncogenicity: dominant-negative or gain-of-function?,” *Carcinogenesis*, vol. 41, no. 12, pp. 1635–1647, 2020, doi: 10.1093/carcin/bgaa117.
[50] V. N. Ngo *et al.*, “Oncogenically active MYD88 mutations in human lymphoma,” *Nature*, pp. 3–9, 2011, doi: 10.1038/nature09671.
[51] X. Yu *et al.*, “MYD88 L265P Elicits Mutation-specific Ubiquitination to Drive NF-κB Activation and Lymphomagenesis,” *Blood*, 2020, doi: 10.1182/blood.2020004918.

[52] G. Knittel *et al.*, “B-cell-specific conditional expression of Myd88p.L252P leads to the development of diffuse large B-cell lymphoma in mice,” *Blood*, vol. 127, no. 22, pp. 2732–2741, 2016, doi: 10.1182/blood-2015-11-684183.
[53] J. D. Phelan *et al.*, “A multiprotein supercomplex controlling oncogenic signalling in lymphoma,” *Nature*, vol. 560, no. 7718, pp. 387–391, Aug. 2018, doi: 10.1038/s41586-018-0290-0.
[54] E. Cerami *et al.*, “The cBio Cancer Genomics Portal: An Open Platform for Exploring Multidimensional Cancer Genomics Data,” *Cancer Discov.*, vol. 2, no. 5, pp. 401–404, May 2012, doi: 10.1158/2159-8290.CD-12-0095.
[55] J. Gao *et al.*, “Integrative Analysis of Complex Cancer Genomics and Clinical Profiles Using the cBioPortal,” *Sci. Signal.*, vol. 6, no. 269, pp. pl1–pl1, Apr. 2013, doi: 10.1126/scisignal.2004088.
[56] I. de Bruijn *et al.*, “Analysis and Visualization of Longitudinal Genomic and Clinical Data from the AACR Project GENIE Biopharma Collaborative in cBioPortal,” *Cancer Res.*, vol. 83, no. 23, pp. 3861–3867, Dec. 2023, doi: 10.1158/0008-5472.CAN-23-0816.
[57] D. Chakravarty *et al.*, “OncoKB: A Precision Oncology Knowledge Base,” *JCO Precis. Oncol.*, no. 1, pp. 1–16, Nov. 2017, doi: 10.1200/po.17.00011.
[58] S. P. Suehnholz *et al.*, “Quantifying the Expanding Landscape of Clinical Actionability for Patients with Cancer,” *Cancer Discov.*, vol. 14, no. 1, pp. 49–65, Jan. 2024, doi: 10.1158/2159-8290.CD-23-0467.

Table S2. List of individual alterations that lead to an aberrant cell state and their induced effect size. CN gain/loss: Copy number gain/loss, SV: Structural variant, mutation [GOF]: gain-of-function mutation, mutation [MA]: mutation causing modified activity (increased or decreased activity), mutation [LOF]: loss-of-function mutation, mutation [info n/a]: mutation with missing information about the mutation type (LOF or MA).

Gene	alteration type	apoptosis time [d]	div rate [1/d]
TNFAIP3	mutation [info n/a]	10	1.7
	mutation [LOF]	10	1.7
MYC	SV	6.32	1.74
NFKBIA	mutation [LOF]	10	1
MYC	mutation [MA]	6.27	1.28
REL	CN gain	6.04	1.16
CCNB1	CN gain	6.3	1.11
NFKBIA	mutation [info n/a]	10	0.7
	mutation [MA]	10	0.7
PTEN	mutation [info n/a]	10	0.7
	mutation [MA]	10	0.7
	mutation [LOF]	10	0.7
CD79B	mutation [info n/a]	5.27	1.14
	mutation [MA]	5.27	1.14
PRDM1	mutation [LOF]	5.52	1.09
CREBBP	mutation [LOF]	5.52	1.09
EP300	mutation [LOF]	5.52	1.09
FBXO11	mutation [LOF]	5.52	1.09
CREBBP	mutation [info n/a]	5.52	1.09
	mutation [MA]	5.52	1.09
EP300	mutation [info n/a]	5.52	1.09
	mutation [MA]	5.52	1.09
FBXO11	mutation [MA]	5.52	1.09
EZH2	mutation [info n/a]	5.52	1.09
	mutation [MA]	5.52	1.09
PRDM1	mutation [info n/a]	5.52	1.09
	mutation [MA]	5.52	1.09
IRF4	mutation [MA]	5.53	1.09
EZH2	CN gain	5.53	1.08
MEF2B	mutation [info n/a]	5.53	1.08
	mutation [MA]	5.53	1.08
BCL6	CN gain	5.54	1.08
PRDM1	CN loss	5.54	1.08
SPIB	CN gain	5.54	1.08
BCL6	SV	5.55	1.08
NFKBIB	CN gain	5.55	1.08
CDK2	CN gain	6.34	0.95
CCNA1	CN gain	6.34	0.95
PIK3CA	mutation [MA]	6.61	0.91
TNFAIP3	CN loss	7.12	0.84
MYD88	mutation [info n/a]	10	0.6
	mutation [GOF]	10	0.6

Table S3. Alterations forming a synergistic effect with mutated *NFKBIE*. CN gain/loss: Copy number gain/loss, SV: Structural variant, mutation [GOF]: gain-of-function mutation, mutation [MA]: mutation causing modified activity (increased or decreased activity), mutation [LOF]: loss-of-function mutation, mutation [info n/a]: mutation with missing information about the mutation type (LOF or MA).

alteration 1	alteration 2	apop [d]	div [1/d]	score	exp. score
BCL6 CN gain	NFKBIE mutation [info n/a]	10	1.6	1.1	0.2
	NFKBIE mutation [MA]	10	1.6	1.1	0.2
BCL6 SV	NFKBIE mutation [info n/a]	10	1.6	1.1	0.2
	NFKBIE mutation [MA]	10	1.6	1.1	0.2
	NFKBIE mutation [LOF]	10	1.8	1.3	0.2
CARD11 mutation [LOF]	NFKBIE mutation [info n/a]	10	1.1	0.6	-2.91
	NFKBIE mutation [MA]	10	1.1	0.6	-2.91
	NFKBIE mutation [LOF]	9.55	0.94	0.42	-2.86
CD79B mutation [LOF]	NFKBIE mutation [info n/a]	10	0.9	0.4	-3.1
	NFKBIE mutation [MA]	10	0.9	0.4	-3.1
	NFKBIE mutation [LOF]	9.35	0.96	0.43	-3.05
CREBBP mutation [LOF]	NFKBIE mutation [info n/a]	10	1.6	1.1	0.21
	NFKBIE mutation [MA]	10	1.6	1.1	0.21
	NFKBIE mutation [LOF]	10	1.8	1.3	0.2
CREBBP mutation [MA]	NFKBIE mutation [info n/a]	10	1.6	1.1	0.21
	NFKBIE mutation [MA]	10	1.6	1.1	0.21
	NFKBIE mutation [LOF]	10	1.8	1.3	0.2
CREBBP mutation [info n/a]	NFKBIE mutation [info n/a]	10	1.6	1.1	0.21
	NFKBIE mutation [MA]	10	1.6	1.1	0.21
	NFKBIE mutation [LOF]	10	1.8	1.3	0.2
EP300 mutation [LOF]	NFKBIE mutation [info n/a]	10	1.6	1.1	0.21
	NFKBIE mutation [MA]	10	1.6	1.1	0.21
	NFKBIE mutation [LOF]	10	1.8	1.3	0.2
EP300 mutation [MA]	NFKBIE mutation [info n/a]	10	1.6	1.1	0.21
	NFKBIE mutation [MA]	10	1.6	1.1	0.21
	NFKBIE mutation [LOF]	10	1.8	1.3	0.2
EP300 mutation [info n/a]	NFKBIE mutation [info n/a]	10	1.6	1.1	0.21
	NFKBIE mutation [MA]	10	1.6	1.1	0.21
	NFKBIE mutation [LOF]	10	1.8	1.3	0.2
EZH2 CN gain	NFKBIE mutation [info n/a]	10	1.6	1.1	0.21
	NFKBIE mutation [MA]	10	1.6	1.1	0.21
	NFKBIE mutation [LOF]	10	1.8	1.3	0.2
EZH2 mutation [MA]	NFKBIE mutation [info n/a]	10	1.6	1.1	0.21
	NFKBIE mutation [MA]	10	1.6	1.1	0.21
	NFKBIE mutation [LOF]	10	1.8	1.3	0.2
EZH2 mutation [info n/a]	NFKBIE mutation [info n/a]	10	1.6	1.1	0.21
	NFKBIE mutation [MA]	10	1.6	1.1	0.21
	NFKBIE mutation [LOF]	10	1.8	1.3	0.2
FBXO11 mutation [LOF]	NFKBIE mutation [info n/a]	10	1.6	1.1	0.21
	NFKBIE mutation [MA]	10	1.6	1.1	0.21
	NFKBIE mutation [LOF]	10	1.8	1.3	0.2
FBXO11 mutation [MA]	NFKBIE mutation [info n/a]	10	1.6	1.1	0.21
	NFKBIE mutation [MA]	10	1.6	1.1	0.21
	NFKBIE mutation [LOF]	10	1.8	1.3	0.2
IRF4 mutation [MA]	NFKBIE mutation [info n/a]	10	1.6	1.1	0.21
	NFKBIE mutation [MA]	10	1.6	1.1	0.21
	NFKBIE mutation [LOF]	10	1.8	1.3	0.2
MEF2B mutation [MA]	NFKBIE mutation [info n/a]	10	1.6	1.1	0.21
	NFKBIE mutation [MA]	10	1.6	1.1	0.21

alteration 1	alteration 2	apop [d]	div [1/d]	score	exp. score
	NFKBIE mutation [LOF]	10	1.8	1.3	0.2
MEF2B mutation [info n/a]	NFKBIE mutation [info n/a]	10	1.6	1.1	0.21
	NFKBIE mutation [MA]	10	1.6	1.1	0.21
	NFKBIE mutation [LOF]	10	1.8	1.3	0.2
PRDM1 mutation [LOF]	NFKBIE mutation [info n/a]	10	1.6	1.1	0.21
	NFKBIE mutation [MA]	10	1.6	1.1	0.21
	NFKBIE mutation [LOF]	10	1.8	1.3	0.2
PRDM1 mutation [MA]	NFKBIE mutation [info n/a]	10	1.6	1.1	0.21
	NFKBIE mutation [MA]	10	1.6	1.1	0.21
	NFKBIE mutation [LOF]	10	1.8	1.3	0.2
PRDM1 mutation [info n/a]	NFKBIE mutation [info n/a]	10	1.6	1.1	0.21
	NFKBIE mutation [MA]	10	1.6	1.1	0.21
	NFKBIE mutation [LOF]	10	1.8	1.3	0.2

Table S4. Implementation of alterations. CN gain/loss: Copy number gain/loss, SV: Structural variant, mutation [GOF]: gain-of-function mutation, mutation [MA]: mutation causing modified activity (increased or decreased activity), mutation [LOF]: loss-of-function mutation, mutation [info n/a]: mutation with missing information about the mutation type (LOF or MA).

Gene	alteration type	parameter_label	log10_parameter_value	implementation
APAF1	CN gain	init_Apaf	0.17609	direct
BAX	CN gain	k86	0.17609	direct
BCL10	mutation [info n/a]	pikk1	0.5	indirect
	mutation [info n/a]	pikk3	0.5	indirect
	mutation [MA]	pikk1	0.5	indirect
	mutation [MA]	pikk3	0.5	indirect
	mutation [LOF]	pikk1	0.5	indirect
	mutation [LOF]	pikk3	0.5	indirect
BCL2	CN gain	k2_80	0.17609	direct
	mutation [info n/a]	k36	0.5	direct
	mutation [info n/a]	k40	0.5	direct
	mutation [info n/a]	k44	0.5	direct
	mutation [MA]	k36	0.5	direct
	mutation [MA]	k40	0.5	direct
	mutation [MA]	k44	0.5	direct
	SV	ke_bcl2	1	direct
	SV	k2_80	-10	direct
BCL6	CN gain	kASC42	0.17609	direct
	CN loss	kASC42	-0.17609	direct
	mutation [info n/a]	k_bclRep	-2	direct
	mutation [info n/a]	k_bclRep2	-2	direct
	mutation [MA]	k_bclRep	-2	direct
	mutation [MA]	k_bclRep2	-2	direct
	mutation [LOF]	k_bclRep	-10	direct
	mutation [LOF]	k_bclRep2	-10	direct
	SV	ke_bcl6	0.69897	direct
	SV	kASC42	-10	direct
	SV	k_bclRep	-10	direct
CARD11	mutation [info n/a]	pikk1	0.5	indirect
	mutation [info n/a]	pikk3	0.5	indirect
	mutation [MA]	pikk1	0.5	indirect
	mutation [MA]	pikk3	0.5	indirect
	mutation [LOF]	pikk1	-10	indirect
	mutation [LOF]	pikk3	-10	indirect
CASP3	CN loss	k101	-0.17609	direct
CCNA1	CN gain	k2_21	0.17609	direct
CCNB1	CN gain	k2_23	0.17609	direct
	CN gain	k2_24	0.17609	direct
CCND1	CN gain	k2_78	0.17609	direct
CCND3	CN gain	k2_78	0.17609	indirect
	mutation [info n/a]	k2_9	-0.30103	indirect
	mutation [MA]	k2_9	-0.30103	indirect
	mutation [LOF]	k2_10	-10	indirect
	mutation [LOF]	k2_36	-10	indirect
CCNE1	CN gain	k2_12	0.17609	direct
	CN gain	k2_13	0.17609	direct
CD79B	mutation [info n/a]	pikk1	0.5	indirect
	mutation [info n/a]	pikk3	0.5	indirect
	mutation [info n/a]	kp_PMBC	0.5	indirect

Gene	alteration type	parameter_label	log10_parameter_value	implementation
	mutation [MA]	pikk1	0.5	indirect
	mutation [MA]	pikk3	0.5	indirect
	mutation [MA]	kp_PMBC	0.5	indirect
	mutation [LOF]	pikk1	-10	indirect
	mutation [LOF]	pikk3	-10	indirect
	mutation [LOF]	kp_PMBC	-10	indirect
CDK2	CN gain	k2_21	0.17609	indirect
	CN gain	k2_12	0.17609	indirect
	CN gain	k2_13	0.17609	indirect
CDK4	CN gain	k2_78	0.17609	indirect
CDK6	CN gain	k2_78	0.17609	indirect
CDKN1B	CN loss	k2_29	-0.17609	direct
	mutation [LOF]	k2_29	-10	direct
CREBBP	mutation [info n/a]	kASC48	-2	indirect
	mutation [MA]	kASC48	-2	indirect
	mutation [LOF]	kASC48	-10	indirect
CYCS	CN gain	k113	0.17609	direct
DIABLO	CN gain	k97	0.17609	direct
EP300	mutation [info n/a]	kASC48	-2	indirect
	mutation [MA]	kASC48	-2	indirect
	mutation [LOF]	kASC48	-10	indirect
EZH2	CN gain	kASC22	-0.17609	indirect
	CN gain	kASC15	-0.17609	indirect
	CN gain	kASC12	-0.17609	indirect
	mutation [info n/a]	kASC22	-2	indirect
	mutation [info n/a]	kASC15	-2	indirect
	mutation [info n/a]	kASC12	-2	indirect
	mutation [MA]	kASC22	-2	indirect
	mutation [MA]	kASC15	-2	indirect
	mutation [MA]	kASC12	-2	indirect
FADD	CN gain	k3	0.17609	indirect
FAS	CN loss	k71	-0.17609	direct
	mutation [info n/a]	k1	-2	direct
	mutation [MA]	k1	-2	direct
	mutation [LOF]	k1	-10	direct
FBXO11	mutation [MA]	kASC48	-2	indirect
	mutation [LOF]	kASC48	-10	indirect
IRF4	CN gain	kASC15	0.17609	direct
	mutation [MA]	kirfmut	-2	direct
KMT2D	CN gain	k71	0.17609	indirect
	mutation [info n/a]	k71	-2	indirect
	mutation [MA]	k71	-2	indirect
	mutation [LOF]	k71	-10	indirect
MALT1	CN gain	pikk7	0.17609	indirect
MCL1	CN gain	k_mcl	0.17609	direct
MEF2B	mutation [info n/a]	ke_bcl6	0.69897	indirect
	mutation [MA]	ke_bcl6	0.69897	indirect
	mutation [LOF]	kASC42	-10	indirect
MYC	mutation [MA]	k2_86	-0.30103	direct

Gene	alteration type	parameter_label	log10_parameter_value	implementation
MYC	SV	ke_myc	0	direct
	SV	k2_85	-10	direct
MYD88	mutation [info n/a]	ktlr	12	indirect
	mutation [GOF]	ktlr	12	indirect
NFKBIA	mutation [info n/a]	pdi111	-2	direct
	mutation [info n/a]	pdi211	-2	direct
	mutation [info n/a]	pdi121	-2	direct
	mutation [info n/a]	pdi221	-2	direct
	mutation [info n/a]	pdi131	-2	direct
	mutation [info n/a]	pdi231	-2	direct
	mutation [info n/a]	pdi141	-2	direct
	mutation [info n/a]	pdi241	-2	direct
	mutation [MA]	pdi111	-2	direct
	mutation [MA]	pdi211	-2	direct
	mutation [MA]	pdi121	-2	direct
	mutation [MA]	pdi221	-2	direct
	mutation [MA]	pdi131	-2	direct
	mutation [MA]	pdi231	-2	direct
	mutation [MA]	pdi141	-2	direct
	mutation [MA]	pdi241	-2	direct
	mutation [LOF]	pdi111	-10	direct
	mutation [LOF]	pdi211	-10	direct
	mutation [LOF]	pdi121	-10	direct
	mutation [LOF]	pdi221	-10	direct
	mutation [LOF]	pdi131	-10	direct
	mutation [LOF]	pdi231	-10	direct
	mutation [LOF]	pdi141	-10	direct
	mutation [LOF]	pdi241	-10	direct
NFKBIB	CN gain	pii12	0.17609	direct
NFKBIE	CN gain	pii13	0.17609	direct
	mutation [info n/a]	pdi113	-2	direct
	mutation [info n/a]	pdi213	-2	direct
	mutation [info n/a]	pdi123	-2	direct
	mutation [info n/a]	pdi223	-2	direct
	mutation [info n/a]	pdi133	-2	direct
	mutation [info n/a]	pdi233	-2	direct
	mutation [info n/a]	pdi143	-2	direct
	mutation [info n/a]	pdi243	-2	direct
	mutation [MA]	pdi113	-2	direct
	mutation [MA]	pdi213	-2	direct
	mutation [MA]	pdi123	-2	direct
	mutation [MA]	pdi223	-2	direct
	mutation [MA]	pdi133	-2	direct
	mutation [MA]	pdi233	-2	direct
	mutation [MA]	pdi143	-2	direct
	mutation [MA]	pdi243	-2	direct
	mutation [LOF]	pdi113	-10	direct
	mutation [LOF]	pdi213	-10	direct
	mutation [LOF]	pdi123	-10	direct
	mutation [LOF]	pdi223	-10	direct

Gene	alteration type	parameter_label	log10_parameter_value	implementation
	mutation [LOF]	pdi133	-10	direct
	mutation [LOF]	pdi233	-10	direct
	mutation [LOF]	pdi143	-10	direct
	mutation [LOF]	pdi243	-10	direct
PARP1	CN gain	k108	0.17609	direct
	CN loss	k108	-0.17609	direct
	mutation [MA]	k23	-2	direct
PAX5	mutation [MA]	kpax5mut	-2	direct
	mutation [LOF]	kpax5mut	-10	direct
PIK3CA	mutation [MA]	pakt1	0.5	indirect
	mutation [MA]	pakt3	0.5	indirect
	mutation [LOF]	pakt1	-10	indirect
	mutation [LOF]	pakt3	-10	indirect
PRDM1	CN loss	kASC22	-0.17609	direct
	mutation [info n/a]	kASC22	-2	direct
	mutation [MA]	kASC22	-2	direct
	mutation [LOF]	kASC22	-10	direct
PTEN	CN loss	pakt4	-0.17609	direct
	mutation [info n/a]	kpi3kmut	-2	direct
	mutation [info n/a]	kpi3kmut	-2	direct
	mutation [MA]	kpi3kmut	-2	direct
	mutation [LOF]	kpi3kmut	-10	direct
RB1	CN gain	init_ppRb	0.17609	direct
	CN gain	init_Rb	0.17609	direct
	CN gain	init_E2FRb	0.17609	direct
	CN gain	init_pE2FRb	0.17609	direct
	CN loss	init_ppRb	-0.17609	direct
	CN loss	init_Rb	-0.17609	direct
	CN loss	init_E2FRb	-0.17609	direct
	CN loss	init_pE2FRb	-0.17609	direct
	mutation [MA]	k2_72	-2	direct
REL	CN gain	pm13	0.17609	direct
RELA	CN gain	pm11	0.17609	direct
SPIB	CN gain	kASC22	-0.17609	indirect
TNFAIP3	CN loss	pikk4	-0.17609	direct
	mutation [info n/a]	ka20mut	-2	direct
	mutation [LOF]	ka20mut	-10	direct
TP53	CN loss	k86	-0.17609	indirect
	mutation [info n/a]	k86	-2	indirect
	mutation [MA]	k86	-2	indirect
	mutation [LOF]	k86	-10	indirect

1 ODE system

$$\frac{d\left(\mathrm{tIkBa}\right)}{\mathrm{dt}} = \frac{\mathrm{pii\_11} \cdot \left(\mathrm{pdi\_721} \cdot \left(\frac{\mathrm{A50n}}{\mathrm{pii\_101}}\right)^{\mathrm{pii\_91}} + \mathrm{pdi\_711} \cdot \left(\frac{\mathrm{AAn}}{\mathrm{pii\_101}}\right)^{\mathrm{pii\_91}} + \mathrm{pdi\_741} \cdot \left(\frac{\mathrm{C50n}}{\mathrm{pii\_101}}\right)^{\mathrm{pii\_91}} + 1\right)}{\left(\frac{\mathrm{A50n}}{\mathrm{pii\_101}}\right)^{\mathrm{pii\_91}} + \left(\frac{\mathrm{AAn}}{\mathrm{pii\_101}}\right)^{\mathrm{pii\_91}} + \left(\frac{\mathrm{C50n}}{\mathrm{pii\_101}}\right)^{\mathrm{pii\_91}} + 1} - \mathrm{pii\_21} \cdot \mathrm{tIkBa} \tag{1.1}$$

$$\begin{aligned}\frac{d\left(\mathrm{IkBa}\right)}{\mathrm{dt}} = {} & \mathrm{IkBaA50} \cdot \mathrm{pd\_112} + \mathrm{IkBaC50} \cdot \mathrm{pd\_114} + \mathrm{IkBaAA} \cdot \mathrm{pd\_111} + \mathrm{IkBa5050} \cdot \mathrm{pd\_113} + \mathrm{IkBaA50} \cdot \mathrm{pdi\_321} + \mathrm{IkBaAA} \cdot \mathrm{pdi\_311} \\ & + \mathrm{IkBaC50} \cdot \mathrm{pdi\_341} + \mathrm{IkBa5050} \cdot \mathrm{pdi\_331} - \mathrm{IkBa} \cdot \mathrm{pii\_41} - \mathrm{IkBa} \cdot \mathrm{pii\_61} + \mathrm{IkBan} \cdot \mathrm{pii\_71} - \mathrm{A50} \cdot \mathrm{IkBa} \cdot \mathrm{pdi\_121} \\ & - \mathrm{AA} \cdot \mathrm{IkBa} \cdot \mathrm{pdi\_111} - \mathrm{C50} \cdot \mathrm{IkBa} \cdot \mathrm{pdi\_141} - \mathrm{IkBa} \cdot \mathrm{P50P50} \cdot \mathrm{pdi\_131} - \mathrm{IkBa} \cdot \mathrm{pIKK} \cdot \mathrm{pii\_111} + \mathrm{k2\_77} \cdot \mathrm{pii\_31} \cdot \mathrm{tIkBa}\end{aligned} \tag{1.2}$$

$$\begin{aligned}\frac{d\left(\mathrm{IkBan}\right)}{\mathrm{dt}} = {} & \mathrm{IkBaA50n} \cdot \mathrm{pd\_122} + \mathrm{IkBaC50n} \cdot \mathrm{pd\_124} + \mathrm{IkBaAAn} \cdot \mathrm{pd\_121} + \mathrm{IkBa5050n} \cdot \mathrm{pd\_123} + \mathrm{IkBaA50n} \cdot \mathrm{pdi\_421} \\ & + \mathrm{IkBaAAn} \cdot \mathrm{pdi\_411} + \mathrm{IkBaC50n} \cdot \mathrm{pdi\_441} + \mathrm{IkBa5050n} \cdot \mathrm{pdi\_431} + \mathrm{IkBa} \cdot \mathrm{pii\_61} - \mathrm{IkBan} \cdot \mathrm{pii\_51} - \mathrm{IkBan} \\ & \cdot \mathrm{pii\_71} - \mathrm{A50n} \cdot \mathrm{IkBan} \cdot \mathrm{pdi\_221} - \mathrm{AAn} \cdot \mathrm{IkBan} \cdot \mathrm{pdi\_211} - \mathrm{C50n} \cdot \mathrm{IkBan} \cdot \mathrm{pdi\_241} - \mathrm{IkBan} \cdot \mathrm{P50P50n} \cdot \mathrm{pdi\_231}\end{aligned} \tag{1.3}$$

$$\frac{d\left(\mathrm{tIkBb}\right)}{\mathrm{dt}} = \frac{\mathrm{pii\_12} \cdot \left(\mathrm{pdi\_722} \cdot \left(\frac{\mathrm{A50n}}{\mathrm{pii\_102}}\right)^{\mathrm{pii\_92}} + \mathrm{pdi\_712} \cdot \left(\frac{\mathrm{AAn}}{\mathrm{pii\_102}}\right)^{\mathrm{pii\_92}} + \mathrm{pdi\_742} \cdot \left(\frac{\mathrm{C50n}}{\mathrm{pii\_102}}\right)^{\mathrm{pii\_92}} + 1\right)}{\left(\frac{\mathrm{A50n}}{\mathrm{pii\_102}}\right)^{\mathrm{pii\_92}} + \left(\frac{\mathrm{AAn}}{\mathrm{pii\_102}}\right)^{\mathrm{pii\_92}} + \left(\frac{\mathrm{C50n}}{\mathrm{pii\_102}}\right)^{\mathrm{pii\_92}} + 1} - \mathrm{pii\_22} \cdot \mathrm{tIkBb} \tag{1.4}$$

$$\begin{aligned}\frac{d\left(\mathrm{IkBb}\right)}{\mathrm{dt}} = {} & \mathrm{IkBbA50} \cdot \mathrm{pd\_112} + \mathrm{IkBbC50} \cdot \mathrm{pd\_114} + \mathrm{IkBbAA} \cdot \mathrm{pd\_111} + \mathrm{IkBb5050} \cdot \mathrm{pd\_113} + \mathrm{IkBbA50} \cdot \mathrm{pdi\_322} + \mathrm{IkBbAA} \cdot \mathrm{pdi\_312} \\ & + \mathrm{IkBbC50} \cdot \mathrm{pdi\_342} + \mathrm{IkBb5050} \cdot \mathrm{pdi\_332} - \mathrm{IkBb} \cdot \mathrm{pii\_42} - \mathrm{IkBb} \cdot \mathrm{pii\_62} + \mathrm{IkBbn} \cdot \mathrm{pii\_72} - \mathrm{A50} \cdot \mathrm{IkBb} \cdot \mathrm{pdi\_122} \\ & - \mathrm{AA} \cdot \mathrm{IkBb} \cdot \mathrm{pdi\_112} - \mathrm{C50} \cdot \mathrm{IkBb} \cdot \mathrm{pdi\_142} - \mathrm{IkBb} \cdot \mathrm{P50P50} \cdot \mathrm{pdi\_132} - \mathrm{IkBb} \cdot \mathrm{pIKK} \cdot \mathrm{pii\_112} + \mathrm{k2\_77} \cdot \mathrm{pii\_32} \cdot \mathrm{tIkBb}\end{aligned} \tag{1.5}$$

$$\frac{d\left(\mathrm{IkBbn}\right)}{\mathrm{dt}} = \mathrm{IkBbA50n} \cdot \mathrm{pd\_122} + \mathrm{IkBbC50n} \cdot \mathrm{pd\_124} + \mathrm{IkBbAAn} \cdot \mathrm{pd\_121} + \mathrm{IkBb5050n} \cdot \mathrm{pd\_123} + \mathrm{IkBbA50n} \cdot \mathrm{pdi\_422} + \mathrm{IkBbAAn} \cdot \mathrm{pdi\_412} + \mathrm{IkBbC50n} \cdot \mathrm{pdi\_442} + \mathrm{IkBb5050n} \cdot \mathrm{pdi\_432} + \mathrm{IkBb} \cdot \mathrm{pii\_62} - \mathrm{IkBbn} \cdot \mathrm{pii\_52} - \mathrm{IkBbn} \cdot \mathrm{pii\_72} - \mathrm{A50n} \cdot \mathrm{IkBbn} \cdot \mathrm{pdi\_222} - \mathrm{AAn} \cdot \mathrm{IkBbn} \cdot \mathrm{pdi\_212} - \mathrm{C50n} \cdot \mathrm{IkBbn} \cdot \mathrm{pdi\_242} - \mathrm{IkBbn} \cdot \mathrm{P50P50n} \cdot \mathrm{pdi\_232} \tag{1.6}$$

$$\frac{d\left(\mathrm{tIkBe}\right)}{\mathrm{dt}} = \mathrm{kdel\_e1} \cdot \mathrm{tpre\_IkBe1} - \mathrm{pii\_23} \cdot \mathrm{tIkBe} + \frac{\mathrm{pii\_13}}{\left(\frac{\mathrm{A50n}}{\mathrm{pii\_103}}\right)^{\mathrm{pii\_93}} + \left(\frac{\mathrm{AAn}}{\mathrm{pii\_103}}\right)^{\mathrm{pii\_93}} + \left(\frac{\mathrm{C50n}}{\mathrm{pii\_103}}\right)^{\mathrm{pii\_93}} + 1} \tag{1.7}$$

$$\frac{d\left(\mathrm{IkBe}\right)}{\mathrm{dt}} = \mathrm{IkBeA50} \cdot \mathrm{pd\_112} + \mathrm{IkBeC50} \cdot \mathrm{pd\_114} + \mathrm{IkBeAA} \cdot \mathrm{pd\_111} + \mathrm{IkBe5050} \cdot \mathrm{pd\_113} + \mathrm{IkBeA50} \cdot \mathrm{pdi\_323} + \mathrm{IkBeAA} \cdot \mathrm{pdi\_313} + \mathrm{IkBeC50} \cdot \mathrm{pdi\_343} + \mathrm{IkBe5050} \cdot \mathrm{pdi\_333} - \mathrm{IkBe} \cdot \mathrm{pii\_43} - \mathrm{IkBe} \cdot \mathrm{pii\_63} + \mathrm{IkBen} \cdot \mathrm{pii\_73} - \mathrm{A50} \cdot \mathrm{IkBe} \cdot \mathrm{pdi\_123} - \mathrm{AA} \cdot \mathrm{IkBe} \cdot \mathrm{pdi\_113} - \mathrm{C50} \cdot \mathrm{IkBe} \cdot \mathrm{pdi\_143} - \mathrm{IkBe} \cdot \mathrm{P50P50} \cdot \mathrm{pdi\_133} - \mathrm{IkBe} \cdot \mathrm{pIKK} \cdot \mathrm{pii\_113} + \mathrm{k2\_77} \cdot \mathrm{pii\_33} \cdot \mathrm{tIkBe} \tag{1.8}$$

$$\frac{d\left(\mathrm{IkBen}\right)}{\mathrm{dt}} = \mathrm{IkBeA50n} \cdot \mathrm{pd\_122} + \mathrm{IkBeC50n} \cdot \mathrm{pd\_124} + \mathrm{IkBeAAn} \cdot \mathrm{pd\_121} + \mathrm{IkBe5050n} \cdot \mathrm{pd\_123} + \mathrm{IkBeA50n} \cdot \mathrm{pdi\_423} + \mathrm{IkBeAAn} \cdot \mathrm{pdi\_413} + \mathrm{IkBeC50n} \cdot \mathrm{pdi\_443} + \mathrm{IkBe5050n} \cdot \mathrm{pdi\_433} + \mathrm{IkBe} \cdot \mathrm{pii\_63} - \mathrm{IkBen} \cdot \mathrm{pii\_53} - \mathrm{IkBen} \cdot \mathrm{pii\_73} - \mathrm{A50n} \cdot \mathrm{IkBen} \cdot \mathrm{pdi\_223} - \mathrm{AAn} \cdot \mathrm{IkBen} \cdot \mathrm{pdi\_213} - \mathrm{C50n} \cdot \mathrm{IkBen} \cdot \mathrm{pdi\_243} - \mathrm{IkBen} \cdot \mathrm{P50P50n} \cdot \mathrm{pdi\_233} \tag{1.9}$$

$$\frac{d\left(\mathrm{tRelA}\right)}{\mathrm{dt}} = \mathrm{pm\_11} - \mathrm{pm\_21} \cdot \mathrm{tRelA} \tag{1.10}$$

$$\frac{d\left(\mathrm{RelA}\right)}{\mathrm{dt}} = \mathrm{A50} \cdot \mathrm{pd\_52} + 2 \cdot \mathrm{AA} \cdot \mathrm{pd\_51} - \mathrm{RelA} \cdot \mathrm{pm\_41} - 2 \cdot \mathrm{RelA}^2 \cdot \mathrm{pd\_31} - \mathrm{P50} \cdot \mathrm{RelA} \cdot \mathrm{pd\_32} + \mathrm{k2\_77} \cdot \mathrm{pm\_31} \cdot \mathrm{tRelA} \tag{1.11}$$

$$\frac{d\left(\mathrm{RelAn}\right)}{\mathrm{dt}} = \mathrm{A50n} \cdot \mathrm{pd\_62} + 2 \cdot \mathrm{AAn} \cdot \mathrm{pd\_61} - \mathrm{RelAn} \cdot \mathrm{pm\_51} - 2 \cdot \mathrm{RelAn}^2 \cdot \mathrm{pd\_41} - \mathrm{P50n} \cdot \mathrm{RelAn} \cdot \mathrm{pd\_42} \tag{1.12}$$

$$\frac{d\left(\mathrm{tP50}\right)}{\mathrm{dt}} = \frac{\mathrm{pm\_12}}{\left(\frac{\mathrm{A50n}}{\mathrm{pm\_82}}\right)^{\mathrm{pm\_72}} + \left(\frac{\mathrm{C50n}}{\mathrm{pm\_82}}\right)^{\mathrm{pm\_72}} + 1} + \mathrm{kdel\_p501} \cdot \mathrm{tpre\_P501} - \mathrm{pm\_22} \cdot \mathrm{tP50} \tag{1.13}$$

$$\frac{d\,(\mathrm{P50})}{\mathrm{dt}} = \mathrm{A50}\cdot \mathrm{pd\_52} + \mathrm{C50}\cdot \mathrm{pd\_54} + 2\cdot \mathrm{P50P50}\cdot \mathrm{pd\_53} - \mathrm{P50}\cdot \mathrm{pm\_42} - 2\cdot \mathrm{P50}^2 \cdot \mathrm{pd\_33} - \mathrm{P50}\cdot \mathrm{RelA}\cdot \mathrm{pd\_32} - \mathrm{P50}\cdot \mathrm{cRel}\cdot \mathrm{pd\_34} + \mathrm{k2\_77}\cdot \mathrm{pm\_32}\cdot \mathrm{tP50} \tag{1.14}$$

$$\frac{d\,(\mathrm{P50n})}{\mathrm{dt}} = \mathrm{A50n}\cdot \mathrm{pd\_62} + \mathrm{C50n}\cdot \mathrm{pd\_64} + 2\cdot \mathrm{P50P50n}\cdot \mathrm{pd\_63} - \mathrm{P50n}\cdot \mathrm{pm\_52} - 2\cdot \mathrm{P50n}^2\cdot \mathrm{pd\_43} - \mathrm{P50n}\cdot \mathrm{RelAn}\cdot \mathrm{pd\_42} - \mathrm{P50n}\cdot \mathrm{cReln}\cdot \mathrm{pd\_44} \tag{1.15}$$

$$\frac{d\,(\mathrm{tcRel})}{\mathrm{dt}} = \mathrm{kdel\_crel1}\cdot \mathrm{tpre\_cRel1} - \mathrm{pm\_23}\cdot \mathrm{tcRel} + \frac{\mathrm{kASC\_66}^{\mathrm{kASC\_67}}\cdot \mathrm{pm\_13}}{\left(\mathrm{Blimp\_1}^{\mathrm{kASC\_67}} + \mathrm{kASC\_66}^{\mathrm{kASC\_67}}\right)\cdot\left(\left(\frac{\mathrm{A50n}}{\mathrm{pm\_83}}\right)^{\mathrm{pm\_73}} + \left(\frac{\mathrm{C50n}}{\mathrm{pm\_83}}\right)^{\mathrm{pm\_73}} + 1\right)} \tag{1.16}$$

$$\frac{d\,(\mathrm{cRel})}{\mathrm{dt}} = \mathrm{C50}\cdot \mathrm{pd\_54} - \mathrm{cRel}\cdot \mathrm{pm\_43} - \mathrm{P50}\cdot \mathrm{cRel}\cdot \mathrm{pd\_34} + \mathrm{k2\_77}\cdot \mathrm{pm\_33}\cdot \mathrm{tcRel} \tag{1.17}$$

$$\frac{d\,(\mathrm{cReln})}{\mathrm{dt}} = \mathrm{C50n}\cdot \mathrm{pd\_64} - \mathrm{cReln}\cdot \mathrm{pm\_53} - \mathrm{P50n}\cdot \mathrm{cReln}\cdot \mathrm{pd\_44} \tag{1.18}$$

$$\frac{d\,(\mathrm{AA})}{\mathrm{dt}} = \mathrm{pd\_31}\cdot \mathrm{RelA}^2 - \mathrm{AA}\cdot \mathrm{pd\_51} - \mathrm{AA}\cdot \mathrm{pd\_71} - \mathrm{AA}\cdot \mathrm{pd\_91} + \mathrm{AAn}\cdot \mathrm{pd\_81} + \mathrm{IkBaAA}\cdot \mathrm{pdi\_311} + \mathrm{IkBbAA}\cdot \mathrm{pdi\_312} + \mathrm{IkBeAA}\cdot \mathrm{pdi\_313} + \mathrm{IkBaAA}\cdot \mathrm{pii\_131} + \mathrm{IkBbAA}\cdot \mathrm{pii\_132} + \mathrm{IkBeAA}\cdot \mathrm{pii\_133} - \mathrm{AA}\cdot \mathrm{IkBa}\cdot \mathrm{pdi\_111} - \mathrm{AA}\cdot \mathrm{IkBb}\cdot \mathrm{pdi\_112} - \mathrm{AA}\cdot \mathrm{IkBe}\cdot \mathrm{pdi\_113} + \mathrm{IkBaAA}\cdot \mathrm{pIKK}\cdot \mathrm{pii\_121} + \mathrm{IkBbAA}\cdot \mathrm{pIKK}\cdot \mathrm{pii\_122} + \mathrm{IkBeAA}\cdot \mathrm{pIKK}\cdot \mathrm{pii\_123} \tag{1.19}$$

$$\frac{d\,(\mathrm{AAn})}{\mathrm{dt}} = \mathrm{pd\_41}\cdot \mathrm{RelAn}^2 + \mathrm{AA}\cdot \mathrm{pd\_71} - \mathrm{AAn}\cdot \mathrm{pd\_61} - \mathrm{AAn}\cdot \mathrm{pd\_81} - \mathrm{AAn}\cdot \mathrm{pd\_101} + \mathrm{IkBaAAn}\cdot \mathrm{pdi\_411} + \mathrm{IkBbAAn}\cdot \mathrm{pdi\_412} + \mathrm{IkBeAAn}\cdot \mathrm{pdi\_413} + \mathrm{IkBaAAn}\cdot \mathrm{pii\_141} + \mathrm{IkBbAAn}\cdot \mathrm{pii\_142} + \mathrm{IkBeAAn}\cdot \mathrm{pii\_143} - \mathrm{AAn}\cdot \mathrm{IkBan}\cdot \mathrm{pdi\_211} - \mathrm{AAn}\cdot \mathrm{IkBbn}\cdot \mathrm{pdi\_212} - \mathrm{AAn}\cdot \mathrm{IkBen}\cdot \mathrm{pdi\_213} \tag{1.20}$$

$$\frac{d\,(\mathrm{IkBaAA})}{\mathrm{dt}} = \mathrm{IkBaAAn}\cdot \mathrm{pdi\_611} - \mathrm{IkBaAA}\cdot \mathrm{pdi\_311} - \mathrm{IkBaAA}\cdot \mathrm{pdi\_511} - \mathrm{IkBaAA}\cdot \mathrm{pd\_111} - \mathrm{IkBaAA}\cdot \mathrm{pii\_131} + \mathrm{AA}\cdot \mathrm{IkBa}\cdot \mathrm{pdi\_111} - \mathrm{IkBaAA}\cdot \mathrm{pIKK}\cdot \mathrm{pii\_121} \tag{1.21}$$

$$\frac{d\left(\mathrm{IkBaAAn}\right)}{\mathrm{dt}} = \mathrm{IkBaAA} \cdot \mathrm{pdi\_511} - \mathrm{IkBaAAn} \cdot \mathrm{pd\_121} - \mathrm{IkBaAAn} \cdot \mathrm{pdi\_411} - \mathrm{IkBaAAn} \cdot \mathrm{pdi\_611} - \mathrm{IkBaAAn} \cdot \mathrm{pii\_141} + \mathrm{AAn} \cdot \mathrm{IkBan} \cdot \mathrm{pdi\_211} \tag{1.22}$$

$$\frac{d\left(\mathrm{IkBbAA}\right)}{\mathrm{dt}} = \mathrm{IkBbAAn} \cdot \mathrm{pdi\_612} - \mathrm{IkBbAA} \cdot \mathrm{pdi\_312} - \mathrm{IkBbAA} \cdot \mathrm{pdi\_512} - \mathrm{IkBbAA} \cdot \mathrm{pd\_111} - \mathrm{IkBbAA} \cdot \mathrm{pii\_132} + \mathrm{AA} \cdot \mathrm{IkBb} \cdot \mathrm{pdi\_112} - \mathrm{IkBbAA} \cdot \mathrm{pIKK} \cdot \mathrm{pii\_122} \tag{1.23}$$

$$\frac{d\left(\mathrm{IkBbAAn}\right)}{\mathrm{dt}} = \mathrm{IkBbAA} \cdot \mathrm{pdi\_512} - \mathrm{IkBbAAn} \cdot \mathrm{pd\_121} - \mathrm{IkBbAAn} \cdot \mathrm{pdi\_412} - \mathrm{IkBbAAn} \cdot \mathrm{pdi\_612} - \mathrm{IkBbAAn} \cdot \mathrm{pii\_142} + \mathrm{AAn} \cdot \mathrm{IkBbn} \cdot \mathrm{pdi\_212} \tag{1.24}$$

$$\frac{d\left(\mathrm{IkBeAA}\right)}{\mathrm{dt}} = \mathrm{IkBeAAn} \cdot \mathrm{pdi\_613} - \mathrm{IkBeAA} \cdot \mathrm{pdi\_313} - \mathrm{IkBeAA} \cdot \mathrm{pdi\_513} - \mathrm{IkBeAA} \cdot \mathrm{pd\_111} - \mathrm{IkBeAA} \cdot \mathrm{pii\_133} + \mathrm{AA} \cdot \mathrm{IkBe} \cdot \mathrm{pdi\_113} - \mathrm{IkBeAA} \cdot \mathrm{pIKK} \cdot \mathrm{pii\_123} \tag{1.25}$$

$$\frac{d\left(\mathrm{IkBeAAn}\right)}{\mathrm{dt}} = \mathrm{IkBeAA} \cdot \mathrm{pdi\_513} - \mathrm{IkBeAAn} \cdot \mathrm{pd\_121} - \mathrm{IkBeAAn} \cdot \mathrm{pdi\_413} - \mathrm{IkBeAAn} \cdot \mathrm{pdi\_613} - \mathrm{IkBeAAn} \cdot \mathrm{pii\_143} + \mathrm{AAn} \cdot \mathrm{IkBen} \cdot \mathrm{pdi\_213} \tag{1.26}$$

$$\begin{aligned}\frac{d\left(\mathrm{A50}\right)}{\mathrm{dt}} = {} & \mathrm{A50n} \cdot \mathrm{pd\_82} - \mathrm{A50} \cdot \mathrm{pd\_72} - \mathrm{A50} \cdot \mathrm{pd\_92} - \mathrm{A50} \cdot \mathrm{pd\_52} + \mathrm{IkBaA50} \cdot \mathrm{pdi\_321} + \mathrm{IkBbA50} \cdot \mathrm{pdi\_322} + \mathrm{IkBeA50} \cdot \mathrm{pdi\_323} \\ & + \mathrm{IkBaA50} \cdot \mathrm{pii\_131} + \mathrm{IkBbA50} \cdot \mathrm{pii\_132} + \mathrm{IkBeA50} \cdot \mathrm{pii\_133} - \mathrm{A50} \cdot \mathrm{IkBa} \cdot \mathrm{pdi\_121} - \mathrm{A50} \cdot \mathrm{IkBb} \cdot \mathrm{pdi\_122} - \mathrm{A50} \cdot \mathrm{IkBe} \\ & \cdot \mathrm{pdi\_123} + \mathrm{P50} \cdot \mathrm{RelA} \cdot \mathrm{pd\_32} + \mathrm{IkBaA50} \cdot \mathrm{pIKK} \cdot \mathrm{pii\_121} + \mathrm{IkBbA50} \cdot \mathrm{pIKK} \cdot \mathrm{pii\_122} + \mathrm{IkBeA50} \cdot \mathrm{pIKK} \cdot \mathrm{pii\_123}\end{aligned} \tag{1.27}$$

$$\frac{d\left(\mathrm{A50n}\right)}{\mathrm{dt}} = \mathrm{A50} \cdot \mathrm{pd\_72} - \mathrm{A50n} \cdot \mathrm{pd\_62} - \mathrm{A50n} \cdot \mathrm{pd\_82} - \mathrm{A50n} \cdot \mathrm{pd\_102} + \mathrm{IkBaA50n} \cdot \mathrm{pdi\_421} + \mathrm{IkBbA50n} \cdot \mathrm{pdi\_422} + \mathrm{IkBeA50n} \cdot \mathrm{pdi\_423} + \mathrm{IkBaA50n} \cdot \mathrm{pii\_141} + \mathrm{IkBbA50n} \cdot \mathrm{pii\_142} + \mathrm{IkBeA50n} \cdot \mathrm{pii\_143} - \mathrm{A50n} \cdot \mathrm{IkBan} \cdot \mathrm{pdi\_221} - \mathrm{A50n} \cdot \mathrm{IkBbn} \cdot \mathrm{pdi\_222} - \mathrm{A50n} \cdot \mathrm{IkBen} \cdot \mathrm{pdi\_223} + \mathrm{P50n} \cdot \mathrm{RelAn} \cdot \mathrm{pd\_42} \tag{1.28}$$

$$\frac{d\,(\mathrm{IkBaA50})}{\mathrm{dt}} = \mathrm{IkBaA50n} \cdot \mathrm{pdi\_621} - \mathrm{IkBaA50} \cdot \mathrm{pdi\_321} - \mathrm{IkBaA50} \cdot \mathrm{pdi\_521} - \mathrm{IkBaA50} \cdot \mathrm{pd\_112} - \mathrm{IkBaA50} \cdot \mathrm{pii\_131} + \mathrm{A50} \cdot \mathrm{IkBa} \cdot \mathrm{pdi\_121} - \mathrm{IkBaA50} \cdot \mathrm{pIKK} \cdot \mathrm{pii\_121} \tag{1.29}$$

$$\frac{d\,(\mathrm{IkBaA50n})}{\mathrm{dt}} = \mathrm{IkBaA50} \cdot \mathrm{pdi\_521} - \mathrm{IkBaA50n} \cdot \mathrm{pd\_122} - \mathrm{IkBaA50n} \cdot \mathrm{pdi\_421} - \mathrm{IkBaA50n} \cdot \mathrm{pdi\_621} - \mathrm{IkBaA50n} \cdot \mathrm{pii\_141} + \mathrm{A50n} \cdot \mathrm{IkBan} \cdot \mathrm{pdi\_221} \tag{1.30}$$

$$\frac{d\,(\mathrm{IkBbA50})}{\mathrm{dt}} = \mathrm{IkBbA50n} \cdot \mathrm{pdi\_622} - \mathrm{IkBbA50} \cdot \mathrm{pdi\_322} - \mathrm{IkBbA50} \cdot \mathrm{pdi\_522} - \mathrm{IkBbA50} \cdot \mathrm{pd\_112} - \mathrm{IkBbA50} \cdot \mathrm{pii\_132} + \mathrm{A50} \cdot \mathrm{IkBb} \cdot \mathrm{pdi\_122} - \mathrm{IkBbA50} \cdot \mathrm{pIKK} \cdot \mathrm{pii\_122} \tag{1.31}$$

$$\frac{d\,(\mathrm{IkBbA50n})}{\mathrm{dt}} = \mathrm{IkBbA50} \cdot \mathrm{pdi\_522} - \mathrm{IkBbA50n} \cdot \mathrm{pd\_122} - \mathrm{IkBbA50n} \cdot \mathrm{pdi\_422} - \mathrm{IkBbA50n} \cdot \mathrm{pdi\_622} - \mathrm{IkBbA50n} \cdot \mathrm{pii\_142} + \mathrm{A50n} \cdot \mathrm{IkBbn} \cdot \mathrm{pdi\_222} \tag{1.32}$$

$$\frac{d\,(\mathrm{IkBeA50})}{\mathrm{dt}} = \mathrm{IkBeA50n} \cdot \mathrm{pdi\_623} - \mathrm{IkBeA50} \cdot \mathrm{pdi\_323} - \mathrm{IkBeA50} \cdot \mathrm{pdi\_523} - \mathrm{IkBeA50} \cdot \mathrm{pd\_112} - \mathrm{IkBeA50} \cdot \mathrm{pii\_133} + \mathrm{A50} \cdot \mathrm{IkBe} \cdot \mathrm{pdi\_123} - \mathrm{IkBeA50} \cdot \mathrm{pIKK} \cdot \mathrm{pii\_123} \tag{1.33}$$

$$\frac{d\,(\mathrm{IkBeA50n})}{\mathrm{dt}} = \mathrm{IkBeA50} \cdot \mathrm{pdi\_523} - \mathrm{IkBeA50n} \cdot \mathrm{pd\_122} - \mathrm{IkBeA50n} \cdot \mathrm{pdi\_423} - \mathrm{IkBeA50n} \cdot \mathrm{pdi\_623} - \mathrm{IkBeA50n} \cdot \mathrm{pii\_143} + \mathrm{A50n} \cdot \mathrm{IkBen} \cdot \mathrm{pdi\_223} \tag{1.34}$$

$$\frac{d\,(\mathrm{P50P50})}{\mathrm{dt}} = \mathrm{pd\_33} \cdot \mathrm{P50}^2 + \mathrm{IkBa5050} \cdot \mathrm{pdi\_331} + \mathrm{IkBb5050} \cdot \mathrm{pdi\_332} + \mathrm{IkBe5050} \cdot \mathrm{pdi\_333} + \mathrm{IkBa5050} \cdot \mathrm{pii\_131} + \mathrm{IkBb5050} \cdot \mathrm{pii\_132} + \mathrm{IkBe5050} \cdot \mathrm{pii\_133} - \mathrm{P50P50} \cdot \mathrm{pd\_53} - \mathrm{P50P50} \cdot \mathrm{pd\_73} - \mathrm{P50P50} \cdot \mathrm{pd\_93} + \mathrm{P50P50n} \cdot \mathrm{pd\_83} - \mathrm{IkBa} \cdot \mathrm{P50P50} \cdot \mathrm{pdi\_131} - \mathrm{IkBb} \cdot \mathrm{P50P50} \cdot \mathrm{pdi\_132} - \mathrm{IkBe} \cdot \mathrm{P50P50} \cdot \mathrm{pdi\_133} + \mathrm{IkBa5050} \cdot \mathrm{pIKK} \cdot \mathrm{pii\_121} + \mathrm{IkBb5050} \cdot \mathrm{pIKK} \cdot \mathrm{pii\_122} + \mathrm{IkBe5050} \cdot \mathrm{pIKK} \cdot \mathrm{pii\_123} \tag{1.35}$$

$$\frac{d\,(\mathrm{P50P50n})}{\mathrm{dt}} = \mathrm{pd\_43} \cdot \mathrm{P50n}^2 + \mathrm{IkBa5050n} \cdot \mathrm{pdi\_431} + \mathrm{IkBb5050n} \cdot \mathrm{pdi\_432} + \mathrm{IkBe5050n} \cdot \mathrm{pdi\_433} + \mathrm{IkBa5050n} \cdot \mathrm{pii\_141} + \mathrm{IkBb5050n} \cdot \mathrm{pii\_142} + \mathrm{IkBe5050n} \cdot \mathrm{pii\_143} + \mathrm{P50P50} \cdot \mathrm{pd\_73} - \mathrm{P50P50n} \cdot \mathrm{pd\_63} - \mathrm{P50P50n} \cdot \mathrm{pd\_83} - \mathrm{P50P50n} \cdot \mathrm{pd\_103} - \mathrm{IkBan} \cdot \mathrm{P50P50n} \cdot \mathrm{pdi\_231} - \mathrm{IkBbn} \cdot \mathrm{P50P50n} \cdot \mathrm{pdi\_232} - \mathrm{IkBen} \cdot \mathrm{P50P50n} \cdot \mathrm{pdi\_233} \tag{1.36}$$

$$\frac{d\,(\mathrm{IkBa5050})}{\mathrm{dt}} = \mathrm{IkBa5050n} \cdot \mathrm{pdi\_631} - \mathrm{IkBa5050} \cdot \mathrm{pdi\_331} - \mathrm{IkBa5050} \cdot \mathrm{pdi\_531} - \mathrm{IkBa5050} \cdot \mathrm{pd\_113} - \mathrm{IkBa5050} \cdot \mathrm{pii\_131} + \mathrm{IkBa} \cdot \mathrm{P50P50} \cdot \mathrm{pdi\_131} - \mathrm{IkBa5050} \cdot \mathrm{pIKK} \cdot \mathrm{pii\_121} \tag{1.37}$$

$$\frac{d\,(\mathrm{IkBa5050n})}{\mathrm{dt}} = \mathrm{IkBa5050} \cdot \mathrm{pdi\_531} - \mathrm{IkBa5050n} \cdot \mathrm{pd\_123} - \mathrm{IkBa5050n} \cdot \mathrm{pdi\_431} - \mathrm{IkBa5050n} \cdot \mathrm{pdi\_631} - \mathrm{IkBa5050n} \cdot \mathrm{pii\_141} + \mathrm{IkBan} \cdot \mathrm{P50P50n} \cdot \mathrm{pdi\_231} \tag{1.38}$$

$$\frac{d\,(\mathrm{IkBb5050})}{\mathrm{dt}} = \mathrm{IkBb5050n} \cdot \mathrm{pdi\_632} - \mathrm{IkBb5050} \cdot \mathrm{pdi\_332} - \mathrm{IkBb5050} \cdot \mathrm{pdi\_532} - \mathrm{IkBb5050} \cdot \mathrm{pd\_113} - \mathrm{IkBb5050} \cdot \mathrm{pii\_132} + \mathrm{IkBb} \cdot \mathrm{P50P50} \cdot \mathrm{pdi\_132} - \mathrm{IkBb5050} \cdot \mathrm{pIKK} \cdot \mathrm{pii\_122} \tag{1.39}$$

$$\frac{d\,(\mathrm{IkBb5050n})}{\mathrm{dt}} = \mathrm{IkBb5050} \cdot \mathrm{pdi\_532} - \mathrm{IkBb5050n} \cdot \mathrm{pd\_123} - \mathrm{IkBb5050n} \cdot \mathrm{pdi\_432} - \mathrm{IkBb5050n} \cdot \mathrm{pdi\_632} - \mathrm{IkBb5050n} \cdot \mathrm{pii\_142} + \mathrm{IkBbn} \cdot \mathrm{P50P50n} \cdot \mathrm{pdi\_232} \tag{1.40}$$

$$\frac{d\,(\mathrm{IkBe5050})}{\mathrm{dt}} = \mathrm{IkBe5050n} \cdot \mathrm{pdi\_633} - \mathrm{IkBe5050} \cdot \mathrm{pdi\_333} - \mathrm{IkBe5050} \cdot \mathrm{pdi\_533} - \mathrm{IkBe5050} \cdot \mathrm{pd\_113} - \mathrm{IkBe5050} \cdot \mathrm{pii\_133} + \mathrm{IkBe} \cdot \mathrm{P50P50} \cdot \mathrm{pdi\_133} - \mathrm{IkBe5050} \cdot \mathrm{pIKK} \cdot \mathrm{pii\_123} \tag{1.41}$$

$$\frac{d\,(\mathrm{IkBe5050n})}{\mathrm{dt}} = \mathrm{IkBe5050} \cdot \mathrm{pdi\_533} - \mathrm{IkBe5050n} \cdot \mathrm{pd\_123} - \mathrm{IkBe5050n} \cdot \mathrm{pdi\_433} - \mathrm{IkBe5050n} \cdot \mathrm{pdi\_633} - \mathrm{IkBe5050n} \cdot \mathrm{pii\_143} + \mathrm{IkBen} \cdot \mathrm{P50P50n} \cdot \mathrm{pdi\_233} \tag{1.42}$$

$$\frac{d\,(\mathrm{C50})}{\mathrm{dt}} = \mathrm{C50n}\cdot\mathrm{pd\_84} - \mathrm{C50}\cdot\mathrm{pd\_74} - \mathrm{C50}\cdot\mathrm{pd\_94} - \mathrm{C50}\cdot\mathrm{pd\_54} + \mathrm{IkBaC50}\cdot\mathrm{pdi\_341} + \mathrm{IkBbC50}\cdot\mathrm{pdi\_342} + \mathrm{IkBeC50}\cdot\mathrm{pdi\_343} + \mathrm{IkBaC50}\cdot\mathrm{pii\_131} + \mathrm{IkBbC50}\cdot\mathrm{pii\_132} + \mathrm{IkBeC50}\cdot\mathrm{pii\_133} - \mathrm{C50}\cdot\mathrm{IkBa}\cdot\mathrm{pdi\_141} - \mathrm{C50}\cdot\mathrm{IkBb}\cdot\mathrm{pdi\_142} - \mathrm{C50}\cdot\mathrm{IkBe}\cdot\mathrm{pdi\_143} + \mathrm{P50}\cdot\mathrm{cRel}\cdot\mathrm{pd\_34} + \mathrm{IkBaC50}\cdot\mathrm{pIKK}\cdot\mathrm{pii\_121} + \mathrm{IkBbC50}\cdot\mathrm{pIKK}\cdot\mathrm{pii\_122} + \mathrm{IkBeC50}\cdot\mathrm{pIKK}\cdot\mathrm{pii\_123} \tag{1.43}$$

$$\frac{d\,(\mathrm{C50n})}{\mathrm{dt}} = \mathrm{C50}\cdot\mathrm{pd\_74} - \mathrm{C50n}\cdot\mathrm{pd\_64} - \mathrm{C50n}\cdot\mathrm{pd\_84} - \mathrm{C50n}\cdot\mathrm{pd\_104} + \mathrm{IkBaC50n}\cdot\mathrm{pdi\_441} + \mathrm{IkBbC50n}\cdot\mathrm{pdi\_442} + \mathrm{IkBeC50n}\cdot\mathrm{pdi\_443} + \mathrm{IkBaC50n}\cdot\mathrm{pii\_141} + \mathrm{IkBbC50n}\cdot\mathrm{pii\_142} + \mathrm{IkBeC50n}\cdot\mathrm{pii\_143} - \mathrm{C50n}\cdot\mathrm{IkBan}\cdot\mathrm{pdi\_241} - \mathrm{C50n}\cdot\mathrm{IkBbn}\cdot\mathrm{pdi\_242} - \mathrm{C50n}\cdot\mathrm{IkBen}\cdot\mathrm{pdi\_243} + \mathrm{P50n}\cdot\mathrm{cReln}\cdot\mathrm{pd\_44} \tag{1.44}$$

$$\frac{d\,(\mathrm{IkBaC50})}{\mathrm{dt}} = \mathrm{IkBaC50n}\cdot\mathrm{pdi\_641} - \mathrm{IkBaC50}\cdot\mathrm{pdi\_341} - \mathrm{IkBaC50}\cdot\mathrm{pdi\_541} - \mathrm{IkBaC50}\cdot\mathrm{pd\_114} - \mathrm{IkBaC50}\cdot\mathrm{pii\_131} + \mathrm{C50}\cdot\mathrm{IkBa}\cdot\mathrm{pdi\_141} - \mathrm{IkBaC50}\cdot\mathrm{pIKK}\cdot\mathrm{pii\_121} \tag{1.45}$$

$$\frac{d\,(\mathrm{IkBaC50n})}{\mathrm{dt}} = \mathrm{IkBaC50}\cdot\mathrm{pdi\_541} - \mathrm{IkBaC50n}\cdot\mathrm{pd\_124} - \mathrm{IkBaC50n}\cdot\mathrm{pdi\_441} - \mathrm{IkBaC50n}\cdot\mathrm{pdi\_641} - \mathrm{IkBaC50n}\cdot\mathrm{pii\_141} + \mathrm{C50n}\cdot\mathrm{IkBan}\cdot\mathrm{pdi\_241} \tag{1.46}$$

$$\frac{d\,(\mathrm{IkBbC50})}{\mathrm{dt}} = \mathrm{IkBbC50n}\cdot\mathrm{pdi\_642} - \mathrm{IkBbC50}\cdot\mathrm{pdi\_342} - \mathrm{IkBbC50}\cdot\mathrm{pdi\_542} - \mathrm{IkBbC50}\cdot\mathrm{pd\_114} - \mathrm{IkBbC50}\cdot\mathrm{pii\_132} + \mathrm{C50}\cdot\mathrm{IkBb}\cdot\mathrm{pdi\_142} - \mathrm{IkBbC50}\cdot\mathrm{pIKK}\cdot\mathrm{pii\_122} \tag{1.47}$$

$$\frac{d\,(\mathrm{IkBbC50n})}{\mathrm{dt}} = \mathrm{IkBbC50}\cdot\mathrm{pdi\_542} - \mathrm{IkBbC50n}\cdot\mathrm{pd\_124} - \mathrm{IkBbC50n}\cdot\mathrm{pdi\_442} - \mathrm{IkBbC50n}\cdot\mathrm{pdi\_642} - \mathrm{IkBbC50n}\cdot\mathrm{pii\_142} + \mathrm{C50n}\cdot\mathrm{IkBbn}\cdot\mathrm{pdi\_242} \tag{1.48}$$

$$\frac{d\,(\mathrm{IkBeC50})}{\mathrm{dt}} = \mathrm{IkBeC50n}\cdot\mathrm{pdi\_643} - \mathrm{IkBeC50}\cdot\mathrm{pdi\_343} - \mathrm{IkBeC50}\cdot\mathrm{pdi\_543} - \mathrm{IkBeC50}\cdot\mathrm{pd\_114} - \mathrm{IkBeC50}\cdot\mathrm{pii\_133} + \mathrm{C50}\cdot\mathrm{IkBe}\cdot\mathrm{pdi\_143} - \mathrm{IkBeC50}\cdot\mathrm{pIKK}\cdot\mathrm{pii\_123} \tag{1.49}$$

$$\frac{d\left(\text{IkBeC50n}\right)}{\text{dt}} = \text{IkBeC50} \cdot \text{pdi\_543} - \text{IkBeC50n} \cdot \text{pd\_124} - \text{IkBeC50n} \cdot \text{pdi\_443} - \text{IkBeC50n} \cdot \text{pdi\_643} - \text{IkBeC50n} \cdot \text{pii\_143} + \text{C50n} \cdot \text{IkBen} \cdot \text{pdi\_243} \tag{1.50}$$

$$\frac{d\left(\text{LL}\right)}{\text{dt}} = 0 \tag{1.51}$$

$$\frac{d\left(\text{RR}\right)}{\text{dt}} = \text{LR} \cdot k\_2 - \text{RR} \cdot k\_72 + k\_71 \cdot \text{k2\_77} + \text{LL} \cdot \text{RR} \cdot k\_1 \cdot \left(\frac{\text{Blimp\_1}}{\text{Blimp\_1} + 4} - 1\right) \tag{1.52}$$

$$\frac{d\left(\text{LR}\right)}{\text{dt}} = -\text{LR} \cdot k\_2 - \text{LR} \cdot k\_3 - \text{LL} \cdot \text{RR} \cdot k\_1 \cdot \left(\frac{\text{Blimp\_1}}{\text{Blimp\_1} + 4} - 1\right) \tag{1.53}$$

$$\frac{d\left(\text{DISC}\right)}{\text{dt}} = \text{DISCpC\_8} \cdot k\_7 + \text{DISCpC\_8} \cdot k\_8 + \text{LR} \cdot k\_3 + \text{flipDISC} \cdot k\_5 - \text{DISC} \cdot \text{flipp} \cdot k\_4 - \text{DISC} \cdot k\_6 \cdot \text{pC\_8} \tag{1.54}$$

$$\frac{d\left(\text{flipp}\right)}{\text{dt}} = \text{flipDISC} \cdot k\_5 - \text{flipp} \cdot k\_74 + k\_73 \cdot \text{k2\_77} - \text{DISC} \cdot \text{flipp} \cdot k\_4 \tag{1.55}$$

$$\frac{d\left(\text{flipDISC}\right)}{\text{dt}} = \text{DISC} \cdot \text{flipp} \cdot k\_4 - \text{flipDISC} \cdot k\_75 - \text{flipDISC} \cdot k\_5 \tag{1.56}$$

$$\frac{d\left(\text{pC\_8}\right)}{\text{dt}} = \text{C6pC\_8} \cdot k\_18 + \text{DISCpC\_8} \cdot k\_7 + k\_76 \cdot \text{k2\_77} - k\_77 \cdot \text{pC\_8} - C\_6 \cdot k\_17 \cdot \text{pC\_8} - \text{DISC} \cdot k\_6 \cdot \text{pC\_8} \tag{1.57}$$

$$\frac{d\left(\text{DISCpC\_8}\right)}{\text{dt}} = \text{DISC} \cdot k\_6 \cdot \text{pC\_8} - \text{DISCpC\_8} \cdot k\_8 - \text{DISCpC\_8} \cdot k\_7 \tag{1.58}$$

$$\frac{d\left(C\_8\right)}{\text{dt}} = \text{BarC\_8} \cdot k\_10 + \text{C8Bid} \cdot k\_27 + \text{C8Bid} \cdot k\_28 + \text{C6pC\_8} \cdot k\_19 + \text{C8pC\_3} \cdot k\_12 + \text{C8pC\_3} \cdot k\_13 + \text{DISCpC\_8} \cdot k\_8 - \text{Barp} \cdot C\_8 \cdot k\_9 - \text{Bid} \cdot C\_8 \cdot k\_26 - C\_8 \cdot k\_11 \cdot \text{pC\_3} \tag{1.59}$$

$$\frac{d\,(\mathrm{Barp})}{\mathrm{dt}} = \mathrm{BarC\_8} \cdot k\_10 - \mathrm{Barp} \cdot k\_79 + k\_78 \cdot \mathrm{k2\_77} - \mathrm{Barp} \cdot C\_8 \cdot k\_9 \tag{1.60}$$

$$\frac{d\,(\mathrm{BarC\_8})}{\mathrm{dt}} = \mathrm{Barp} \cdot C\_8 \cdot k\_9 - \mathrm{BarC\_8} \cdot k\_80 - \mathrm{BarC\_8} \cdot k\_10 \tag{1.61}$$

$$\frac{d\,(\mathrm{pC\_3})}{\mathrm{dt}} = \mathrm{ApoppC\_3} \cdot k\_63 + \mathrm{C8pC\_3} \cdot k\_12 + k\_101 \cdot \mathrm{k2\_77} - k\_102 \cdot \mathrm{pC\_3} - \mathrm{Apop} \cdot k\_62 \cdot \mathrm{pC\_3} - C\_8 \cdot k\_11 \cdot \mathrm{pC\_3} \tag{1.62}$$

$$\frac{d\,(\mathrm{C8pC\_3})}{\mathrm{dt}} = C\_8 \cdot k\_11 \cdot \mathrm{pC\_3} - \mathrm{C8pC\_3} \cdot k\_13 - \mathrm{C8pC\_3} \cdot k\_12 \tag{1.63}$$

$$\begin{aligned}\frac{d\,(C\_3)}{\mathrm{dt}} = {} & \mathrm{ApoppC\_3} \cdot k\_64 + \mathrm{C3PARP} \cdot k\_24 + \mathrm{C3PARP} \cdot k\_25 + \mathrm{C3pC\_6} \cdot k\_15 + \mathrm{C3pC\_6} \cdot k\_16 \\ & + \mathrm{C8pC\_3} \cdot k\_13 + \mathrm{XIAPC\_3} \cdot k\_21 - C\_3 \cdot \mathrm{PARP} \cdot k\_23 - C\_3 \cdot \mathrm{XIAP} \cdot k\_20 - C\_3 \cdot k\_14 \cdot \mathrm{pC\_6}\end{aligned} \tag{1.64}$$

$$\frac{d\,(\mathrm{pC\_6})}{\mathrm{dt}} = \mathrm{C3pC\_6} \cdot k\_15 + k\_104 \cdot \mathrm{k2\_77} - k\_105 \cdot \mathrm{pC\_6} - C\_3 \cdot k\_14 \cdot \mathrm{pC\_6} \tag{1.65}$$

$$\frac{d\,(\mathrm{C3pC\_6})}{\mathrm{dt}} = C\_3 \cdot k\_14 \cdot \mathrm{pC\_6} - \mathrm{C3pC\_6} \cdot k\_16 - \mathrm{C3pC\_6} \cdot k\_15 \tag{1.66}$$

$$\frac{d\,(C\_6)}{\mathrm{dt}} = \mathrm{C3pC\_6} \cdot k\_16 - C\_6 \cdot k\_106 + \mathrm{C6pC\_8} \cdot k\_18 + \mathrm{C6pC\_8} \cdot k\_19 - C\_6 \cdot k\_17 \cdot \mathrm{pC\_8} \tag{1.67}$$

$$\frac{d\,(\mathrm{C6pC\_8})}{\mathrm{dt}} = C\_6 \cdot k\_17 \cdot \mathrm{pC\_8} - \mathrm{C6pC\_8} \cdot k\_19 - \mathrm{C6pC\_8} \cdot k\_18 \tag{1.68}$$

$$\begin{aligned}\frac{d\,(\mathrm{XIAP})}{\mathrm{dt}} = {} & \mathrm{ApopXIAP} \cdot k\_68 + \mathrm{XIAPC\_3} \cdot k\_21 + \mathrm{XIAPC\_3} \cdot k\_22 - \mathrm{XIAP} \cdot k\_96 + \mathrm{cSmacXIAP} \\ & \cdot k\_70 + k\_95 \cdot \mathrm{k2\_77} - \mathrm{Apop} \cdot \mathrm{XIAP} \cdot k\_67 - C\_3 \cdot \mathrm{XIAP} \cdot k\_20 - \mathrm{XIAP} \cdot \mathrm{cSmac} \cdot k\_69\end{aligned} \tag{1.69}$$

$$\frac{d\,(\mathrm{XIAPC\_3})}{\mathrm{dt}} = C\_3 \cdot \mathrm{XIAP} \cdot k\_20 - \mathrm{XIAPC\_3} \cdot k\_22 - \mathrm{XIAPC\_3} \cdot k\_21 \tag{1.70}$$

$$\frac{d\,(\mathrm{PARP})}{\mathrm{dt}} = \mathrm{C3PARP} \cdot k\_24 - \mathrm{PARP} \cdot k\_109 + k\_108 \cdot \mathrm{k2\_77} - C\_3 \cdot \mathrm{PARP} \cdot k\_23 \tag{1.71}$$

$$\frac{d\,(\mathrm{C3PARP})}{\mathrm{dt}} = C\_3 \cdot \mathrm{PARP} \cdot k\_23 - \mathrm{C3PARP} \cdot k\_25 - \mathrm{C3PARP} \cdot k\_24 \tag{1.72}$$

$$\frac{d\,(\mathrm{CPARP})}{\mathrm{dt}} = \mathrm{C3PARP} \cdot k\_25 - \mathrm{CPARP} \cdot k\_110 \tag{1.73}$$

$$\frac{d\,(\mathrm{Bid})}{\mathrm{dt}} = \mathrm{C8Bid} \cdot k\_27 - \mathrm{Bid} \cdot k\_82 + k\_81 \cdot \mathrm{k2\_77} - \mathrm{Bid} \cdot C\_8 \cdot k\_26 \tag{1.74}$$

$$\frac{d\,(\mathrm{C8Bid})}{\mathrm{dt}} = \mathrm{Bid} \cdot C\_8 \cdot k\_26 - \mathrm{C8Bid} \cdot k\_28 - \mathrm{C8Bid} \cdot k\_27 \tag{1.75}$$

$$\frac{d\,(\mathrm{tBid})}{\mathrm{dt}} = \mathrm{C8Bid} \cdot k\_28 + \mathrm{Mcl1tBid} \cdot k\_30 + k\_32 \cdot \mathrm{tBidBax} + k\_33 \cdot \mathrm{tBidBax} - \mathrm{Bax} \cdot k\_31 \cdot \mathrm{tBid} - \mathrm{Mcl\_1} \cdot k\_29 \cdot \mathrm{tBid} \tag{1.76}$$

$$\begin{aligned}\frac{d\,(\mathrm{Mcl\_1})}{\mathrm{dt}} = {} & \mathrm{Mcl1tBid} \cdot k\_30 - \mathrm{Mcl\_1} \cdot k\_84 + \mathrm{k2\_77} \cdot k\_\mathrm{mcl} + \mathrm{MCLMCLi} \cdot \mathrm{kimcli} \\ & \cdot \mathrm{phase} - \mathrm{Mcl\_1} \cdot k\_29 \cdot \mathrm{tBid} - \mathrm{MCLi} \cdot \mathrm{Mcl\_1} \cdot \mathrm{kmcli} \cdot \mathrm{phase}\end{aligned} \tag{1.77}$$

$$\frac{d\,(\mathrm{Mcl1tBid})}{\mathrm{dt}} = \mathrm{Mcl\_1} \cdot k\_29 \cdot \mathrm{tBid} - \mathrm{Mcl1tBid} \cdot k\_85 - \mathrm{Mcl1tBid} \cdot k\_30 \tag{1.78}$$

$$\frac{d\,(\mathrm{Bax})}{\mathrm{dt}} = k\_86 \cdot \mathrm{k2\_77} - \mathrm{Bax} \cdot k\_87 + k\_32 \cdot \mathrm{tBidBax} - \mathrm{Bax} \cdot k\_31 \cdot \mathrm{tBid} \tag{1.79}$$

$$\frac{d\,(\mathrm{tBidBax})}{\mathrm{dt}} = \mathrm{Bax} \cdot k\_31 \cdot \mathrm{tBid} - k\_33 \cdot \mathrm{tBidBax} - k\_32 \cdot \mathrm{tBidBax} \tag{1.80}$$

$$\frac{d\,(\text{act\_Bax})}{\text{dt}} = \text{Baxm} \cdot k\_35 - \text{act\_Bax} \cdot k\_34 + k\_33 \cdot \text{tBidBax} \tag{1.81}$$

$$\frac{d\,(\text{Baxm})}{\text{dt}} = 2 \cdot \text{Bax\_2} \cdot k\_39 - \text{Baxm} \cdot k\_35 + \text{BaxmBcl\_2} \cdot k\_37 + \text{act\_Bax} \cdot k\_34 - \frac{2 \cdot \text{Baxm}^2 \cdot k\_38}{\text{mvol}} - \frac{\text{Baxm} \cdot \text{Bcl\_2} \cdot k\_36}{\text{mvol}} \tag{1.82}$$

$$\begin{aligned}\frac{d\,(\text{Bcl\_2})}{\text{dt}} = {} & \text{Bax2Bcl\_2} \cdot k\_41 + \text{Bax4Bcl\_2} \cdot k\_45 + \text{BaxmBcl\_2} \cdot k\_37 - \text{Bcl\_2} \cdot k\_89 - 277.2133 \cdot \text{k2\_77} \cdot (\text{phase} - 1) \\ & + 0.3070 \cdot \text{k2\_77} \cdot \text{mBcl\_2} \cdot \text{phase} - \frac{\text{Bax\_2} \cdot \text{Bcl\_2} \cdot k\_40}{\text{mvol}} - \frac{\text{Bax\_4} \cdot \text{Bcl\_2} \cdot k\_44}{\text{mvol}} - \frac{\text{Baxm} \cdot \text{Bcl\_2} \cdot k\_36}{\text{mvol}}\end{aligned} \tag{1.83}$$

$$\frac{d\,(\text{BaxmBcl\_2})}{\text{dt}} = \frac{\text{Baxm} \cdot \text{Bcl\_2} \cdot k\_36}{\text{mvol}} - \text{BaxmBcl\_2} \cdot k\_90 - \text{BaxmBcl\_2} \cdot k\_37 \tag{1.84}$$

$$\frac{d\,(\text{Bax\_2})}{\text{dt}} = 2 \cdot \text{Bax\_4} \cdot k\_43 - \text{Bax\_2} \cdot k\_39 + \text{Bax2Bcl\_2} \cdot k\_41 - \frac{2 \cdot \text{Bax\_2}^2 \cdot k\_42}{\text{mvol}} + \frac{\text{Baxm}^2 \cdot k\_38}{\text{mvol}} - \frac{\text{Bax\_2} \cdot \text{Bcl\_2} \cdot k\_40}{\text{mvol}} \tag{1.85}$$

$$\frac{d\,(\text{Bax2Bcl\_2})}{\text{dt}} = \frac{\text{Bax\_2} \cdot \text{Bcl\_2} \cdot k\_40}{\text{mvol}} - \text{Bax2Bcl\_2} \cdot k\_91 - \text{Bax2Bcl\_2} \cdot k\_41 \tag{1.86}$$

$$\frac{d\,(\text{Bax\_4})}{\text{dt}} = \text{Bax4M} \cdot k\_47 - \text{Bax\_4} \cdot k\_43 + \text{Bax4Bcl\_2} \cdot k\_45 + \frac{\text{Bax\_2}^2 \cdot k\_42}{\text{mvol}} - \frac{\text{Bax\_4} \cdot \text{Bcl\_2} \cdot k\_44}{\text{mvol}} - \frac{\text{Bax\_4} \cdot \text{MM} \cdot k\_46}{\text{mvol}} \tag{1.87}$$

$$\frac{d\,(\text{Bax4Bcl\_2})}{\text{dt}} = \frac{\text{Bax\_4} \cdot \text{Bcl\_2} \cdot k\_44}{\text{mvol}} - \text{Bax4Bcl\_2} \cdot k\_92 - \text{Bax4Bcl\_2} \cdot k\_45 \tag{1.88}$$

$$\frac{d\,(\text{MM})}{\text{dt}} = \text{AMito} \cdot k\_93 + \text{Bax4M} \cdot k\_47 - \frac{\text{Bax\_4} \cdot \text{MM} \cdot k\_46}{\text{mvol}} \tag{1.89}$$

$$\frac{d\,(\text{Bax4M})}{\text{dt}} = \frac{\text{Bax\_4} \cdot \text{MM} \cdot k\_46}{\text{mvol}} - \text{Bax4M} \cdot k\_48 - \text{Bax4M} \cdot k\_47 \tag{1.90}$$

$$\frac{d\,(\mathrm{AMito})}{\mathrm{dt}} = \mathrm{AMitomSmac}\cdot k\_53 - \mathrm{AMito}\cdot k\_93 + \mathrm{AMitomSmac}\cdot k\_54 + \mathrm{AMitomCytoC}\cdot k\_50 + \mathrm{AMitomCytoC}\cdot k\_51 + \mathrm{Bax4M}\cdot k\_48 - \frac{\mathrm{AMito}\cdot k\_49\cdot \mathrm{mCytoC}}{\mathrm{mvol}} - \frac{\mathrm{AMito}\cdot k\_52\cdot \mathrm{mSmac}}{\mathrm{mvol}} \tag{1.91}$$

$$\frac{d\,(\mathrm{mCytoC})}{\mathrm{dt}} = \mathrm{AMitomCytoC}\cdot k\_50 + k\_113\cdot \mathrm{k2\_77} - k\_114\cdot \mathrm{mCytoC} - \frac{\mathrm{AMito}\cdot k\_49\cdot \mathrm{mCytoC}}{\mathrm{mvol}} \tag{1.92}$$

$$\frac{d\,(\mathrm{AMitomCytoC})}{\mathrm{dt}} = \frac{\mathrm{AMito}\cdot k\_49\cdot \mathrm{mCytoC}}{\mathrm{mvol}} - \mathrm{AMitomCytoC}\cdot k\_51 - \mathrm{AMitomCytoC}\cdot k\_50 \tag{1.93}$$

$$\frac{d\,(\mathrm{ACytoC})}{\mathrm{dt}} = \mathrm{AMitomCytoC}\cdot k\_51 - \mathrm{ACytoC}\cdot k\_55 + \mathrm{CytoC}\cdot k\_56 \tag{1.94}$$

$$\frac{d\,(\mathrm{mSmac})}{\mathrm{dt}} = \mathrm{AMitomSmac}\cdot k\_53 + k\_97\cdot \mathrm{k2\_77} - k\_98\cdot \mathrm{mSmac} - \frac{\mathrm{AMito}\cdot k\_52\cdot \mathrm{mSmac}}{\mathrm{mvol}} \tag{1.95}$$

$$\frac{d\,(\mathrm{AMitomSmac})}{\mathrm{dt}} = \frac{\mathrm{AMito}\cdot k\_52\cdot \mathrm{mSmac}}{\mathrm{mvol}} - \mathrm{AMitomSmac}\cdot k\_54 - \mathrm{AMitomSmac}\cdot k\_53 \tag{1.96}$$

$$\frac{d\,(\mathrm{ASmac})}{\mathrm{dt}} = \mathrm{AMitomSmac}\cdot k\_54 - \mathrm{ASmac}\cdot k\_65 + \mathrm{cSmac}\cdot k\_66 \tag{1.97}$$

$$\frac{d\,(\mathrm{CytoC})}{\mathrm{dt}} = \mathrm{ACytoC}\cdot k\_55 + \mathrm{ApafCytoC}\cdot k\_57 + \mathrm{ApafCytoC}\cdot k\_59 - \mathrm{CytoC}\cdot k\_56 - \mathrm{CytoC}\cdot k\_115 - \mathrm{Apaf}\cdot \mathrm{CytoC}\cdot k\_58 \tag{1.98}$$

$$\frac{d\,(\mathrm{Apaf})}{\mathrm{dt}} = \mathrm{ApafCytoC}\cdot k\_59 + \mathrm{act\_Apaf}\cdot k\_94 - \mathrm{Apaf}\cdot \mathrm{CytoC}\cdot k\_58 \tag{1.99}$$

$$\frac{d\,(\mathrm{ApafCytoC})}{\mathrm{dt}} = \mathrm{Apaf}\cdot \mathrm{CytoC}\cdot k\_58 - \mathrm{ApafCytoC}\cdot k\_59 - \mathrm{ApafCytoC}\cdot k\_57 \tag{1.100}$$

$$\frac{d\left(\text{act\_Apaf}\right)}{\text{dt}} = \text{ApafCytoC} \cdot k\_57 + \text{Apop} \cdot k\_61 - \text{act\_Apaf} \cdot k\_94 - \text{act\_Apaf} \cdot k\_60 \cdot \text{pC\_9} \tag{1.101}$$

$$\frac{d\left(\text{pC\_9}\right)}{\text{dt}} = \text{Apop} \cdot k\_61 - \text{act\_Apaf} \cdot k\_60 \cdot \text{pC\_9} \tag{1.102}$$

$$\begin{aligned}\frac{d\left(\text{Apop}\right)}{\text{dt}} = {} & \text{ApoppC\_3} \cdot k\_63 - \text{Apop} \cdot k\_61 + \text{ApoppC\_3} \cdot k\_64 + \text{ApopXIAP} \cdot k\_68 + \text{ApopXIAP} \\ & \cdot k\_107 - \text{Apop} \cdot \text{XIAP} \cdot k\_67 - \text{Apop} \cdot k\_62 \cdot \text{pC\_3} + \text{act\_Apaf} \cdot k\_60 \cdot \text{pC\_9}\end{aligned} \tag{1.103}$$

$$\frac{d\left(\text{ApoppC\_3}\right)}{\text{dt}} = \text{Apop} \cdot k\_62 \cdot \text{pC\_3} - \text{ApoppC\_3} \cdot k\_64 - \text{ApoppC\_3} \cdot k\_63 \tag{1.104}$$

$$\frac{d\left(\text{cSmac}\right)}{\text{dt}} = \text{ASmac} \cdot k\_65 - \text{cSmac} \cdot k\_66 - \text{cSmac} \cdot k\_99 + \text{cSmacXIAP} \cdot k\_70 - \text{XIAP} \cdot \text{cSmac} \cdot k\_69 \tag{1.105}$$

$$\frac{d\left(\text{ApopXIAP}\right)}{\text{dt}} = \text{Apop} \cdot \text{XIAP} \cdot k\_67 - \text{ApopXIAP} \cdot k\_107 - \text{ApopXIAP} \cdot k\_68 \tag{1.106}$$

$$\frac{d\left(\text{cSmacXIAP}\right)}{\text{dt}} = \text{XIAP} \cdot \text{cSmac} \cdot k\_69 - \text{cSmacXIAP} \cdot k\_100 - \text{cSmacXIAP} \cdot k\_70 \tag{1.107}$$

$$\frac{d\left(C\_3\text{\_Ub}\right)}{\text{dt}} = \text{XIAPC\_3} \cdot k\_22 - C\_3\text{\_Ub} \cdot k\_103 \tag{1.108}$$

$$\begin{aligned}\frac{d\left(\text{CycA}\right)}{\text{dt}} = {} & \text{expr\_3} + \text{CA} \cdot \text{k2\_17} + \text{CA} \cdot (\text{k2\_30} + \text{k2\_31} \cdot (\text{CycA} \cdot \text{k2\_34} + \text{CycB} \cdot \text{k2\_33} + \text{CycE} \cdot \text{k2\_32})) \\ & - \text{CDc\_20} \cdot \text{CycA} \cdot \text{k2\_22} - \text{CycA} \cdot \text{k2\_16} \cdot \text{p27}\end{aligned} \tag{1.109}$$

$$\frac{d\left(\text{CycB}\right)}{\text{dt}} = \text{k2\_77} \cdot \left(\text{k2\_23} + \frac{\text{CycB}^2 \cdot \text{k2\_24}}{\text{k2\_25}^2 \cdot \left(\frac{\text{CycB}^2}{\text{k2\_25}^2} + 1\right)}\right) - \text{CycB} \cdot (\text{CDc\_20} \cdot \text{k2\_28} + \text{Cdh\_1} \cdot \text{k2\_27} - \text{k2\_26} \cdot (\text{Cdh\_1} - 1)) \tag{1.110}$$

$$\frac{d\left(\mathrm{CycD}\right)}{\mathrm{dt}} = \mathrm{CD}\cdot \mathrm{k2\_11} - \mathrm{CycD}\cdot \mathrm{k2\_9} + \mathrm{CD}\cdot \left(\mathrm{k2\_30} + \mathrm{k2\_31}\cdot \left(\mathrm{CycA}\cdot \mathrm{k2\_34} + \mathrm{CycB}\cdot \mathrm{k2\_33} + \mathrm{CycE}\cdot \mathrm{k2\_32}\right)\right) - \mathrm{CycD}\cdot \mathrm{k2\_10}\cdot \mathrm{p27} + \mathrm{k2\_8}\cdot \mathrm{k2\_77}\cdot \mathrm{mCycD} \tag{1.111}$$

$$\frac{d\left(\mathrm{CycE}\right)}{\mathrm{dt}} = \mathrm{CE}\cdot \mathrm{k2\_17} - \mathrm{CycE}\cdot \left(\mathrm{k2\_14} + \frac{\mathrm{k2\_15}\cdot \left(\mathrm{CycB}\cdot \mathrm{k2\_20} + \mathrm{k2\_19}\cdot \left(\mathrm{CycA} + \mathrm{CycE}\right)\right)}{\mathrm{CE} + \mathrm{CycE} + \mathrm{k2\_18}}\right) + \mathrm{k2\_77}\cdot \left(\mathrm{k2\_12} + \mathrm{E2F}\cdot \mathrm{k2\_13}\right) + \mathrm{CE}\cdot \left(\mathrm{k2\_30} + \mathrm{k2\_31}\cdot \left(\mathrm{CycA}\cdot \mathrm{k2\_34} + \mathrm{CycB}\cdot \mathrm{k2\_33} + \mathrm{CycE}\cdot \mathrm{k2\_32}\right)\right) - \mathrm{CycE}\cdot \mathrm{k2\_16}\cdot \mathrm{p27} \tag{1.112}$$

$$\frac{d\left(\mathrm{mCycD}\right)}{\mathrm{dt}} = \mathrm{k2\_78}\cdot \left(\frac{0.9900\cdot \left(\mathrm{A50n}\cdot \mathrm{kp\_NC} + \mathrm{C50n}\cdot \mathrm{kp\_NC} + \mathrm{kp\_mtb}\cdot \mathrm{otherTFs\_activity} + \mathrm{kmtb\_off}\cdot \mathrm{kp\_PMBC}\cdot \mathrm{otherTFs\_activity}\right)^2}{\mathrm{CYCD\_THRESHOLD}^2\cdot \left(\frac{\left(\mathrm{A50n}\cdot \mathrm{kp\_NC} + \mathrm{C50n}\cdot \mathrm{kp\_NC} + \mathrm{kp\_mtb}\cdot \mathrm{otherTFs\_activity} + \mathrm{kmtb\_off}\cdot \mathrm{kp\_PMBC}\cdot \mathrm{otherTFs\_activity}\right)^2}{\mathrm{CYCD\_THRESHOLD}^2} + 1\right)} + 0.0100\right) - \mathrm{k2\_79}\cdot \mathrm{mCycD} \tag{1.113}$$

$$\frac{d\left(\mathrm{mBcl\_2}\right)}{\mathrm{dt}} = \mathrm{expr\_4} + \mathrm{ke\_bcl2} - \mathrm{k2\_81}\cdot \mathrm{mBcl\_2} \tag{1.114}$$

$$\frac{d\left(\mathrm{Cdh\_1}\right)}{\mathrm{dt}} = \mathrm{expr\_1} - \frac{\mathrm{Cdh\_1}\cdot \mathrm{k2\_51}\cdot \left(\mathrm{CycA}\cdot \mathrm{k2\_54} + \mathrm{CycB}\cdot \mathrm{k2\_53} + \mathrm{CycE}\cdot \mathrm{k2\_52}\right)}{\mathrm{Cdh\_1} + \mathrm{k2\_50}} \tag{1.115}$$

$$\frac{d\left(\mathrm{CA}\right)}{\mathrm{dt}} = \mathrm{CycA}\cdot \mathrm{k2\_16}\cdot \mathrm{p27} - \mathrm{CA}\cdot \left(\mathrm{k2\_30} + \mathrm{k2\_31}\cdot \left(\mathrm{CycA}\cdot \mathrm{k2\_34} + \mathrm{CycB}\cdot \mathrm{k2\_33} + \mathrm{CycE}\cdot \mathrm{k2\_32}\right)\right) - \mathrm{CA}\cdot \mathrm{CDc\_20}\cdot \mathrm{k2\_22} - \mathrm{CA}\cdot \mathrm{k2\_17} \tag{1.116}$$

$$\frac{d\left(\mathrm{CD}\right)}{\mathrm{dt}} = \mathrm{CycD}\cdot \mathrm{k2\_10}\cdot \mathrm{p27} - \mathrm{CD}\cdot \mathrm{k2\_11} - \mathrm{CD}\cdot \left(\mathrm{k2\_30} + \mathrm{k2\_31}\cdot \left(\mathrm{CycA}\cdot \mathrm{k2\_34} + \mathrm{CycB}\cdot \mathrm{k2\_33} + \mathrm{CycE}\cdot \mathrm{k2\_32}\right)\right) - \mathrm{CD}\cdot \mathrm{k2\_9} \tag{1.117}$$

$$\frac{d\left(\mathrm{CDc\_20}\right)}{\mathrm{dt}} = -\mathrm{CDc\_20} \cdot \mathrm{k2\_63} - \frac{\mathrm{CDc\_20} \cdot \mathrm{k2\_65}}{\mathrm{CDc\_20} + \mathrm{k2\_67}} - \frac{\mathrm{IEP} \cdot \mathrm{k2\_64} \cdot \left(\mathrm{CDc\_20} - \mathrm{CDc20T}\right)}{\mathrm{CDc20T} - \mathrm{CDc\_20} + \mathrm{k2\_66}} \tag{1.118}$$

$$\frac{d\left(\mathrm{CDc20T}\right)}{\mathrm{dt}} = \mathrm{k2\_77} \cdot \left(\mathrm{k2\_61} + \mathrm{CycB} \cdot \mathrm{k2\_62}\right) - \mathrm{CDc20T} \cdot \mathrm{k2\_63} \tag{1.119}$$

$$\begin{aligned}\frac{d\left(\mathrm{CE}\right)}{\mathrm{dt}} = {} & \mathrm{CycE} \cdot \mathrm{k2\_16} \cdot \mathrm{p27} - \mathrm{CE} \cdot \mathrm{k2\_17} - \mathrm{CE} \cdot \left(\mathrm{k2\_30} + \mathrm{k2\_31} \cdot \left(\mathrm{CycA} \cdot \mathrm{k2\_34} + \mathrm{CycB} \cdot \mathrm{k2\_33} + \mathrm{CycE} \cdot \mathrm{k2\_32}\right)\right) \\ & - \mathrm{CE} \cdot \left(\mathrm{k2\_14} + \frac{\mathrm{k2\_15} \cdot \left(\mathrm{CycB} \cdot \mathrm{k2\_20} + \mathrm{k2\_19} \cdot \left(\mathrm{CycA} + \mathrm{CycE}\right)\right)}{\mathrm{CE} + \mathrm{CycE} + \mathrm{k2\_18}}\right)\end{aligned} \tag{1.120}$$

$$\frac{d\left(\mathrm{GM}\right)}{\mathrm{dt}} = \mathrm{expr\_2} - \mathrm{GM} \cdot \mathrm{k2\_75} \tag{1.121}$$

$$\frac{d\left(\mathrm{IEP}\right)}{\mathrm{dt}} = -\frac{\mathrm{CycB} \cdot \mathrm{k2\_57} \cdot \left(\mathrm{IEP} - 1\right)}{\mathrm{k2\_59} - \mathrm{IEP} + 1} - \frac{\mathrm{IEP} \cdot \mathrm{PPX} \cdot \mathrm{k2\_58}}{\mathrm{IEP} + \mathrm{k2\_60}} \tag{1.122}$$

$$\frac{d\left(\mathrm{Mass}\right)}{\mathrm{dt}} = \mathrm{GM} \cdot \mathrm{k2\_76} \cdot \mathrm{k2\_77} - \mathrm{Mass} \cdot \mathrm{k2\_84} \tag{1.123}$$

$$\begin{aligned}\frac{d\left(\mathrm{p27}\right)}{\mathrm{dt}} = {} & \mathrm{CE} \cdot \left(\mathrm{k2\_14} + \frac{\mathrm{k2\_15} \cdot \left(\mathrm{CycB} \cdot \mathrm{k2\_20} + \mathrm{k2\_19} \cdot \left(\mathrm{CycA} + \mathrm{CycE}\right)\right)}{\mathrm{CE} + \mathrm{CycE} + \mathrm{k2\_18}}\right) + \mathrm{CA} \cdot \mathrm{k2\_17} + \mathrm{CD} \cdot \mathrm{k2\_9} + \mathrm{CD} \cdot \mathrm{k2\_11} + \mathrm{CE} \\ & \cdot \mathrm{k2\_17} + \mathrm{k2\_29} \cdot \mathrm{k2\_77} - \mathrm{p27} \cdot \left(\mathrm{k2\_30} + \mathrm{k2\_31} \cdot \left(\mathrm{CycA} \cdot \mathrm{k2\_34} + \mathrm{CycB} \cdot \mathrm{k2\_33} + \mathrm{CycE} \cdot \mathrm{k2\_32}\right)\right) \\ & + \mathrm{CA} \cdot \mathrm{CDc\_20} \cdot \mathrm{k2\_22} - \mathrm{CycD} \cdot \mathrm{k2\_10} \cdot \mathrm{p27} - \mathrm{CycA} \cdot \mathrm{k2\_16} \cdot \mathrm{p27} - \mathrm{CycE} \cdot \mathrm{k2\_16} \cdot \mathrm{p27}\end{aligned} \tag{1.124}$$

$$\frac{d\left(\mathrm{PPX}\right)}{\mathrm{dt}} = \mathrm{k2\_55} \cdot \mathrm{k2\_77} - \mathrm{PPX} \cdot \mathrm{k2\_56} \tag{1.125}$$

$$\begin{aligned}\frac{d\left(\mathrm{ppRb}\right)}{\mathrm{dt}} = {} & \mathrm{E2FRb} \cdot \mathrm{k2\_40} \cdot \left(\mathrm{CycA} \cdot \mathrm{k2\_39} + \mathrm{CycB} \cdot \mathrm{k2\_38} + \mathrm{CycE} \cdot \mathrm{k2\_37} + \mathrm{k2\_36} \cdot \left(\mathrm{CD} + \mathrm{CycD}\right)\right) - \mathrm{ppRb} \cdot \left(\mathrm{k2\_41}\right. \\ & \left. \cdot \left(\mathrm{k2\_44} - \frac{\mathrm{k2\_44}}{\mathrm{k2\_43} \cdot \left(\mathrm{CycB} \cdot \mathrm{k2\_46} + \mathrm{k2\_45} \cdot \left(\mathrm{CycA} + \mathrm{CycE}\right)\right) + 1}\right) + \frac{\mathrm{k2\_42} \cdot \mathrm{k2\_44}}{\mathrm{k2\_43} \cdot \left(\mathrm{CycB} \cdot \mathrm{k2\_46} + \mathrm{k2\_45} \cdot \left(\mathrm{CycA} + \mathrm{CycE}\right)\right) + 1}\right) \\ & + \mathrm{Rb} \cdot \mathrm{k2\_40} \cdot \left(\mathrm{CycA} \cdot \mathrm{k2\_39} + \mathrm{CycB} \cdot \mathrm{k2\_38} + \mathrm{CycE} \cdot \mathrm{k2\_37} + \mathrm{k2\_36} \cdot \left(\mathrm{CD} + \mathrm{CycD}\right)\right) + \mathrm{k2\_40} \\ & \cdot \mathrm{pE2FRb} \cdot \left(\mathrm{CycA} \cdot \mathrm{k2\_39} + \mathrm{CycB} \cdot \mathrm{k2\_38} + \mathrm{CycE} \cdot \mathrm{k2\_37} + \mathrm{k2\_36} \cdot \left(\mathrm{CD} + \mathrm{CycD}\right)\right)\end{aligned} \tag{1.126}$$

$$\frac{d\left(\mathrm{E2F}\right)}{\mathrm{dt}} = \mathrm{E2FRb} \cdot \mathrm{k2\_73} - \mathrm{E2F} \cdot \left(\mathrm{k2\_70} + \mathrm{k2\_71} \cdot \left(\mathrm{CycA} + \mathrm{CycB}\right)\right) + \mathrm{k2\_69} \cdot \mathrm{pE2F} + \mathrm{E2FRb} \cdot \mathrm{k2\_40} \cdot \left(\mathrm{CycA} \cdot \mathrm{k2\_39} + \mathrm{CycB} \cdot \mathrm{k2\_38} + \mathrm{CycE} \cdot \mathrm{k2\_37} + \mathrm{k2\_36} \cdot \left(\mathrm{CD} + \mathrm{CycD}\right)\right) - \mathrm{E2F} \cdot \mathrm{Rb} \cdot \mathrm{k2\_72} \tag{1.127}$$

$$\frac{d\left(\mathrm{pE2F}\right)}{\mathrm{dt}} = \mathrm{E2F} \cdot \left(\mathrm{k2\_70} + \mathrm{k2\_71} \cdot \left(\mathrm{CycA} + \mathrm{CycB}\right)\right) - \mathrm{k2\_69} \cdot \mathrm{pE2F} + \mathrm{k2\_73} \cdot \mathrm{pE2FRb} + \mathrm{k2\_40} \cdot \mathrm{pE2FRb} \cdot \left(\mathrm{CycA} \cdot \mathrm{k2\_39} + \mathrm{CycB} \cdot \mathrm{k2\_38} + \mathrm{CycE} \cdot \mathrm{k2\_37} + \mathrm{k2\_36} \cdot \left(\mathrm{CD} + \mathrm{CycD}\right)\right) - \mathrm{Rb} \cdot \mathrm{k2\_72} \cdot \mathrm{pE2F} \tag{1.128}$$

$$\frac{d\left(\mathrm{Rb}\right)}{\mathrm{dt}} = \mathrm{E2FRb} \cdot \mathrm{k2\_73} + \mathrm{ppRb} \cdot \left(\mathrm{k2\_41} \cdot \left(\mathrm{k2\_44} - \frac{\mathrm{k2\_44}}{\mathrm{k2\_43} \cdot \left(\mathrm{CycB} \cdot \mathrm{k2\_46} + \mathrm{k2\_45} \cdot \left(\mathrm{CycA} + \mathrm{CycE}\right)\right) + 1}\right) + \frac{\mathrm{k2\_42} \cdot \mathrm{k2\_44}}{\mathrm{k2\_43} \cdot \left(\mathrm{CycB} \cdot \mathrm{k2\_46} + \mathrm{k2\_45} \cdot \left(\mathrm{CycA} + \mathrm{CycE}\right)\right) + 1}\right) + \mathrm{k2\_73} \cdot \mathrm{pE2FRb} - \mathrm{Rb} \cdot \mathrm{k2\_40} \cdot \left(\mathrm{CycA} \cdot \mathrm{k2\_39} + \mathrm{CycB} \cdot \mathrm{k2\_38} + \mathrm{CycE} \cdot \mathrm{k2\_37} + \mathrm{k2\_36} \cdot \left(\mathrm{CD} + \mathrm{CycD}\right)\right) - \mathrm{E2F} \cdot \mathrm{Rb} \cdot \mathrm{k2\_72} - \mathrm{Rb} \cdot \mathrm{k2\_72} \cdot \mathrm{pE2F} \tag{1.129}$$

$$\frac{d\left(\mathrm{E2FRb}\right)}{\mathrm{dt}} = \mathrm{k2\_69} \cdot \mathrm{pE2FRb} - \mathrm{E2FRb} \cdot \left(\mathrm{k2\_70} + \mathrm{k2\_71} \cdot \left(\mathrm{CycA} + \mathrm{CycB}\right)\right) - \mathrm{E2FRb} \cdot \mathrm{k2\_73} - \mathrm{E2FRb} \cdot \mathrm{k2\_40} \cdot \left(\mathrm{CycA} \cdot \mathrm{k2\_39} + \mathrm{CycB} \cdot \mathrm{k2\_38} + \mathrm{CycE} \cdot \mathrm{k2\_37} + \mathrm{k2\_36} \cdot \left(\mathrm{CD} + \mathrm{CycD}\right)\right) + \mathrm{E2F} \cdot \mathrm{Rb} \cdot \mathrm{k2\_72} \tag{1.130}$$

$$\frac{d\left(\mathrm{pE2FRb}\right)}{\mathrm{dt}} = \mathrm{E2FRb} \cdot \left(\mathrm{k2\_70} + \mathrm{k2\_71} \cdot \left(\mathrm{CycA} + \mathrm{CycB}\right)\right) - \mathrm{k2\_69} \cdot \mathrm{pE2FRb} - \mathrm{k2\_73} \cdot \mathrm{pE2FRb} - \mathrm{k2\_40} \cdot \mathrm{pE2FRb} \cdot \left(\mathrm{CycA} \cdot \mathrm{k2\_39} + \mathrm{CycB} \cdot \mathrm{k2\_38} + \mathrm{CycE} \cdot \mathrm{k2\_37} + \mathrm{k2\_36} \cdot \left(\mathrm{CD} + \mathrm{CycD}\right)\right) + \mathrm{Rb} \cdot \mathrm{k2\_72} \cdot \mathrm{pE2F} \tag{1.131}$$

$$\frac{d\left(\mathrm{Growth}\right)}{\mathrm{dt}} = \mathrm{MYC} \cdot \mathrm{k2\_82} - \mathrm{Growth} \cdot \mathrm{k2\_83} \tag{1.132}$$

$$\frac{d\left(\mathrm{MYC}\right)}{\mathrm{dt}} = \mathrm{ke\_myc} - \mathrm{MYC} \cdot \mathrm{k2\_86} + \mathrm{k2\_85} \cdot \left(\frac{0.9900 \cdot \left(\mathrm{A50n} \cdot \mathrm{kp\_NM} + \mathrm{C50n} \cdot \mathrm{kp\_NM} + \mathrm{kp\_mtb} \cdot \mathrm{otherTFs\_activity} + \mathrm{kmtb\_off} \cdot \mathrm{kp\_PMBC} \cdot \mathrm{otherTFs\_activity}\right)^2}{\mathrm{MYC\_THRESHOLD}^2 \cdot \left(\frac{\left(\mathrm{A50n}\cdot\mathrm{kp\_NM}+\mathrm{C50n}\cdot\mathrm{kp\_NM}+\mathrm{kp\_mtb}\cdot\mathrm{otherTFs\_activity}+\mathrm{kmtb\_off}\cdot\mathrm{kp\_PMBC}\cdot\mathrm{otherTFs\_activity}\right)^2}{\mathrm{MYC\_THRESHOLD}^2} + 1 \right)} + 0.0100 \right) \tag{1.133}$$

$$\frac{d\left(\mathrm{IRF}\right)}{\mathrm{dt}} = \frac{\mathrm{kASC\_16}^{\mathrm{kASC\_17}} \cdot \left(\mathrm{kASC\_15} + \frac{\mathrm{A50n}^{\mathrm{kASC\_13}}\cdot\mathrm{kASC\_11}\cdot\mathrm{kASC\_12}}{40\cdot\mathrm{A50n}^{\mathrm{kASC\_13}}+40\cdot\left(50\cdot\mathrm{kASC\_11}\right)^{\mathrm{kASC\_13}}} + \frac{\mathrm{C50n}^{\mathrm{kASC\_13}}\cdot\mathrm{kASC\_11}\cdot\mathrm{kASC\_12}}{40\cdot\mathrm{C50n}^{\mathrm{kASC\_13}}+40\cdot\left(3\cdot\mathrm{kASC\_11}\right)^{\mathrm{kASC\_13}}} + \frac{\mathrm{Blimp\_1}^{\mathrm{kASC\_13}}\cdot\mathrm{kASC\_11}\cdot\mathrm{kASC\_12}}{3\cdot\left(\mathrm{kASC\_11}\cdot\mathrm{kASC\_14}\right)^{\mathrm{kASC\_13}}+3\cdot\mathrm{Blimp\_1}^{\mathrm{kASC\_13}}} \right)}{\mathrm{kASC\_16}^{\mathrm{kASC\_17}} + 0^{\mathrm{kASC\_17}}} - \mathrm{IRF} \cdot \mathrm{kASC\_18} \tag{1.134}$$

$$\frac{d\left(\mathrm{Blimp\_1}\right)}{\mathrm{dt}} = \frac{\mathrm{kASC\_26}^{\mathrm{kASC\_27}} \cdot \left(\frac{\mathrm{A50n}^{\mathrm{kASC\_23}}\cdot\mathrm{kASC\_21}\cdot\mathrm{kASC\_22}}{\mathrm{A50n}^{\mathrm{kASC\_23}}+\left(50\cdot\mathrm{kASC\_21}\right)^{\mathrm{kASC\_23}}} + \frac{\mathrm{IRF}^{\mathrm{kASC\_23}}\cdot\mathrm{kASC\_21}\cdot\mathrm{kASC\_22}\cdot\mathrm{kirfmut}}{\left(\mathrm{kASC\_21}\cdot\mathrm{kASC\_24}\right)^{\mathrm{kASC\_23}}+\mathrm{IRF}^{\mathrm{kASC\_23}}} \right)}{\mathrm{kASC\_26}^{\mathrm{kASC\_27}} + \left(\mathrm{Bcl} \cdot k\_\mathrm{bclRep2}\right)^{\mathrm{kASC\_27}}} - \mathrm{Blimp\_1} \cdot \mathrm{kASC\_28} \tag{1.135}$$

$$\frac{d\left(\mathrm{Pax\_5}\right)}{\mathrm{dt}} = \frac{\mathrm{kASC\_35} \cdot \mathrm{kASC\_36}^{\mathrm{kASC\_37}}}{\mathrm{Blimp\_1}^{\mathrm{kASC\_37}} + \mathrm{kASC\_36}^{\mathrm{kASC\_37}}} - \mathrm{Pax\_5} \cdot \mathrm{kASC\_38} \tag{1.136}$$

$$\frac{d\left(\mathrm{Bcl}\right)}{\mathrm{dt}} = \mathrm{ke\_bcl6} - \mathrm{Bcl} \cdot \mathrm{kASC\_48} + \frac{\mathrm{kASC\_46}^{\mathrm{kASC\_47}} \cdot \left(\frac{\mathrm{C50n}^{\mathrm{kASC\_43}}\cdot\mathrm{kASC\_41}\cdot\mathrm{kASC\_42}}{\mathrm{C50n}^{\mathrm{kASC\_43}}+\left(3\cdot\mathrm{kASC\_41}\right)^{\mathrm{kASC\_43}}} + \frac{\mathrm{kASC\_41}\cdot\mathrm{kASC\_42}\cdot\left(\mathrm{Pax\_5}\cdot\mathrm{kpax5mut}\right)^{\mathrm{kASC\_43}}}{\left(\mathrm{kASC\_41}\cdot\mathrm{kASC\_44}\right)^{\mathrm{kASC\_43}}+\left(\mathrm{Pax\_5}\cdot\mathrm{kpax5mut}\right)^{\mathrm{kASC\_43}}} \right)}{\mathrm{kASC\_46}^{\mathrm{kASC\_47}} + \mathrm{Blimp\_1}^{\mathrm{kASC\_47}} \cdot k\_\mathrm{bclRep} + \mathrm{IRF}^{\mathrm{kASC\_47}} \cdot k\_\mathrm{bclRep} \cdot \mathrm{kirfmut}} \tag{1.137}$$

$$\frac{d\left(\mathrm{Aid}\right)}{\mathrm{dt}} = \frac{\mathrm{kASC\_56}^{\mathrm{kASC\_57}} \cdot \left(\frac{\mathrm{A50n}^{\mathrm{kASC\_53}}\cdot\mathrm{kASC\_51}\cdot\mathrm{kASC\_52}}{\mathrm{A50n}^{\mathrm{kASC\_53}}+\left(50\cdot\mathrm{kASC\_51}\right)^{\mathrm{kASC\_53}}} + \frac{\mathrm{C50n}^{\mathrm{kASC\_53}}\cdot\mathrm{kASC\_51}\cdot\mathrm{kASC\_52}}{\mathrm{C50n}^{\mathrm{kASC\_53}}+\left(3\cdot\mathrm{kASC\_51}\right)^{\mathrm{kASC\_53}}} + \frac{\mathrm{kASC\_51}\cdot\mathrm{kASC\_52}\cdot\mathrm{kirfmut}\cdot\mathrm{kpax5mut}\cdot\left(\mathrm{IRF}\cdot\mathrm{Pax\_5}^2\right)^{\mathrm{kASC\_53}}}{\left(\mathrm{kASC\_51}\cdot\mathrm{kASC\_54}\right)^{\mathrm{kASC\_53}}+\left(\mathrm{IRF}\cdot\mathrm{Pax\_5}^2\right)^{\mathrm{kASC\_53}}} \right)}{\mathrm{kASC\_56}^{\mathrm{kASC\_57}} + 0^{\mathrm{kASC\_57}}} - \mathrm{Aid} \cdot \mathrm{kASC\_58} \tag{1.138}$$

$$\frac{d\left(\text{tpre\_IkBe1}\right)}{\text{dt}} = \frac{\text{pii\_13} \cdot \left(\text{pdi\_723} \cdot \left(\frac{\text{A50n}}{\text{pii\_103}}\right)^{\text{pii\_93}} + \text{pdi\_713} \cdot \left(\frac{\text{AAn}}{\text{pii\_103}}\right)^{\text{pii\_93}} + \text{pdi\_743} \cdot \left(\frac{\text{C50n}}{\text{pii\_103}}\right)^{\text{pii\_93}}\right)}{\left(\frac{\text{A50n}}{\text{pii\_103}}\right)^{\text{pii\_93}} + \left(\frac{\text{AAn}}{\text{pii\_103}}\right)^{\text{pii\_93}} + \left(\frac{\text{C50n}}{\text{pii\_103}}\right)^{\text{pii\_93}} + 1} - \text{kdel\_e1} \cdot \text{tpre\_IkBe1} \tag{1.139}$$

$$\frac{d\left(\text{tpre\_P501}\right)}{\text{dt}} = \frac{\text{pm\_12} \cdot \left(\text{pdm\_122} \cdot \left(\frac{\text{A50n}}{\text{pm\_82}}\right)^{\text{pm\_72}} + \text{pdm\_142} \cdot \left(\frac{\text{C50n}}{\text{pm\_82}}\right)^{\text{pm\_72}}\right)}{\left(\frac{\text{A50n}}{\text{pm\_82}}\right)^{\text{pm\_72}} + \left(\frac{\text{C50n}}{\text{pm\_82}}\right)^{\text{pm\_72}} + 1} - \text{kdel\_p501} \cdot \text{tpre\_P501} \tag{1.140}$$

$$\frac{d\left(\text{tpre\_cRel1}\right)}{\text{dt}} = \frac{\text{kASC\_66}^{\text{kASC\_67}} \cdot \text{pm\_13} \cdot \left(\text{pdm\_123} \cdot \left(\frac{\text{A50n}}{\text{pm\_83}}\right)^{\text{pm\_73}} + \text{pdm\_143} \cdot \left(\frac{\text{C50n}}{\text{pm\_83}}\right)^{\text{pm\_73}}\right)}{\left(\text{Blimp\_1}^{\text{kASC\_67}} + \text{kASC\_66}^{\text{kASC\_67}}\right) \cdot \left(\left(\frac{\text{A50n}}{\text{pm\_83}}\right)^{\text{pm\_73}} + \left(\frac{\text{C50n}}{\text{pm\_83}}\right)^{\text{pm\_73}} + 1\right)} - \text{kdel\_crel1} \cdot \text{tpre\_cRel1} \tag{1.141}$$

$$\begin{aligned}\frac{d\left(\text{pIKK}\right)}{\text{dt}} = {} & \frac{\text{kmtb}}{\text{kmtb} + \text{A20} \cdot \text{ka20mut}} + \frac{\text{ktlr}}{\text{ktlr} + \text{A20} \cdot \text{ka20mut}} - \text{pIKK} \cdot \text{pikk\_2} \\ & + \frac{\text{kmtb\_off} \cdot \text{pikk\_1}}{\text{pikk\_1} + \text{A20} \cdot \text{ka20mut}} + \text{kmtb\_off} \cdot \text{phase} \cdot \text{pikk\_3} \cdot \text{e}^{-\text{A20} \cdot \text{ka20mut}}\end{aligned} \tag{1.142}$$

$$\frac{d\left(tA20\right)}{\text{dt}} = \text{A50n} \cdot \text{pikk\_4} - \text{pikk\_5} \cdot tA20 \tag{1.143}$$

$$\frac{d\left(\text{A20}\right)}{\text{dt}} = \text{pikk\_6} \cdot tA20 - \text{A20} \cdot \text{pikk\_7} \tag{1.144}$$

$$\frac{d\left(\text{pAKT}\right)}{\text{dt}} = \text{pakt\_1} - \text{pAKT} \cdot \text{pakt\_2} + \text{pakt\_3} \cdot \text{phase} \cdot \text{e}^{-\text{PTEN} \cdot \text{kpi3kmut}} \tag{1.145}$$

$$\frac{d\left(\text{tPTEN}\right)}{\text{dt}} = \text{pakt\_4} \cdot \text{e}^{-\text{A50n}} - \text{pakt\_5} \cdot \text{tPTEN} \tag{1.146}$$

$$\frac{d\left(\text{PTEN}\right)}{\text{dt}} = \text{pakt\_6} \cdot \text{tPTEN} - \text{PTEN} \cdot \text{pakt\_7} \tag{1.147}$$

2 Definitions of expressions

$$expr\_1 = \left\{ \begin{array}{ll} \frac{((k2\_47+k2\_48\cdot CDc20)\cdot(1-Cdh1))}{(k2\_49-Cdh1+1)}, & Cdh1 \leq 1 \\ 0, & Cdh1 > 1 \end{array} \right\} \tag{2.1}$$

$$expr\_2 = \left\{ \begin{array}{ll} k2\_74 \cdot (0.01 + 0.99 \cdot GrowthMultiplier \cdot GMgrowth), & \frac{numerator}{denominator} < 0.8 \\ k2\_74 \cdot 0.01, & otherwise \end{array} \right\} \tag{2.2}$$

$$expr\_3 = \left\{ \begin{array}{ll} k2\_77 \cdot k2\_21 \cdot E2F \cdot max(0, (GrowthMultiplier \cdot (GM \cdot k2\_76 \cdot k2\_77 - Mass \cdot k2\_84) \cdot 30)), & Mass > 0.5 \\ 0, & otherwise \end{array} \right\} \tag{2.3}$$

$$expr\_4 = \left\{ \begin{array}{ll} max(k2\_80 \cdot Bcl2Activity, \frac{k2\_80}{100}) & \\ \frac{k2\_80}{100}, & otherwise \end{array} \right\} \tag{2.4}$$

$$numerator = Rb + E2FRb + pE2FRb \tag{2.5}$$

$$denominator = numerator + ppRb \tag{2.6}$$

$$GMgrowth = (2.8 \cdot Mass^2)^{\cdot(-0.14*Mass^2)} \tag{2.7}$$

$$GrowthMultiplier = \frac{(\frac{Growth}{GROWTH\_THRESHOLD})^2}{(1 + \frac{Growth}{GROWTH\_THRESHOLD})^2} \tag{2.8}$$

$$BclNumerator = \left(\frac{0.3 * A50n + 0.6 \cdot C50n + 0.1 \cdot otherTFs\_activity}{BCL2\_THRESHOLD} \right)^2 \tag{2.9}$$

$$Bcl2Activity = \frac{BclNumerator}{1 + BclNumerator} \cdot (1 - 0.01) + 0.01 \tag{2.10}$$

(2.11)